Accepted Manuscript

A Review of Some Advanced Sensors used for Health Diagnosis of Civil Engineering Structures

Swagato Das, Purnachandra Saha

PII: S0263-2241(18)30601-8
DOI: https://doi.org/10.1016/j.measurement.2018.07.008
Reference: MEASUR 5692

To appear in: *Measurement*

Received Date: 30 January 2018
Revised Date: 2 July 2018
Accepted Date: 4 July 2018

Please cite this article as: S. Das, P. Saha, A Review of Some Advanced Sensors used for Health Diagnosis of Civil Engineering Structures, *Measurement* (2018), doi: https://doi.org/10.1016/j.measurement.2018.07.008

A Review of Some Advanced Sensors used for Health Diagnosis of Civil Engineering Structures

Swagato Das[1], Purnachandra Saha[2]

[1](Ph.D. Scholar, School of Civil Engineering, KIIT, deemed to be University, Bhubaneswar, Odisha, India.)
[2](Senior Associate Professor, School of Civil Engineering, KIIT, deemed to be University, Bhubaneswar, Odisha, India)

Abstract

The developments in structural health monitoring techniques have led to the invention of various sensors that can be effective damage indicator. Due to environmental or electromagnetic effects and need for constant energy source, the traditional sensors are unable to provide accurate and continuous measurements. In light of these events, new and improved sensors have been developed, along with wireless technology, to assist the monitoring process. With the need of detecting more than one damage parameters, multiplexed sensors have been the main interest of researchers. This paper deals with the different sensors used for determination of strain, acceleration and corrosion. A brief comparative study has been performed and presented in the following review paper. Multiplexed Fiber optics sensor have proved quite effective for SHM and proved to be a good competitor with other sensors. Optimum Sensor Placement technique developed for low level damage diagnosis is Iterated Improved Reduced System (IIRS) Method.

Keywords: Non-Contact sensor, Strain Sensors, Dynamic Monitoring, Accelerometers, Corrosion Sensors, Multiplexed Sensor, MEMS, Fiber Optic Sensors, Optimal Sensor Placement

1. Introduction

Structural Health Monitoring (SHM) of civil structures, as the name suggests means a proper evaluation of the civil structural condition. SHM based techniques are Non-Destructive Damage Evaluation (NDE) or Non-Destructive Testing (ND/T) techniques which are able to identify damage in a structure at an early stage and evaluate the damage extent so that the engineers can carry out the maintenance with the help of this data. The main functions of SHM are: 1) damage detection or validating the performance of large-scale complicated structures, 2) accurate identification of damage location, 3) check the severity of damage or evaluation of health status and predicting the service life of the structure, and 4) real-time data collection and diagnosis of structural condition [1]. Previously, the most common monitoring process carried out to evaluate damage was only by visual examination. With the development of technology, various other methods have been introduced to evaluate the structural health. Non - destructive monitoring techniques used previously were the X-rays, thermography, radiography and many others which required direct access to all the parts of the structure. This condition is not possible to achieve in case of complex structures. SHM had a breakthrough when it was integrated with different modern technologies such as; magnetic, electrical, thermal, and photic and computer science technology [2]. The modern SHM technique includes sensing technology, data collecting or acquisition, transmission, storage or management and diagnosis of the structural health. These techniques, with integrated remote sensing, use of smart materials and computer biased knowledge system, allow a civil engineer to observe the performance of large infrastructures; tunnels, bridges, offshore platforms, railways and at other places where it is not possible for onsite field test [3]. The traditional sensors used for the purpose of health diagnostics were the electronic strain sensors, accelerometers, displacement transducers, which provided the global and local parameters such as frequency, mode shapes, and frequency. These methods, however, posed a problem in measurement due to the environmental interference.

The modern NDE methods for monitoring the structural parameters are eddy current [4], radioscopy [5], acoustic emission (AE) [6], Lamb waves [7], comparative vacuum [8], methods based on electromagnetic impedance principle [9] and on fiber optics [10]. The methods involving eddy current and radioscopy make use of expensive and large transducers which have to be installed in large quantities for a structure. Therefore these methods proved to be uneconomical [11]. Compared to these methods, SHM carried out with the help of accelerometers, strain gage, piezoceramic material sensor, fiber optics, corrosion sensors and acoustic emission sensors are more commonly used. These sensors, being economical and light, can be installed at a larger scale [2, 5]. A huge amount of data is being generated which has to be arranged accurately which is a costly and challenging process [12]. With the improvement in SHM technologies, sensor fusion technique has been introduced in the field. This technique enhances the decision making performance, thus reducing the uncertainty, by the use of multiple sensors [13]. The complex data set obtained from multiple sensors has to be merged such that no relevant data is skipped out. The final analysis of SHM system is done based on increased safety, reduced maintenance, economic approach, reduced design margins and possibly zero false alarm rate [14]. A state of the art review has been performed in this paper for the different sensors in order to obtain a uniform base of comparison among different sensing techniques.

The researchers are mainly focussing their attention on the development of innovative sensing technologies for health diagnostic approach. For observing the structural behaviour, an appropriate sensor network is required for efficient signal processing and damage calculation from the extracted data [15]. The most basic health monitoring technique ever developed was based on the modal properties the structures: Vibration based SHM [16]. These methods include the use of dynamic measurements to calculate the local and global behaviours of the structure. Non contact damage detection technique has been developed to study the growth of cracks in structure. The local behaviour is measured in terms of change in strain which can be measured with the help of strain-based sensors: strain gauge [17]. The global behaviours are measured as displacement, frequency and mode shapes which can be measured with the help of sensors such as velocimeters, accelerometers and displacement transducers [18]. The data collected from these sensors are used for the mathematical calculations of damage in these structures using frequency response method, Modal Assurance criterion method, modal strain energy and modal flexibility method and mode shapes and curvature [16, 18-20]. Out of these methods, frequency response method, which gives a precise location of damage in global coordinates, is unable to measure local damage [21]. Other parameters, such as modal flexibility and modal energy, which are theoretically more sensitive, pick up errors due to measurement and environment along with the damage signals [22]. Some of the notable damage algorithms developed for SHM of bridges is based on load ratings, ambient truck load, traffic loads or Weigh-in-Motion (WIM) data [23-25]. However the all these algorithms are dependent on the strain data for the damage algorithms to detect damage [26]. Strain as a local coordinate has proved to be more sensitive in case of local damage detection. The traditional strain sensors or strain gage can detect damage precisely only if the damaged area is present under the influence or radius of the gage. This sensor is unable to pick up signals if the damage occurs in the surrounding areas outside the gage influence. Therefore, the strain gage cannot be employed for complex civil structures [17]. Also, the sensors are vulnerable to surrounding electromagnetic interference. Thereafter the study of damage with the help of piezoelectric sensor or transducers became popular. The PZT used are practically immune to the interference of electromagnetism. Therefore the damage recorded using this sensor is more precise than the strain gauge sensor. The electromechanical impedance (EMI) method and Lamb wave method utilizes mainly the piezometric transducers (PZT) for monitoring the structure. In the former method, the piezoelectric sensor can detect changes or damage in the mechanical properties of the structure by electrical impedance recorded by the sensor [27]. Whereas the latter method utilizes PZT to monitor Lamb waves which can travel long distances with a little loss in amplitude [28]. This method can be efficiently utilized if the number of PZT used is more [29]. The above sensors are mainly used to measure the damage due to change in strain that occurs in the structure after a particular force has acted on it, ex. earthquake force. Such type of damage is normally referred to as the static damage in the structure. For structures, such as towers or bridges, continuous horizontal force, in form of wind load, is acting. For assessment of such structures, dynamic parameters have to be measured. This condition is achieved by the use of accelerometers. These sensors measure the acceleration of the structure continuously and diagnostic is done by converting this acceleration to frequency domain [30]. This measured frequency is then processed to obtain the change in strain and hence structural diagnostic is performed. Another major damage in the structure is due to rebar corrosion which can be detected with the help of embedded sensors such as piezoceramic lead zirconate transducer and galvanic couple [31]. In order to incorporate all the sensing properties, i.e. for damage results from strain gauge, accelerometer and corrosion sensor, a new type of sensor - fiber optic sensors have been introduced and are the most widely used sensor of the present time. These optics are light, easy to handle, occupy little amount of space and are not affected by electromagnetic interference, unlike the other sensors [32]. The main advantage of these sensors is multiplexing [33]. These sensors can be used for measurement of a number of structural parameters; strain, temperature, humidity, acceleration, corrosion. This technology has been beneficial in reducing the number of different types of sensors employed for SHM [34]. Sensor placement is also an important aspect for efficient sensor placement such that maximum number of structural data is obtained with deployment of minimum number of sensors. Study of Optimal Sensor Placement (OSP) is advantageous for determining the efficiency of sensor network [35].

This paper deals with the development of SHM techniques in the field of sensor used. Different types of sensors used for SHM till date has been reviewed according to their loading and a brief comparative study have been performed citing the advancement of sensors and their sensing technology. A brief OSP study has also been conducted for finding the efficient sensor network placement.

2. Sensors Vision based SHM

Vision-based monitoring is a measurement technology used for detecting damage in structure since the beginning of health monitoring. In normal monitoring, the mode shapes are calculated from the sensor data, which involves a great number of calculations [16]. With an acute measurement of the vision-based system, the error sources were carefully examined such as gray level interpolation [36], subset function [37] and shape functions [38]. With recent development, non-contact machine-based vision technology was introduced which can measure the quasi-distributed displacement of structures. The techniques involved in vision-based displacement sensors are digital image correlation (DIC) [39], pattern matching [40], RANSAC algorithm [41] and others.

Machine-based vision technology includes measurement of strain from digital image obtained from high resolution industrial charge-coupled device (CCD) camera using multi-point pattern matching algorithm [42, 43]. The pre-designed patterns are compared with the images captured and the count is made for a number of times the patterns match with the images. When this count is maximum, it indicates that the target position is identified as damaged [44]. This process is sensitive to the variation of amplitude of geometric size. After the pattern matching is completed, the change in the image is converted into actual structural displacement in order to measure the damage.

One of the factors that have to be taken into consideration while obtaining images is the illumination which plays an important part as inferior illumination may lead to images captured not real to the original structure. The effect of bad weather, fog, may also be a hindrance to measurement. The vision-based measurement was tested against the magnetostrictive displacement sensor (MDS). The lab experiments for these factors proved to be satisfactory. However, in case of field experiments, a large angle of elevation for the digital camera has to be taken keeping in mind the sensitivity and accuracy of the measuring system. For a large angle of elevation, the longitudinal axis of the digital camera may not be perpendicular to the object, hence causing a problem in measurement. The digital image processing can be used along vision-based technology for health monitoring and was compared with linear variable differential transformer (LVDT). The result was found to be reliable and effective for multipoint structural displacement measurement [45].

Side by side, video camera based vibration measurement was also developed for NDT. The video-based monitoring can be applied for analysis of small motions, small subpixel displacement, and the accuracy is more as compared to camera-based measurement [46]. Computer-based programming can be used to convert displacement units obtained in pixels to mm. The process of converting video signals to displacement signals was proved to be effective and was validated using signals measured from laser vibrometer and accelerometer [47]. In order to increase the signal to noise ratio, the video signals may be downsampled. Fast Fourier Transform is implemented to convert the displacement signal to the frequency domain. The frequency obtained is compared for health monitoring.

The limitations are similar to that of the high-resolution camera-based monitoring, i.e., illumination, hindrance due to weather conditions. However for non contact based monitoring the measurement of noise is greater. Also for vibration of small amplitude, the sensor might now be as effective as strain gauges or accelerometer.

3. Sensors for Strain Measurement in SHM

The principal parameter used to detect damage in a structure is the change in strain. The change in strain may occur due to various reasons; change in temperature, dynamic forces acting on the structure, tension and compression forces due to loading or unloading and others. The change in strain is measured after the deformations have occurred due to the application of external force or load.

A wide range of sensors has been available for the purpose of SHM. But most of the sensors have a problem of measurement due to environmental disturbances. One of the major environmental issues is the change in temperature; due to which the structure experiences change in strain. Therefore it is hard to distinguish the strain measurements occurring due to change in temperature or due to change in other parameters. In order to measure this strain change, different strain sensors have been introduced. There are mainly three different strain sensors; electrical [48], wireless [49] and optical [50]. The electrical strain gauges are inexpensive and suitable for dynamic load conditions. Electrical resistance strain gauge (ERS) and vibrating wire strain gauge (VWSG) comes under this category. VWSG has the ability to measure temperature as well as strain without any electromagnetic interference. But due to the limited sampling rate, VWSG are not suitable for long-term monitoring of live load [51]. The wireless sensors require no cable for data transmission but their monitoring time is limited due to battery life [49]. The optical sensors used are Fiber Bragg Sensors (FBG) and Fiber-Optics sensor (FOS). These sensors are immune to noise and electromagnetic interferences. Also, they can be safely integrated with the structure for long-term monitoring [52]. Commercially three types of strain sensors are available; discrete strain sensor or point sensors, quasi-distributed strain sensor and highly distributed strain sensor [53]. Discrete strain sensors can measure only localised strain, quasi-distributed sensors are series of discrete sensors connected together and highly distributed strain sensors can measure the complete profile of strain along the entire length. Quasi-distributed sensors are a continuous series of discrete sensors connected together for strain measurement. Fibre Bragg Grating sensors (FBG) connected in series is the most widely used quasi-distributed strain sensor. The highly distributed strain sensors, distributed optical fibre (FO) cables, provide strain data over the whole length of the optical fibres. Therefore this sensor can be used for long-term monitoring of structures as it measures the strain for the entire profile of the structure whereas the former sensors only provided the strain data for the region they were installed in [54].

3.1 Metallic thin film strain gauge

The metallic thin film strain gauges are electrical sensors perfect for detection of a change in structural parameters and have been used for a long period of time. These sensors are economical, compact, and stable and provide a stable output signal for data acquisition. But the sensors have faced a challenge during measurement of dynamic loads of large scale [55]. Thus these sensors are not suitable to measure the dynamic strain of off-shore structures which can experience strain more than 5000με. The normal metallic thin foil strain gauges are unable to measure dynamic strain more than 2000με for 10^6 alternating load cycles [56].

To counter all the above drawbacks, strain shunt has been designed Xia and Quial [55] to incorporate the metallic thin film sensor gauge for measurement of large dynamic strain. The design of strain shunt includes installation of a strain gauge on an elastic shunt sheet which is supported by two elastic columns as shown in Fig. 1. Due to deformation in structure, the supporting columns will get deformed, thus disturbing the strain gauge. Therefore the strain can be measured by the gauge without undergoing large deformations. It was experimented and observed that the 11.5% strain was overestimated which may be due to not considering the height of the supporting columns which may undergo bending and tension/compression.

3.2 Thick film ceramic strain sensors

Measurement of strains in structures has been widely performed with the help of Foil Film Strain Gauge or Strain Gauges (FSG) [57]. With inclusions of new technology, Thick Film Sensors (TFSs) have been used for strain measurement. The thick film materials used are chosen such that they have high longevity, more robust, survive high mechanical stresses and extreme temperatures [58]. These sensors also measure strain with the help of piezoresistive effect. The piezo-resistive materials mainly used for strain gauge are thick film resistors, thin metal films and semiconductors [59]. The comparison of the above materials is provided in Table 1. It can be seen that thick film resistor is a good bridge between the other two sensors. It is economical, reliable and has a good gauge factor which is important from a sensitivity point of view.

To describe the sensitivity of a strain sensor, the gauge factor plays an important role Eq. 1 [60].

$$G_F = \frac{\Delta R/R_0}{\Delta L/L_0} \quad (1)$$

where ΔR, ΔL, R_0 and L_0 are change in resistance, change in displacement, initial resistance and length of composite sensor respectively.

The gauge factor is calculated using Quarter Bridge configuration which gives the relation between unbalanced output voltage and strain due to the load applied (Eq. 2) [61].

$$GF = (4V_0/V) * (1/\varepsilon) \quad (2)$$

where GF is the gauge factor, V is bridge excitation voltage, V_0 is unbalance bridge voltage due to the load applied and ε is the strain of the specimen.

Out of all the TFSs, Thick Film Ceramic Strain Gauge Sensor (TFCS) has been recognized as an effective strain measuring device. Ceramic has high elasticity, shock resistant, corrosion and abrasion resistant, has an operating thermal range from -20^{0}C to 80^{0}C and can withstand high voltages (2kW) [61].

Jabir and Gupta [61] conducted a comparative Four-Point Bending Test (4PBT) experiment (ASTM D6272-00 2001) with the help of FSG and TFCS to determine the efficiency of the sensors. Each TFCS was connected to a Wheatstone bridge which in-turn was connected to a data acquisition system. This arrangement is followed so that both tensions on the upper side and compression on the lower side can be recorded for the beam. The response for TFCS having a GF 7.2 was observed to be higher than FSG having GF 2 (Fig. 2).

But for practical applications, the TFCS have not been calibrated for readings due to different atmospheric effects, disturbance due to the application of glue and continuous structural deterioration as the G.F. changes.

3.3 Carbon based graphene sensor

With the advancement in technology, new lightweight sensors have been developed. These sensors are based on carbon nanomaterials; carbon black (CB) [62], graphene [63], carbon nanotube (CNT) [64], carbon nanofiber (CNF) [65] and carbon nanoribbons. Among these graphene has been the widely used nanomaterials. It has a 2D hexagonal honeycomb structure which easily breaks under stress, thus changing the electronic energy band indicating damage in the structure [66].

Zha et al. [60] performed experiments on the piezoelectric strain sensor based on graphene/epoxy materials (f-GnP) for SHM. The behaviour of the sensors was studied under successive tensile loading and incremental cyclic loading. From the results obtained, Fig. 3, it can be concluded that these composite sensors are effective for damage detection. From the graph obtained for tensile loading Fig. 3a, it can be seen that with increased stress, the piezoresistivity increases and the damage is indicated by the irreversible nature of curve. Fig. 3b shows the damage measured by incremental cyclic loading. It can be observed that during first two cycles of loading and unloading, the resistance increased and decreased linearly. But in the third cycle, the resistivity did not return to the original value. The irreversible nature indicates damage to the structure, i.e. the graphene epoxy structure has been damaged and hence the sensor reading is irreversible in nature.

The sensor used had a gauge factor of 45 with Young's Modulus and tensile strength of 2.2 ± 0.2 GPa and 80 ± 3 MPa respectively. These factors ensure good relative sensitivity and mechanical properties thus ensuring the use of the sensor in the field.

3.4 Cement based strain sensor (CBSS)

Neild et al. [67] conducted practical and theoretical experiments to conclude that for sensor embedded in massive concrete structure and sensor on the surface, the readings may vary. In order to extract the exact value of strain, concrete filled steel tubular (CFST) columns have been used for SHM of bridge piers, multi-storeyed buildings, etc [68]. The health diagnostic of these columns is difficult due to the surrounding steel tube. The traditional ultrasonic sensors or transducers can be used for the purpose, but the quantity required may be high. The Cement-based strain sensor (CBSS) is a type of high strength smart sensors used for health monitoring of Ultra-high strength concrete (UHSC) columns. Due to the cementitious nature, these sensors are bonded naturally with the parent structure [69]. This sensor detects damage by the piezoresistive effect, change in volume electric resistivity, with the help of a fractional change in resistance as in Eq. 3 [70]:-

$$\Delta R/R_0 = (R_x - R_0)/R_0 \tag{3}$$

$$R_x = V_x R/V_R \tag{4}$$

where R_0 is the initial resistance of CBSS and R_x is the resistance of CBSS during loading, V_x is the voltage measured across the specimen during SHM process, V_R is the voltage across the known resistor and R is the known resistance of the resistor.

For the piezoresistive phenomenon to take place, conductive materials, such as carbon fibers, carbon black or carbon nanotubes, have to be provided into the cement matrix. These materials enhance the electrical conductivity of the cement composites by a magnitude of order two [71]. Carbon fibers are economic with improved conductivity and mechanical properties and have proved to be useful for monitoring of traffic and cracks in asphalt pavement [72]. Carbon nanofibers (CNTs), which possess good mechanical properties and has good aspect ratio, can be used as reinforcing the cement sensors [73].

Oven dried CBSS, with 0.5% brass coated steel fibers, was used by Sun et al. [70] for the study of UHSC columns under cyclic loading of 60 MPa and 120 MPa. The compressive strength obtained for CBSS was greater than 120 MPa and less noise was recorded by piezoresistivity. The reason for using the oven – dried CBSS is because of its high sensitivity, making it easier to calibrate than the air-dried CBSS (Table 2). The test results show a good relationship as a strain gauge (Fig. 4 and Fig. 5). It the load case of 120 MPa, a difference between stress and $\Delta R/R_0$ can be observed at the bottom region (Fig 5b). This irreversible change in resistance indicates formation of micro cracks on the specimen. Therefore proper monitoring of UHSC can be performed using CBSS.

Azhari and Banthia [69] conducted experiments on the cement based strain sensors with carbon fibers (CF) and carbon nanofibers as the conductive material and compared the result with ordinary 10mm foil strain sensors for the cyclic compressive load. The data measured for the sensors were converted to electrical resistivity (Eq. 5):-

$$\rho = R\frac{A}{l} \tag{5}$$

where ρ is the electrical resistivity (Ω cm), A is the area of the cross-section (cm^2), R is the electrical resistance (Ω) and l is the length between inner electrodes (cm).

To apply the piezoresistive quality of CF cement based sensors, the load applied was compared with the fractional change in resistivity (FCR) in Eq. 6:-

$$FCR = \frac{\rho_t - \rho_0}{\rho_0} \tag{6}$$

where ρ_0 and ρ_t are the electrical resistivity before the test and at time t during the test respectively.

The samples were tested for load amplitude of 30 kN and load rate of 0.06 kN/s. The response of the sensor data points was measured for ordinary strain sensor and hybrid sensor. It was observed that the error margin improved while using the hybrid sensor.

3.5 Wireless strain sensor

The sensors normally used for monitoring are connected the central server via cable. This process is costly and may provide hindrance in data acquisition due to the surrounding conditions [74]. In buildings with complex designs, some structural members may remain inaccessible [75]. Also, the huge amount of data generated has to be arranged accurately which is a costly and challenging process [12].

With advancements in SHM techniques, building information modeling (BIM) along with radio frequency identification (RFID) based wireless structural condition assessment (WSCA) can be employed for such cases [76]. BIM is a universal virtual user interference and computing system adopted for SHM system, which can produce the structural data model of buildings and structures [77]. This system provides good results if it is adopted from the project design and construction phase of a structure. BIM can capture, organize, process and display the sensor data obtained from the structure [75]. The data obtained through BIM can be stored as a digital file and utilized by several applications [78]. This technology utilizes breakage-triggered (BT) strain sensors to detect the critical strain [79]. The BT sensors along with RFID tag can be utilized for wireless communication with BIM-based SHM software. The BT sensors are connected to the structure along with a crack-sensitive brittle bar with RFID tag. RFID antenna or reader is used to scan the RFID tag from a great distance and hence the damage location and information can be recorded. The RFID tag is activated only when the pre-set strain is surpassed in the brittle bar [75].

The use of wireless sensing technology along with Micro-Electro-Mechanical System (MEMS) has proved to be economical and effective and has been considered as a substitute of the conventional sensors [80].

Huynh et al. [81] used wireless sensors and implemented Stochastic Subspace Identification (SSI) analysis and Time-frequency Short Time Fourier Transform (STFT) method to analyze and update the structural parameters. The sensors were installed on a bridge and from the acceleration recorded, the modal parameters were found out. It was observed that with an increase in wind speed, the natural frequencies decreased due to the increment of flexibility and loosening of cables [82]. The modal parameters obtained were analyzed and updated using SSI analysis and STFT method [83, 84]. It was observed that the STFT method produced more significant wind inducted variations than SSI. Therefore, the STFT method can more suitable for computation of dynamic response.

The power source of the wireless sensors has to be recharged periodically. To avoid this process, solar panels and rechargeable battery were attached to each sensor for long-term monitoring process without any hindrance [81]. The system was a success during the sunny time. But at night or cloudy day, the power source is cut off thus compromising the system readings. Attaching solar panels to the sensors placed at the interior points of the structure was costly and complex [85]. Use of thermal energy was studied for an effective power source [86]. This method uses the temperature difference between the atmospheric air and bridge surface to harvest the power for the sensor. However, the temperature variation may be small which can hinder the power harvesting process. Another process investigated by the researchers is the radio frequency (RF) harvesting [87]. This method utilizes the radio frequency available in the atmosphere to recharge the sensor power source. In order to achieve this condition, the RF transmitters have to in close vicinity of the RF harvesters, in order to avoid rapid attenuation of transmission signals [86]. To avoid all these drawbacks, the mechanical or vibrational energy was considered for recharging the sensors. This method proved to be effective in case of bridges, in which the power was harvested during the high traffic and stored for later use [85]. This feat was achieved with the help of resonant vibration harvesters, where the resonant frequency of the harvester at the sensor point was adjusted to the modal frequency of the bridge [88-90]. This method cannot be broadly applied to the bridge as the resonant frequency varies from deck to deck [86]. Attachment of automatic tuning devices to the harvesters may also be used at the cost of a large amount of power or energy [85]. A piezoelectric based self – powered wireless sensor was developed to counter the above problems [91]. This sensor uses a series of memory cells to record the load history profile transferred to data logger system through piezoelectric effect as a voltage signal, which charges the sensor [92]. But the major drawback noted was that a part of data is lost in above process which may give insufficient result [93].

3.6 Acoustic Emission Sensor

With increasing importance of monitoring civil engineering structures, new technology has been developed, acoustic emission (AE), which can work under earthquake load of different frequency (20 kHz to 1 MHz). Acoustic Emission (AE) Method is an NDE method which uses highly sensitive AE sensors to measure the change in strain, mainly useful for detecting crack growth, detection of crack formation, corrosion, deformation and void formation [94]. This method works on the principle of detecting elastic waves due to changes in strain energy released due to change in structural parameters [95].

Though the method has been successfully installed for different structure; pipelines, bridges, and others, it faces problem due to atmospheric interferences, noise interference [96, 97]. Resonant type AE sensors having a narrow bandwidth can be used for such purposes. This type of sensors reduces the background noise created due to low frequencies and increases the accuracy of damage localization. The data acquisition for AE sensor is based on the principle of the threshold; i.e. if the signal level recorded by the sensor is greater than the pre-set threshold level, then the AE data is recorded by the sensor [97]. This data collected is the change in elastic waves occurring due to the newly formed damage. AE signals have high-frequency range having low amplitude. The AE signals are in form of the waveform and are recorded using techniques such as Wavelet Transform (WT) or Continuous Wavelet Transform (CWT) [98]. Single AE sensor approach may also detect the elastic waves from secondary sources occurring due to friction. In order to reduce this unwanted noise, AE sensors along with load-based or strain based sensors can be used [99]. The use of AE based Micro-Electro-Mechanical sensors (MEMS) along with strain sensor has been very commonly used in the detection of initiation and growth of cracks without the influence of friction [97].

Godinez-Azcuaga [99] performed a comparative study between wired and wireless AE sensor. The cumulative energy for both the sensors have been recorded (Fig. 6). It can be clearly seen that the energy required for the wired sensor was much greater than its wireless counterpart. The jump in the curves indicates the points where a sudden growth of damage has occurred.

AE for damage detection was used to detect the local damage in connections to a building under earthquake loads [100]. The data was collected using low-frequency sensor of band 25-80 kHz and the digital filter was used to reduce the undesirable high and low frequency. For seismic simulation, the noises considered to be present are mechanical noise from oil flow in the actuator, friction noise from connections which were minimized by adjustment of sensors. The damage index introduced uses the energy from acoustic signals (energy b-value (bϵ)) instead of amplitude.

$$\log_{10} \mathrm{N(AEE)} = \mathrm{a} - \mathrm{b}\epsilon \log_{10}(\mathrm{AEE}) \quad (7)$$

where AEE is the true energy of reconstructed signals, a is empirical constant and N(AEE) is the total number of signals reconstructed signals with energy higher than AEE. Reconstructed signals are used for calculating AEE; therefore the damage index calculated has little effect on secondary source and primary effect of concrete cracking. The sensor for interior connection and the exterior connection was tested for analysis (Fig. 7). It can be observed that the energy b-value reduces with the increase of peak acceleration. The decrease of energy b-value below 1 indicates severe damage to the structure, which has been cross-checked by visual observation.

Yapar et al. [101] studied the piezoelectric AE sensors for SHM on bridges and applied mathematical tools like artificial neural networks, wavelet transformation, and fast Fourier transformation to eliminate problems related to the prediction of the source, noise elimination, and source characterization respectively. The results obtained were compared with the results of theoretical AE signal measured by Moore et al [102] (Eq. 8).

$$V = V_0 e^{(-Bt) \sin \omega t} \quad (8)$$

where V_0, V, B, ω, and t are input signal amplitude, output voltage, decay constant, angular frequency and time.

The experiment was conducted to study steel beam and reinforced concrete beam and their comparative study with the predicted signal. The experimental results showed good agreement with the predicted signal having an average error of 1.97% and 1.574% respectively. But for practical use, the number of sensors employed has to be large in order to get accurate damage characteristics.

Saboonchi et al. [97] made use of capacitive MEMS AE sensors along with piezoresistive MEMS strain sensor and compared the damage detected with respect to piezoelectric AE sensor.

The capacitive MEMS AE sensor consists of two parallel plates acting as electrodes and separated by a dielectric material. The change in capacitance is calculated from the Eq. 9 [103, 104]:-

$$\frac{\delta C}{C} = \frac{\delta \varepsilon}{\varepsilon} + \frac{\delta A}{A} - \frac{\delta d}{d} \quad (9)$$

where, C = capacitance = $\varepsilon_0 \varepsilon_r \frac{A}{d}$

ε_0 is electric constant ≈ 8.854×10^{-12} $\mathrm{Fm^{-1}}$, ε_r is relative static permittivity of material between the plates, A is the area of plates facing each other, d is the gap between the plates.

Apart from capacitance, the other critical parameter considered for the design of MEMS sensor is the fundamental frequency of the sensor (Eq. 10)

$$f = 2\pi \sqrt{\frac{K_{mech}}{m}} \quad (10)$$

where f is the frequency, m is the mass of the system and K_{mech} is the mechanical stiffness.

The piezoresistive MEMS strain sensor works on the principle of resistance change Eq. 11:-

$$\frac{\delta R}{R} = \frac{\delta p}{p} + \frac{\delta l}{l} - \frac{\delta A}{A} \tag{11}$$

where ρ is the resistivity coefficient, A is cross-sectional area of the resistor and L is the length.

The MEMS sensors encounter a problem related to higher level of drift due to the influence of atmospheric thermal conditions [105]. This problem can be resolved by the use of the narrow window of sensor response [97].

4. Dynamic parameters measurement for SHM

The continuous and large structures, bridges and towers, mainly attract vertical forces, wind force, and have to be analyzed in the frequency domain for safety against dynamic loading [30]. In order to monitor the structures, the acceleration of the structure is monitored from which the frequency can be obtained. In order to achieve such condition, accelerometers have been used for diagnostics of bridges and tall structures.

4.1 Accelerometers

Much like the strain sensors, these sensors are the fundamental building blocks of an SHM system which can detect structural response and use the information for structural diagnostics [106]. A huge amount of data is generated by the acceleration sensors which increases the storage cost for the SHM system. In order to overcome this difficulty, data compression methods have been developed commonly named as compressive sampling (CS). Bao et al. [107] studied this system and concluded that CS using wavelet basis proved to be more effective than the Fourier basis system. In order to directly obtain the compressed data from the structure, various devices have been developed; Compressive wireless sensing [108], CS camera [109], CS analog-to-digital converter (ADC) [110].

4.1.1 Wireless Accelerometers

In order to detect a dynamic response, traditional electronic accelerometers were used for a long period of time. The accelerometers can measure three-way acceleration of a structure and are economic and can be easily installed [111]. These sensors are known to consume a lot of energy and limited resolution capacity [112]. To overcome these drawbacks, the wireless monitoring system has been used to which are economic and reliable for remote monitoring within the range of the sensor [111].

Kilic and Unluturk [112] have successfully validated the deflections occurring in a wind turbine with the help of wireless sensor network (WSN) and conventional accelerometers. The wireless monitoring process has proved to be effective for determining the threshold for wind turbine strength. Wireless sensors have the capability to detect the total vibrational frequencies generated by the wind turbine as accurately as the ordinary accelerometers [113]. These sensors have to be recharged periodically and they have to be in the range of computing system.

Wireless sensor technology measurement was validated using wireless and cable-based accelerometer SHM system on a highway bridge [114]. The wireless and wired accelerometers used were Silicon Designs 2012 accelerometer and Honeywell QA750 accelerometer respectively with sampling rate 100 Hz and 256 Hz respectively. The sensors were placed in 19 locations at the same level along the bridge with a maximum distance of 40 m. The 5s acceleration data obtained for location 6 and 10 has been shown in Fig. 8. It can be seen that the readings of both the sensor system totally match, indicating that wireless sensor system can be used for short-term SHM. The wireless sensor was packed in a waterproof box along with battery pack.

But these sensors come across interference from electromagnetic radiations, thus reducing the accuracy. To reduce this phenomenon, further research in this field has been conducted [112].

4.1.2 GPS Based Accelerometer

The geodetic monitoring system developed for monitoring of structure uses mainly global navigation satellite systems (GNSS) or global positioning system (GPS) [115]. This system measures the positions of monitored points in three directions for both dynamic and static cases and monitoring is done in frequency and time domain.

Monitoring of bridge with help of accelerometer has proved to be difficult due to low vibrational frequency, lower than 0.2 Hz [116]. Most of the accelerometers are unable to detect this low vibrational frequency [117]. In the recent time, wireless GPS sensors have been used to in place of cabled sensors and the measurements are taken under a clear sky in order to minimize the error due to obstruction. Handheld GPS has been used for kinematic point positioning. Also, dual frequency GPS receivers were used for damage detection. But these sensors faced problem to monitor the damage for various cases; a) satellite visibility, b) incorrect tropospheric delay, c) higher sampling rate for higher frequencies, 20 Hz [118]. In the recent advancements, the problem with sampling rate was sorted out by using GPS receivers of sampling rate 100 Hz and improving the signal collection [119, 120]. The monitoring of high rise structures with the help of GPS can be carried out with the help of RTK technology. This method uses a stationary checkpoint as reference station whose coordinates are pre-determined. This station records the difference between its known and its calculated position from the data provided by satellites. The difference in readings indicates an error which is sent to the rover. Rover is the GPS receiver whose position is tracked and the error information is used by the rover to improve the accuracy. If the two receivers are close enough, the error due to clock offset and atmospheric propagation delays can be ignored as errors are strongly correlated. GPS receivers can be used both for the static and dynamic status of the structure. The static status can be determined using short baseline test (SBL) and zero baseline test (ZBL) [121]. SBL is performed with help of two antennas having receivers on each of them, whereas ZBL is performed with the help of single antenna with an antenna splitter and two GPS receivers. For dynamic analysis, the GPS receivers have faced difficulties due to various effects such as data sampling rate, satellite coverage, multi-path effects, receiver noise, etc.

Multipath error occurs when the GPS receiver receives another signal from a duplicate satellite or a reflecting surface, thus inducing error in measurement [122]. A test up was made for GPS based monitoring system and study the multipath effect in a controlled environment using particle filter algorithm. It was concluded that the method was able to reduce the multipath effect significantly for the close reflector.

Differential GPS (DGPS) is an advanced instrument that has been used for the kinematic point positioning or real-time kinematic (RTK) measure. The error due to signal transmission is countered as DGPS uses two GPS instruments, one acts as the stable point (base) and the other is moved to obtain the different points with respect to the stable point (rover receivers). The accuracy of DGPS measurement was found to be 19.2% for horizontal movement and 28.78% for vertical movement [69]. The typical error accuracy for moving points of the structure was found to be 15 mm in the horizontal direction and 25 mm in vertical direction [122-124].

For monitoring of dynamic loads such as an earthquake, high-frequency sampling needs to be used. DGPS needs the base station to be stable for good data analysis. Therefore in case of an earthquake, this sensor is not suitable for measurement as the movement of the base receiver may include the noisy data [125]. In light of this event, Precise Point Positioning (PPP) is a new technique that has been developed. Precise Point Positioning (PPP) is a new technique for accurate positioning for dynamic applications [126]. The accuracy of PPP is around 2 cm in the horizontal direction [125]. This technique makes use of a moving receiver and the corrections are made using the data collected from a relatively large number of remote receivers operating permanently [127]. The limitation of GPS sensors is that a bulk number of observations have to be collected for high-frequency sampling. The use of GNSS-PPP using high rate GPS can be used to overcome this limitation [128].

In order to avoid the other inconsistent problems and to increase reliability and accuracy, an integrated sensor system was introduced. This system may contain GPS receiver, strain gauge, displacement transducers or accelerometers and has proved to increase the productivity of the SHM system [129]. For the integrated type sensors, extraction of structural dynamic properties has to be performed using a proper digital filter or bandpass filter, Chebyshev type digital filter [130].

Meng et al. [118] experimented the integrated sensor consisting of GPS and triaxial accelerometers on a suspension footbridge. The GPS receivers, sampled at 10 Hz, and triaxial accelerators, sampled at 80 Hz, were installed along the span of the bridge. The vertical acceleration obtained for damage event for re-sampled acceleration (10 Hz) and GPS are shown in Fig. 9(a) and Fig. 9(b) respectively. It can be observed from Fig. 9(a) that on the removal of forced excitation, the amplitude of acceleration reduced to 0 gradually, but the random noise of less than 1 cm amplitude was recorded in GPS measurement (Fig. 9(b)). Therefore GPS sensors proved to be more sensitive in detecting the low frequencies and hence more effective than the normal accelerometer.

Therefore integration of both RTK GPS sensor and triaxial accelerometers can be used for effective damage monitoring, as it can gather data for low sample rate (10Hz) and high sample rate (100Hz) respectively[131]. However for the system to work, absolute positioning of sensors has to be pin pointed in order to use an algorithm to integrate the sensors. Keeping the problem of sensor data integration, sensors with high data sampling rates were studied. JNS100 and Leica receivers showed a good sampling frequency of 50 Hz which is close to the normal triaxial accelerometers (80 Hz).

The other obstacle faced by the GPS sensor integration system is the accelerometer and GPS time series synchronization [132]. To avoid this mismatch of time series, a frequency based algorithm was devised to analyse the frequency values of accelerometer and GPS data to obtain the original vibration frequency of the structure. 7% error between the two sensor readings was obtained which was good for damage detection.

For detection of dynamic deformation, sensors such as, high frequency GPS/GLONASS receivers, tachymeters, inductive displacement sensors, code levellers and meteorological station have been set up. The accuracy of GPS/GLONASS receiver was noted as accurate within 2cm and the tachymeter and displacement sensor accuracy was recorded to be within ± 1 mm. Therefore this integrated GPS sensor system was effective for SHM [133].

4.1.3 Micro-Electro-Mechanical System (MEMS) Accelerometer

With the improvement in technology, the researchers are focussed on developing Micro-electro-mechanical systems (MEMS) accelerometers based on the working principles of capacitive, piezoelectric and piezoresistive accelerometers [106, 134]. But only capacitive and piezoresistive accelerometers are used in the modern world. Though piezoresistive accelerometers are more sensitive in high-frequency bands, the capacitive based MEMS accelerometer is popular due to the temperature coefficient problem with the former [80, 135]. The key parameters for the effective design of an accelerometers sensor are deflection, stress sensitivity and resonant frequencies [136]. Accelerometers have sensitivity inversely proportional to the square of first resonant frequency [136, 137]. Accelerometers are mainly designed for sensing high frequency, hence having low sensitivity. But the natural frequency of a structure is less than 100 Hz which cannot be detected by the traditional MEMS accelerometers [106, 135]. In most of the cases, the ambient vibrations occurring in the structures have a small value of g, low amplitude, except for earthquakes having 1-2 g [138]. The readings of these accelerometers are mainly affected by thermal noise caused due to piezoresistors and due to thermal agitation in sensing structure [139]. Therefore MEMS accelerometer with small bandwidth and simple signal conditioning electronics has been designed to improve the sensitivity as well as the power consumption and has ultra low floor noise [137]. This technology can be efficiently used for wireless sensor networks [140].

A study has been performed by Kavitha et al. [136] to compare the performance of piezoresistive MEMS accelerometers and capacitive MEMS accelerometers (Fig. 10) with respect to frequency and deflection sensitivity. It was observed that the capacitive sensor has a response range of 0 – 20 Hz and very low floor noise, hence is suitable for low-frequency acceleration in SHM as well as seismic applications. A brief comparison has been made with that of the available Commercial Off-the-shelf technologies (COTS) accelerometers with the piezoelectric and capacitive accelerometers [141, 142] as shown in Table 3. The capacitive and piezoresistive MEMS sensors proved to be superior to the other sensors used.

Kavitha et al. [137] designed two ADXL series MEMS accelerometers with comb finger type differential capacitive MEMS structure [143], Device A for low-frequency ambient vibrations and Device B for earthquake applications. The capacitive accelerometers are simple in design and have low drift, good sensitivity and noise performance [144]. The performance of both the devices was compared with other MEMS accelerometers widely used (Table 4) [145, 146]. It was noted that Device A provided good noise performance. Device A and Device B proved to have good voltage sensitivity and excellent noise immunity which makes them suitable for SHM and seismic applications respectively.

5. Corrosion Sensors

Another type of damage analysis in case of damage failure is due to corrosion in structural rebar steel [147]. In the case of corrosion, the first time corrosion detection is done directly by determining the thickness of rust layer [148]. The main source of corrosion is due to chloride contamination [149] and change in pH value [150] inside concrete. A number of corrosion detection techniques have been experimentally invested such as; polarization resistance technique [151], Impedance Spectroscopy [152], galvano-static pulse transient technique [153]. However these techniques, in the laboratory have been tested for gradual corrosion and the area of steel was fixed. In the field these techniques posed a problem as corrosion in real life is not gradual.

Embedded sensor such as piezoceramic lead zirconate (PZT) transducer, which uses acoustic emission (AE) technique, has been used for corrosion monitoring of reinforced concrete structure [31, 154]. These sensors use ultrasonic waves to indicate different stages of rebar corrosion [155]. The embedded sensor can be installed at the time of construction, therefore corrosion monitoring of existing structures is not feasible. The surface bonded embedded PZT sensors were compared with embedded PZT sensors for corrosion detection. The surface bonded sensor was able to detect progression of sensors and the embedded sensor was able to detect early stage of rebar corrosion, mainly the percentage of stiffness loss [156].

Likewise various sensor configurations were used for corrosion detection. One among them is the galvanic couple, which makes use of macrocell as cathode and rebar or macrocell as the anode, and the macrocell current measurement can be used for evaluation of corrosion rate [157]. The corrosion rate using macrocell measurements was successful in proving information about passive and active corrosion. However in practical implementation, this sensor faced problem due to interference of environmental wet and dry cycle and electric resistance to concrete [158]. In order to improve the measurements, steel/copper galvanic sensor has been used which provides good corrosion rate of steel bar in concrete [159]. Another sensor configuration is the use of capacitive transducers (CT) which works on the principle of non contact based corrosion detection. This sensor uses two capacitance electrodes on both sides of rebar to detect corrosion as well as the thickness of rust on rebar due to corrosion [148]. The sensor was effective for thick rebar and was also able to detect clean steel from corroded steel.

Printed Circuit Board (PCB) based corrosion sensor was designed which can resonant frequency variation of couple coil resonator to detect corrosion [160]. The difference in resonant frequency can also be detected using wireless sensors at the early stage of corrosion detection [161]. Based on the principle of wireless sensing technology, RFID based corrosion sensors embedded in the concrete have been able to detect the chloride concentration change in concrete [162]. The sensor can be used for long term using small amount of power from Radio Frequency (RF) signals [163].

6. Multiple Damage Detection

The techniques discussed above all deal with detection of a particular type of damage i.e., strain, temperature, acceleration or displacement, etc. The application of all the sensors at a particular structure is not feasible. Therefore the need of sensor that can detect multiple damages was strongly needed. In light of this event sensors based on fiber optic principle was developed which can be utilized for multiple damage detection [33].

6.1 Fiber Optic-Based Sensor

Most of the traditional sensors are attached with the help of cables. These cables over a long distance may suffer from electromagnetic interference (EMI). To overcome this phenomenon, Fiber Optic sensors have been introduced for SHM. The advantages of Fiber Optic based sensor over traditional sensors are that they are lightweight, corrosion resistant and durable. These sensors are immune to electromagnetic and radio interference, due to dielectric materials, thus making them suitable for monitoring metal structures even for small length, 2 micron, with high precision [33, 164]. The fiber optics sensors are also versatile and the same optical fiber sensor can be used for measurement of multiple parameters; humidity, temperature, pressure, displacement, acceleration, magnetic flux and pH value. Therefore the need for multiple traditional sensors is reduced [34]. These sensors are small in size, low cost and low power consumption [165]. Optical fiber consists of a) core, a thin glass fiber, b) cladding, that confines the propagation of light within the fiber core and c) protective coating, which provides mechanical strength and absorbs moisture (Fig. 11) [166]. The basic material of this sensor is silica which can withstand high temperature up to 1000^0C and low temperature of less than 4K, suitable for vacuum condition with good fiber coating and resistant against radiation as the core of pure silica can stabilize the change of refractive index due to radiation [167]. Three technologies of fiber optics present are; point sensor (Fiber Bragg Grating (FBG) sensor) [168], long gauge sensor or quasi-distributed sensor (multiplexed Fiber Bragg Grating sensors) [169] and fully-distributed sensor (Brillouin Optical Time Domain Reflectometry (BOTDR) and Brillouin Optical Time Domain Analysis (BOTDA)) [170]. Out of these sensors, point sensor; Fiber Bragg Grating (FBG) sensor, is mostly used for practical monitoring of structures [171].

6.1.1 FBG Sensor

The Bragg gratings operate by acting as wavelength selective filter that can reflect single particular wavelength, Bragg wavelength, and transmit the other wavelengths (Fig. 12) [166]. For the FBG to function, it is illuminated by a bright light source and the measurements are taken due to the change in wavelength of reflected light [172].

The Bragg wavelength is given as:

$$\lambda_B = 2\Lambda n_{eff} \tag{12}$$

where n_{eff} is the mean refractive index of the core and Λ is the grating pitch.

The installation of FBG to a structure is a major hindrance. They can be attached to a structure by the process of adhesive bonding, mechanically attached and welding [173]. The process of welding of sensors to the structure can alter the chemical properties. Therefore this process is not favoured in the practical field [174].

The major disadvantage of these sensors is that they are fragile [175]. Being fragile, the FBG sensor has to be encapsulated properly before installing it on structural element [176]. The protective system provided for the FBG should be such that it can: a) withstand harsh environment during the construction stage, b) isolation of the sensor so that it might withstand physical shock or pressure and keep the sensor intact, c) in-penetrable to moisture and d) resistant to chemical attacks. Ngoi et al. [177] used cylindrical silicone rubber tube to embed the FBG, which proved to be effective in detecting lateral loads. The silicone rubber tube packed FBG sensor has high Poisson's ratio, low elastic modulus and is thermally stable in the range -100 to 320^0C [171]. Dawood et al. [178] used vacuum infusion technique to embed the FBG sensor between cross-ply laminate of GFRP sandwich material and foam core. This arrangement is useful for microscopic sensing of localized defects at an early stage under dynamic and static loading with great accuracy. Chung and Kang [179] used a technique to embed FBG in steel rebar and bond it with adhesive to the rebar. This is an easy technique than vacuum infusion but the accuracy of strain measurement has to be verified.

The FBG sensors have to be attached to the structures with the help of adequate adhesives, failing to which errors due to temperature, insensitivity and loosening might occur [180]. For long-term monitoring, adhesives with higher service life such as epoxy and acrylic type adhesives are preferred. For short-term and dynamic monitoring, fast cure adhesives like instant cyanoacrylates adhesives are used [172]. The adhesives commonly used to attach the sensor to the structure are cyanoacrylate C2 and epoxy NM BPE Lim 465 [181]. It has been experimentally observed with the help of modified fibre pull-out test that cyanoacrylate can withstand higher failure load than epoxy glue [181]. It was observed by Torres et al. [166] that the presence of packaging material below the sensor can cause errors in reading. For new structures, the FBG can be embedded into the structures during construction phase without any alteration in structural properties [171].

Moyo et al. [175] compared the tensile test of steel rebar and static test results of concrete beams for strain measurement between FBG sensors and electrical resistance strain gauges (ERS). The FBG sensor was packed between two layers of carbon composite material. The tensile test result shows good correlation between the strain measurements of two sensors. The static tests of the concrete beam were conducted on top and bottom parts at mid-point and the results show good linearity between the two sensors. The system had a sensitivity of 1 με and accuracy of 5 με. Thus it was noted that FBG can be used for effective strain measurement. For dynamic loading, the ERS and FBG showed a maximum strain of 58 με and 55 με respectively.

For effective diagnostic of structure, the sensor used should be sensitive to only one parameter. But a bare FBG sensor is sensitive to pressure, strain and temperature. Therefore while measuring strain; it may also detect strain due to thermal variations [175]. In order to minimize this cross-sensitivity, measurement at two different optical modes for which temperature and strain responses are different [182]. A method was developed to measure the strain and temperature with the help of thermochromic material and FBG sensor. The variation of strain was measured with the help of FBG sensor, and the temperature was measured by the change in optical power reflected by the thermochromic material. This complex technique showed good results but limited measurement range [183].

The change in strain and temperature can be identified with the change in wavelength of the FGB [184]:

$$\frac{\Delta\lambda_B}{\lambda_B} = P_e\varepsilon_{zz} + [P_e(\alpha_s - \alpha_f) + \zeta]\Delta T \tag{13}$$

where α_s and α_f are coefficients of thermal expansion of structural material and optical fibre respectively, ζ is the thermo-optic coefficient, ε_{zz} is the axial strain and P_e is strain-optic coefficient.

The effects of temperature, strain and pressure can be modelled by the following equation [175]:

$$\Delta\lambda_B = K_\varepsilon\varepsilon + K_T\Delta T + K_P P \tag{14}$$

where K_ε, K_P and K_T are the coefficients of wavelength sensitivity to strain, pressure and temperature respectively [171].

$$K_\varepsilon = \left[1 - 0.5n_{eff}\left(\rho 12 - \nu(\rho 11 - \rho 12)\right)\right]\lambda_B$$

$$K_T = [\alpha + \xi]\lambda_B$$

$$K_P = \left[-\frac{1-2\nu}{E} + \frac{n^2}{2E}(1-2\nu)(2\rho 12 + \rho 11)\right]\lambda_B$$

where ρ11 and ρ12 are components of fiber optic strain tensor, n is the refractive index of fiber , ξ is fiber thermo-optic coefficient, α is the thermal expansion, ν is Poisson's ratio of fiber and E is Young's Modulus. For wavelength of 1.55 μm, parameters K_e = 1.15 pm/με, K_P = -3.0 pm/MPa and K_T = 11pm/^{0}C remain constant for bare FBG. But the sensitivity coefficients may vary for different OFBGS. Therefore calibration has been to do for individual sensors before installing [185]. It has been observed that for 1^{0}C temperature shift, change in Bragg wavelength is approximately 10 με.

For the measurement of both strain and temperature, a new technique was introduced by the use of optical Fiber Bragg Grating Sensors (OFBGS). In order to protect the bare OFBGS against breaking while installation, they are encapsulated in glass fiber reinforced polymer (GFRP) [186]. With the integration of GFRP bar with OFBGS, the sensing properties, as well as the mechanical properties of the sensors, were found to increase.

The use of distributed FBG sensor in case of bridge monitoring has been very common. In case of bridge monitoring, a number of algorithms have been developed to check the status of the bridge under heavy vehicular loads. These methods make use of strain sensors for measuring the change in strain and then processing the measured data for damage analysis [187]. However, the analysis of data for sensors far away from the damaged area gave false results. The use temperature induced strain from the measured strain data to detect an abnormality in the bridge was used [188]. A Euclidean distance-based damage index method is defined which uses temperature variation and temperature induced strains to detect damage in the structure. This method can be used for long-term monitoring of bridges as stiffness reduction for multiple damage locations can be measured. However, the limitation of this method was that the visual inspections need to be performed for damage of other types as a reduction in stiffness does not occur due to damages such as corrosion.

In order to develop a method for damage location in multiple locations of a structure, the Wind And Structural Health Monitoring System (WASHMS) was used for study in Tsing Ma Bridge [189]. This system uses eight types of sensors such as temperature sensor, dynamic strain gauge, GPS, servo-type accelerometer, anemometer, level sensing stations, displacement transducers and dynamic weigh-in-motion stations for continuous monitoring of loads, structural responses and environmental factors [190]. In order to reduce the number the sensors, multi-purpose sensor such as FBG sensor can be used for analysis owing to its good strain sensing and easy surface mountable property. The measurement result of the FBG system showed good agreement with the dynamic strain recorded on the traditional resistive strain gauge over variable temperature changes [191]. Similar study was conducted on Lezíria Bridge in order to validate the FBG sensor response with conventional strain sensors and FBG proved to be a more robust for strain detection [192].

Newly designed SHM module consisting of wireless sensor network was used on the Jiubao Bridge [193]. The sensor module included several self – devised FBG sensors which were used for strain, tension, and temperature measurement. Other sensors such as an accelerometer, displacement transducers were also a part of the sensor system. The data was transmitted to the workstation via the internet. The strain sensors are embedded in the deck and placed on the surface for measurement. Temperature sensors were placed steel girder, concrete slabs, and arches. The temperature at the middle span of bridge deck was monitored. It was seen that a distinct difference in temperature was observed for top and bottom deck, the top deck being at a lower temperature than the bottom, thus measuring the temperature change in the bridge. The strain data was collected from the FBG strain gauge and the data were combined into average power spectral density. The identified frequency was similar to the results obtained from the 3D FE model. This result verifies the reliability of the monitoring system.

The monitoring of bridge was performed using distributed fiber optical sensors. These sensors are good for measurement of strain in the bridge and measure the change in stiffness for damage identification, locating the damage and measure the extent of damage [194]. Strain influence line theory was the primary proposed method for vehicle load identification, however, the traditional strain gauge was able to obtain readings for local damage [195]. The method was tested on a model bridge having a biaxial model vehicle load and long gauge FBG sensors for measuring strain. The long gauge FBG sensor is made to prevent from the harsh environment with the help of basalt-fiber-reinforced polymer. The model was tested for damage identification both for the analytical model and experimental model. The location and extent of the damaged element were identified with the help of long gauge FBG sensors and the result was not affected due to the velocity of the vehicle. As the initial condition of the bridge is not known, equivalent damage extent is implemented to assess the condition of the bridge. This value is based on the average value of long gauge stiffness coefficient of intact elements. The other two damage extent defined are designed damage extent, based on the variation of the moment of inertia and ideal identified damage extent, which is based on the stiffness coefficient of intact state. For double damage detection, equivalent damage extent is considered as the reference to evaluate the condition of the bridge. The experimental and analytical result for the damage coincides to prove that the proposed long gauge FBG sensors are effective for damage detection.

6.1.2 Fiber Optics Sensor

Fiber Optics Systems (FOSs) use fibers as the signal transmission medium and sensing element over long distances [171]. The FOSs includes Fabry-Perot (FP), Surveillance d'Ouvrange par Fibre Optics (SOFO), and Brillouin sensors [174]. These FOSs are flexible, multiplex, versatile and cost-effective [196].

The FP sensor is an interferometer which uses multi-mode fiber, a simple and economic technology, and can be made temperature self-compensated by taking into account the thermal expansion of the host material. Therefore the strain readings recorded by the sensor is only due to stress-induced [197]. This sensor uses Michelson fiber-optic interferometer arrangement in which one fiber is prestrained (0.5%) and attached to the host structure to act as a sensing arm. The other fiber, reference fiber, is laid close to the previous fiber parallelly so that the temperature variation between the two is negligible [196]. Both the fibers are installed in a tube. The difference in length of the two fibers gives the measurement of strain induced due to compression or tension [198]. SOFO system makes use of an additional broad light source, LED, for damage identification [174]. This configuration is known as low-coherence double Michelson interferometer [199]. The first interferometer is the pair of single mode fibers as the previous sensor. The second interferometer consists of a scanning mirror which with the help of light source (1.3 microns of LED) can detect the difference in length between the two fibers. The stability and precision obtained by this sensor is 2 micron [199]. The data acquisition is performed at an interval of 7s and the dynamic range of measurement is from -0.5% to 1% [164]. Brillouin sensors, BOTDR AND BOTDA, uses Brillouin scattering which is produced due to non-linear interaction of acoustic waves and light. Brillouin Scattering effect may also be defined as the phenomenon which is stimulated when there is a frequency difference between pump pulse light and wave light propagating in the FOS matches with the local Brillouin frequency of fiber core [200]. The relation between light frequency and strain is given by Eq. 15 [201]:

$$\nu(\varepsilon) = \nu(0)(1 + C_\varepsilon * \varepsilon) \tag{15}$$

where $\nu(\varepsilon)$ is Brillouin scattering frequency due to change in strain, C_ε is a constant coefficient due to change in strain, $\nu(0)$ is the reference frequency.

This phenomenon induces small dynamic change, due to change in strain and temperature, in the fiber core refractive index [202]. Therefore, the Brillouin frequency can measure both strain and temperature along the fiber. The only drawback of using FOSs is that they are fragile and has to be installed with extra care [174].

The most economic arrangement of FOS for a bridge is tree pattern with one main cable along with different branches of the optic fiber. This arrangement also helps in multiplexing as the system can incorporate a large number of sensors using only one demodulation system [174].

Uva et al. [164] made use of SOFO sensors to evaluate the health condition of the beams of a bridge. Each beam was fitted with 6 SOFO sensors coupled with 6 thermocouples. The thermocouples were installed to evaluate the change in strain due to temperature change in the beams. The experimental value of strain variation was calculated for time t_1 and t_2 from Eq. 16 and 17 respectively, taking the length of measurement fiber L_S as 300 mm.

$$\Delta\varepsilon_{EXP}(t_1) = \frac{m_s(1)-m_s(0)}{L_S} \tag{16}$$

$$\Delta\varepsilon_{EXP}(t_2) = \frac{m_s(2)-m_s(0)}{L_S} \tag{17}$$

where $m_s(0)$ is the strain measured at the launching of the beam in time t_0, $m_s(1)$ is the strain measured at time t_1 after completion of slab and $m_s(2)$ is strain measured at time t_2 after completion of the bridge. The graphical interpretation of the theoretical and experimental results has been shown in Fig. 13. The structural integrity is obtained from the comparison between the two curves. The red zone shows the data above the predicted strain which indicates an unaccounted phenomenon, i.e. the strain level is above the predicted safety zone.

Hong et al. [201] used the BOTDA based FOS to study the strain inducted in H-piles during pile driving process. The experimentally measured strain data was verified with the theoretical model developed by Misra and Chen [203]. It was observed that most of the data collected from the FOS match with the predicted data. Therefore the BOTDA based FOS can be adopted for practical use.

6.1.3 FBG based Accelerometer

In order to overcome the drawbacks of normal or wireless accelerometers, advanced Fiber Bragg Grating (FBG) based accelerometers have been introduced. These sensors provide immunity against electromagnetic interference, can be monitored from a remote location and is suitable for embedding into the structure [34, 171].

Antunes et al. [30] used this technique for SHM of a tower for bi-axial sensing. The discrepancies or the difference in frequencies obtained are due to the overestimation of stiffness or mass distribution in numerical process. Therefore, the FBG biaxial accelerometer can be used effectively for SHM process.

6.1.4 FBG as Corrosion Sensor

Most of the corrosion sensing techniques require direct contact with the steel rebar for detection which is always not possible. Fiber Optics Sensors have been advantageous for corrosion detection due to its low cost, high resistance to fracture and easy termination [204]. These sensors can be embedded easily with good protective cover and the sensor changes its fluorescence intensity with the change in pH [205]. These sensors, being immune to electromagnetic interferences, have got an upper hand to the normal embedded sensors which are susceptible to external electric field and temperature fluctuations [206].

The FBG sensor for corrosion detection has been tested for without any coating and with Polydimethyl Siloxane (PDMS) coating [207]. The change in strain due to corrosion is sensed by the FBG sensor. The sensors were embedded in concrete for testing. The FBG sensor with PDMS coating was observed to detect corrosion at a more early stage than that of the uncoated FBG. The PDMS coating being soft and thin, acts as a media for transfer of corrosion strain to FBG sensor for detection [208]. Whereas, the uncoated FBG sensor needs the rust to be in close contact with the fiber so that wavelength shift is detected due to early corrosion. However the PDMS layer has a low Young's Modulus which may affect detection in long term [209]. Also the PDMS layer may absorb chemicals in concrete, which may affect the damage detection [207]. To avoid this reaction of the FBG coating layer, a pH-sensitive hydrogel was mixed with the PDMS coating [210]. This coating is used mainly in humid region where the hydrogel layer is pH sensitive and PDMS is strain sensitive [208, 211]. The mixed type coated FBG sensor showed monotonic relation between wavelet shift and corrosion process which makes it a robust corrosion detecting sensor.

The comparative study of different types of strain, acceleration, corrosion and FBG sensors depending on their type, material used, damage detection type, working principle, advantages and limitations have been tabulated in Table 5.

7. A comparative case study among different sensors

7.1 Strain Sensors

It has been observed that normal metallic thin foil strain gauges are unable to measure dynamic strain more than 2000με for 10^6 alternating load cycles [56]. Introduction of optical strain gauges has shown great potential in the measurement of large dynamic strains. They can resist large strains and alternating loads [212]. Experimentally it was seen that optical strain gauges were able to resist alternate loading strain of magnitude ± 1000με for 10^7 loading cycles [213]. But in the practical field, these sensors were not able to provide a significant advantage over the traditional sensors for dynamic loading. Also, the sensors are costly and the power consumption may pose a problem for wireless monitoring [214].

Neild et al. [67] conducted practical and theoretical experiments to conclude that for sensor embedded in massive concrete structure and sensor on the surface, the readings may vary. Sreeshyiarn et al. [215] introduced temperature calibration factor for the embedded sensor as 2.19 $\mu\varepsilon/^0$C and for gauge mounted on the surface as 4.32 $\mu\varepsilon/^0$C. However, they also expressed the need for individual calibration test for each VWSG due to the varied thermal expansion of concrete. A comparative experimental study was conducted by Ge et al. [53] on an RCC beam to investigate the effect of temperature change in different strain sensors; conventional foil electrical resistance strain gauge (ERS), Vibrating Wire Strain Gauge (VWSG), FBG sensor and distributed Brillouin backscattering optic fibre (FO) sensor. The theoretical strain for the beam was calculated considering the thermal expansion coefficient for concrete as 11 $\mu\varepsilon/^0$C [216]. The strain results obtained from the different sensors are being compared with the theoretical strain calculation. Two conditions were maintained during the experiment; (1) the beam is kept in an insulated chamber with temperature change from room temperature to 40^0C by increments of 1^0C (Fig. 14); and (2) the temperature was applied only from above, keeping the bottom part open to ordinary temperature, thus creating temperature gradient (Fig. 15 (a) – at top and Fig. 15 (b) – at bottom). It can be clearly observed that the VWSG has got an upper hand against all the other sensors for measurement of average strain due to dynamic change in temperature. ERS proved to be unreliable for this case study. FBG showed 4% difference the actual strain. This difference can be solved by calibrating each FBG sensor instead of considering an average temperature coefficient. As for FO sensors, it was observed that the measurements were inconsistent, having a difference of 5^0C with the theoretical value. However, it has been observed that for long-term monitoring, where the temperature change is not sudden, FO sensors have been effective.

Costa and Figueiras [174] experimented the static behaviour of a simply supported beam with the help of electric strain gauge (ESG) and fiber optics of length 4cm and 10cm. A maximum load of 60kN has applied in a pair 50cm apart. The FO was protected by polyester sheet and attached with the help of epoxy resin adhesive. In the two cases, the performance of ESG was compared with; (a) FOS of 4cm length and (b) FOS of 10 cm length (long gauge). Differences in strain observed between the two sensors for the first and second case were 20% and 1.5% respectively (Fig. 16 (a) and Fig. 16 (b)). Therefore it was concluded that FOS with 10 cm length can be used for practical use. The researchers also carried out experiments on a steel specimen for determining the efficiency of FOSs in determining strain due to change in temperature. The theoretical strain was calculated using Eq. 18, taking Δp and $\Delta\varepsilon$ as 0 and α_M as $10^{-5}\ {}^0C^{-1}$ [175].

$$\Delta\lambda_B/\lambda_B = P_\varepsilon.\Delta\varepsilon + [P_\varepsilon.(\alpha_M - \alpha_F) + \zeta].\Delta T + G_P.\Delta p \tag{18}$$

where $P\varepsilon$ and ζ are the coefficients of strain and thermo-optic of the FO, G_P is the gain factor for pressure and α_M and α_F are the thermal expansion coefficients for host material and fibre respectively. The test was conducted with the help FOS and resistive thermometer for one temperature cycle ranging between 30^0C and 60^0C. It was observed that the theoretical and experimental strains were exactly the same for the steel specimen (Fig. 17). Therefore the FOS along with the protective cover provides no hindrance to the measurement of strain in different cases.

The efficiency of strain measurement for sensors, carbon nano tube strain sensor, quantum piezo-resistive interphase sensor (sQRS), AE sensor and DIC sensing technique has been studied by Chowdhury et. al. [217] for incremental cyclic loading. The loading were considered for four cycles (Fig. 18) in which the first cycle of damage applied is a classic curve indicating micro cracks [218]. From second cycle loading, the damage curve indicates deformation due to overloading causing damage such as micro cracking, matrix friction or fibre breakage [219]. Finally the stage of ultimate failure is shown in the linear part. In the whole process, the measurement of strain due to damage by sQRS (S_h), AE sensor and DIC sensing technique ($_{\text{ch Armis}}$) were well in agreement.

7.2 GPS sensors

A comparative study was performed for GPS receiver and laser displacement meter against servo-type accelerometers [220]. It can be observed that from Fig. 19, GPS receiver measure the same acceleration data as that of the accelerometer thus proving a good measurement unit.

A comparative study of DGPS and PPP has been performed on a beam under dynamic behaviour to find out the efficiency of the methods [128]. The time series of the DGPS and PPP derived horizontal displacements along with the Fast Fourier Transformation (FFT) has been shown. It can be observed from Fig. 20 that the frequency and displacement results are almost similar stating that PPP can be used efficiently as an alternative to DGPS method.

8. Optimum Sensor Placement (OSP)

Sensors are the electronic devices which are installed on the structures to obtain detailed information on the strain, stress, acceleration, deformation, etc. these data obtained are utilized for the vibrational measurements and structural health monitoring (SHM) [221]. The main factors for data acquisition using sensors are a number of sensors to be placed to the available sensor network and the source of power for the sensors to work [35]. However, the issue of sensor placement draws the attention of different researchers. The sensors installed in the structures are permanent. Due to the design of complex structures, the placement of sensor is difficult. Hence the cost of data acquisition is higher [222]. The problem of sensor accessibility is reduced with the introduction of wireless sensors. However, their application is limited due to the problem of energy source and time synchronization.

The sensor locations were usually determined from the past experience and knowledge of the vibration occurrence. In many health monitoring situations, there was a need for analysis of the measured data to obtain the result of unmeasured parts [221]. There are two types of error: false positives, which denotes false damage to the structure, and false negatives, in which the damage is missed [35]. Therefore optimal placement of sensor is necessary for higher accuracy.

Some of the recent sensor placement methods used are techniques based on Fitness Function approach [221], Bayesian Approach [35], Monkey Algorithm [223, 224], Frequency Effective Independence Approach (FEfi) [222], Distributed Wolf Algorithm [225], Fisher Information Matrix (FIM) norm [226] and Iterated Improved Reduced System (IIRS) method [227]. The advantages and disadvantages of these methods are tabulated in Table 6.

9. Discussion

The comparative study of the performances of some advanced sensors for SHM has been studied. The performance of the sensors supplemented by advanced technology has been discussed as follows. The comparison of the sensors studied has been given in Table 5.

- One of the basic methods for damage detection is non-contact method which makes use of the high-resolution camera to capture images of cracks. These technique makes use of vision-based displacement sensors are digital image correlation (DIC), pattern matching. These images are then superimposed with known templates to determine damage pattern. The method is simple and effective as it requires no extra information about the mode shapes and frequency. However, the environmental factors such as surrounding light, the angle of elevation of the camera and hindrances like fog can cause a problem in acquiring the damage pattern image. A similar method was performed using video-based damage detection.
- The metallic thin film strain gauge has been tested with respect to the theoretical value of strain obtained. The modification made is the introduction of elastic shunt sheet along with the strain gauge to measure dynamic strain. The method showed 11.5% strain overestimation in theoretical value. Also, complexities were faced as the height of the shunt columns were not taken into consideration. Thus improvement in the shunt column design was mandatory for its practical field application. Also the measurements of strain sensors are effected due to electromagnetic interference which may causes distortion in the final result.
- The use of piezoelectric materials in the strain sensors have been a common choice for the researchers. These materials provide immunity to electromagnetic interference which the normal strain sensors are vulnerable to. The thick film ceramic strain sensor is an economic and reliable piezo-based strain sensor with good sensitivity or gauge factor. As compared to other piezo materials, ceramic is shock and corrosion resistant with high elasticity and can operate at high voltages (2kW) and high-temperature range (-20^{0}C to 800C). The drawback of this sensor is that it has to be calibrated for change in atmospheric effect, which is not always feasible.
- The traditional strain sensors used were bulky and had cabled connection. The need for lightweight sensors and wireless sensors were in great demand for improved SHM method. PZT sensor based on carbon nanomaterials was tested and was found to possess good mechanical properties along with high sensitivity which ensured damage detection. These sensors can also be for reinforcing the cement based sensors embedded in the structures.
- To overcome the restrictions due to cabled sensors, wireless sensing technology collaborated with the strain sensors. The technologies commonly used are radio frequency and MEMS. Though these sensors are reliable for damage identification, the power source of the sensors

has to be recharged periodically and the receiver has to be in the range of the sensor. Various solutions have been proposed for self- recharging of the sensors. These include RF harvesting, solar power harvesting, resonant vibration harvesting and piezoelectric-based self-powered sensor. These sensors have to be placed according to the suitable atmospheric conditions.

- The use of AE sensors, which work on the principle of detecting elastic waves due to the difference in strain energy released, have been introduced for structural diagnostics. This method is effective for damage occurring due to crack formation. These sensors also use the piezoelectric, MEMS technology for damage detection. These sensors proved to be effective even for damage detection due to low amplitude and the MEMS sensors provided higher efficiency with lower power consumption. The MEMS sensors have a problem with high drift due to atmospheric thermal conditions, which can be rectified using the narrow window of sensor response. Also, structures under dynamic loads, such as that of the earthquake, can also be determined with the help of AE sensors.
- To measure the dynamic properties of a structure effectively, accelerometers have been used. This sensor provides information about the change in structural parameters due to dynamic loadings, wind load or earthquake load, by measuring the change in acceleration. A wide range of accelerometers have been introduced for SHM; electronic cabled, wireless, GPS based, MEMS. The accuracy of wireless accelerometers has been seen to reduce due to electromagnetic interference.
- GPS based accelerometer showed the good response for detecting damage with low vibrational frequency. But these sensors faced problems due to the high sampling rate and satellite visibility. To avoid this problem, integrated type sensor; strain gauge, GPS receiver, and accelerometer, the arrangement has been used to increase the productivity of the SHM system. The high sampling rate can also be countered with the use of DGPS and PPP which can be used for real-time kinematic measure.
- MEMS accelerometers, working on capacitive and piezoresistive principle, have proved to be effective for the wireless sensor network. These sensors have small bandwidth and ultra-low floor noise, thus improving the sensitivity and power consumption. The voltage sensitivity and noise immunity make them suitable for normal SHM and seismic applications.
- Corrosion sensors can be embedded in the concrete for detection of early stage corrosion. The PZT sensor, which uses AE waves, can be used as surface embedded sensor for detection of corroded rebar in concrete. Galvanic couple, which uses cathode anode configuration, can be used as corrosion sensors because of their high sensitivity. However these sensors are also sensitive to environmental climate change. RF signals based corrosion sensor can also be used for wireless corrosion monitoring.
- Fiber Optic based sensor is the new technology sensor which possesses multiplexing quality. This sensor can be utilized for detection of temperature, humidity, pressure, displacement, acceleration, pH value and magnetic flux. There are three types of sensor included under this technology; FBG sensor, multiplexed FBG sensor and FOS sensor. These sensors are versatile, cost-effective and proved to be a good detector of damage.
- FP, SOFO, BOTDA and BOTDR comes under the FOS. The FP and SOFO systems are of a similar kind except that in SOFO system, a broad LED light is used for measuring the strain difference. This system proved effective in finding out the probable damage region when compared to theoretical strain value.
- Out of BOTDR and BOTDA, BOTDA has been adopted for practical use. This system can detect the difference in strain released during compressive strain or increased frictional

resistance, which is not detected by FBG. This system can measure both strain and temperature, but care has to be taken during installation due to its fragile nature.

- FBG based accelerator has been used due to its ability of electromagnetic immunity. This accelerometer has proved to be effective as it gave an average error of 10.3% when compared with the theoretical value. The reason for the difference may be due to overestimation of mass or stiffness matrix in theoretical calculations.
- An experimental study of different strain sensors, ERS, VWSG, FBG and FO, were performed in the controlled condition of which VWSG gave the best result. This sensor proved to be effective for short-term monitoring. On calibrating the FBG sensors, the error in reading can be reduced. For long-term monitoring, where temperature change is not sudden, FO sensors proved to be more robust for damage identification.
- It was experimentally showed that the strain measured with help of FO sensors is same as the theoretical value for temperature range 30^0C to 60^0C thus making it suitable for measurement of temperature. Also more the length of the FO sensor, more is the accurate measurement. Carbon nano tube strain sensor, AE sensors and DIC sensing technique have been tested for strain measurement and the results were comparable.
- In a comparative study for GPS sensors, it was found that GPS sensors are capable of detecting acceleration with the same accuracy as that of accelerometers. It was also found that both DGPS and PPP are good for measurement of real-time dynamic analysis.
- FBG sensor can be used for corrosion monitoring provided the fiber optic is properly coated. The proper coating provided to FBG sensor is PDMS coating mixed with pH sensitive hydrogel. This coating is sensitive to change in pH and can detect corrosion in the early stage.
- OSP is a major parameter which is applied for proper and efficient measurement of sensor signals. Determination of optimal sensor location for dynamic measurement with good accuracy was achieved with the help of Fitness Function approach, Bayesian approach and FEfi approach (Table 6). However these algorithms include complex calculations which might not be suitable for complex structures. It is observed that the animal cluster based OSP algorithm for efficient for sensor placement. For fast calculation, the AMA algorithm can be used which uses an iterative method for the result to converge. For placement of triaxial sensors, WMA algorithm is implemented which is slow but efficient process for sensor placement, considering six degrees of freedom for assessment.
- The placement of FBG sensors is carried out using FIM norm which makes use of convergence criteria using strain mode shapes to find OSP. The chances of the algorithm to miss out sensor location are reduced as it does not use strain of acceleration data directly. For low level of damage this algorithm may show false sensor placement location. In order to obtain OSP for low damage region, IIRS method has been introduced which uses Jaya algorithm to detect low incomplete modes for damage diagnosis.

10. Conclusion

A number of sensors used in SHM have been studied in this paper. Most of the sensors make use of strain data for the purpose of monitoring the structure. The traditional sensors used for SHM are the electronic types; strain sensors, accelerometer, and displacement transducers. With advancement in technology, these sensors have been modified with the use different systems; fiber optics, MEMS, and PZT. These technologies have improved the quality of sensing damage and proved effective in the modern world.

High-resolution photography has been used to identify damage as it is a good replacement of analytical methods. The method uses predefined damage templates to detect damage. However, this noncontact damage detection technique counters problem due to environmental effects such as illumination, vision hindrance and error due to the large angle of elevation of the camera. Also acquiring high-resolution photographs for small and restricted access is difficult. These sensors have been successful for different building structures situated at a good distance while considering the light conditions to be stable and constant throughout.

The traditional strain sensors used are the bulky cabled electronic strain gauge used to measure the difference in strain occurring in the structure. These sensors are the most common type used for damage detection in any structures. Thin film strain sensors can be used for dynamic strain measurement using supporting columns. However the bending and forces on supporting columns have to be considered for measurement which in real measurement is difficult. CBSS, can be used for column structures, bridge piers, multi storey buildings, etc. because of the cementitious nature which helps these sensors to bond with parent structure. These sensors encountered interference due to surrounding environmental such as electromagnetic effect. To improve the efficiency of the sensor, modified sensors based on piezo and fiber optics have been researched on. These sensors are immune to the electromagnetic influence of the surrounding atmospheric conditions. These sensors are mostly wired to a power source for constant supply of power. In this view, wireless strain sensors have been developed and deployed to remotely detect damage where access for cabled sensor is not feasible, mainly offshore structures.

The piezo materials, immune to electromagnetic interference, used for sensor technology are thick ceramic materials, carbon nano materials and MEMS. These materials have proved to be reliable for practical applications. Nano material based sensors are usually applicable for cyclic loading owing to their grapheme epoxy structure. The AE sensor technology in collaboration with piezo materials and MEMS technique has also proved to be efficient for crack analysis in structures under dynamic loads. The detection of the dynamic properties of the structure with the help of strain sensor was studied. But the prototype used needed improvement for practical application.

To measure the dynamic properties, loading due to wind pressure or earthquakes, accelerometers have been practically assigned. A wide range of accelerometers have been introduced for SHM; electronic cabled, wireless, GPS based, MEMS. Out of these, GPS based and MEMS-based accelerometers have shown accurate measurements with reduced noise interference. The MEMS-based technology for sensor development has been a breakthrough in monitoring techniques. These sensors have been effective in measuring data under different noise environment and can be used for both strain and acceleration data acquisition. Moreover, these sensors can be also integrated with wireless technology, giving them advantages for offshore or remote structural health monitoring. GPS sensor can be used for dynamic monitoring of high rise buildings as this type of sensors are mainly dependant on satellite data provided. The PPP and DGPS sensors are good for measuring damage under earthquake loads and are able to work under high sampling frequency. PZT transducers and Galvanic cathode anode configuration can be used for detection of corrosion in steel rebars.

The last type of sensor discussed is the Fiber Optics based sensors used for multiple damage detection. This sensor uses light as a source of the impulse to detect damage and can be used for long-term health monitoring but has to be installed with good care as the fibers are fragile. This sensor is the upcoming trend in the field of health monitoring. These sensors are resistant to electromagnetic interference and extreme temperature conditions. The long gauge sensors can be used monitoring of bridges under different loads. The main parameters that are measured are strain and temperature.

However, the application of FBG is not limited to only these two parameters. It can detect humidity, acceleration, displacement, corrosion and others. Therefore keeping in mind the careful installation of these sensors, due to their fragile nature, the sensors are robust and can be best used for the damage analysis in the modern day. The sensor has been widely used for monitoring of building and bridge structures as the strain measured is not affected due to change in surrounding conditions, temperature and humidity.

Apart from applications of the sensors, installation of a sensor to a specific point is equally important for the study. Out of the few algorithms discussed, animal cluster algorithm has seen to be a robust method for deciding the crucial location of bi axial and triaxial sensors in case of complex structure. However for low level of damage detection in structure, IIRS method which uses Jaya algorithm has been developed for OSP.

With the advances in technology, the multiplexed sensor such as FBG sensors will be widely used in all the field of SHM. Wireless GPS sensor is advancement in the field of SHM for precise damage diagnosis without any direct connection to power source. Sensor placement is also an important aspect for efficient sensor placement such that maximum number of structural data is obtained with deployment of minimum number of sensors.

References

1. Hong W., Z.J., Wu G., Wu Z., *Comprehensive comparison of macro-strain mode and displacement mode based on different sensing technologies.* Mechanical Systems and Signal Processing, 2015. **50-51**: p. 563-579.
2. Hui, L.I., Jinping, O.U., *Structural Health Monitoring: From Sensing Technology Stepping to Health Diagnosis.* Procedia Engineering, 2011. **14**: p. 753-760.
3. Yi T.H., L.H.N. *Innovative structural health monitoring technologies*. Measurement, 2016. **88**, 343-344.
4. Arjun V., S.B., Purna Chandra Rao B., Mukhopadhyay C.K., Jayakumar T., *Optimisation of pulsed eddy current probe for detection of sub-surfacedefects in stainless steel plates.* Sensors and Actuators A: Physical, 2015. **226**: p. 69-75.
5. Demetgul M., S.V.Y., Uyandik R., Tansel I.N., Yazicioglu O., *Evaluation of the health of riveted joints with active and passive structural health monitoring techniques.* Measurement, 2015. **69**: p. 42-51.
6. Han Q., X.J., Carpinteri A., *Localization of acoustic emission sources instructural health monitoring of masonry bridge.* Structural Control and Health Monitoring, 2015. **22**: p. 314-329.
7. Li F., P.H., Meng G., *Quantitative damage image construction in platestructures using a circular PZT array and lamb waves.* Sensors and Actuators A: Physical, 2014. **214**: p. 66-73.
8. Roach, D., *Real time crack detection using mountable comparative vacuum monitoring sensors.* Smart Structures and Systems, 2009. **5**: p. 317-328.
9. Annamdas V.G.M., S.C.K., *Application of electromechanical impedance technique for engineering structures: review and future issues.* journal of Intelligent Material Systems and Structures, 2010. **21**: p. 41-59.
10. Zhao J., B.T., Amjad U., *Optical fiber sensing of small cracks in isotropic homogeneous materials.* Sensors and Actuators A: Physical, 2015. **225**: p. 133-138.

11. Sun K., M.G., Li F., Ye L., Ye L., *Damage identification in thick steel beam based on guided ultrasonic waves.* Journal of Intelligent Material Systems and Structures, 2010. **21**: p. 225-232.
12. Sundaram, B.A., Ravisankar, K., Senthil, R., Parivalla, S., *Wireless sensors for structural health monitoring and damage detection techniques.* Current Science, 2013. **104**(11): p. 1496-1505.
13. Haynes, C., Todd, M., *Enhanced damage localization for complex structures through statistical modeling and sensor fusion.* Mechanical Systems and Signal Processing, 2015. **54**: p. 195-209.
14. Achenbach, J.D., *Structural health monitoring—what is the prescription?Mech. Res. Commun.* Mechanics Research Communications, 2009. **36**: p. 137-142.
15. Mascarenas D.D.L, F.E.B., Todd M.D., Overly T.G., Farinholt K.M., Park G., Farrar C.R., *Development of capacitance-based and impedance-based wireless sensors and sensor nodes for structural health monitoring applications.* Journal of Sound and Vibration, 2009. **329**: p. 2410-2420.
16. Das, S., Saha, P., Parto, S.K., *Vibration based damage detction techniques used for health monitoring of structrues: a review.* Journal of Civil Structural Health Monitoring, 2016. **6**(3): p. 477-507.
17. Li, Y.Y., *Hypersensitivity of strain-based indicators for structural damage identification: a review.* Mechanical Systems and Signal Processing, 2010. **24**: p. 653-664.
18. Salawu, O.S., *Detection of structural damage through changes in frequency: a review.* Engineering Structures, 1997. **19**(9): p. 718-723.
19. Doebling, S.W., Farrar, C.R. and Prime, M.B. , *A summary review f vibration-based damage identification methods.* Shock and Vibration Digest, 1998. **30**(2): p. 91-105.
20. Carden E. P., F.P., *Vibration based condition monitoring : a review.* Structural Control and Health Monitoring, 2004. **3**(4): p. 355-377.
21. Fox, C.H.J. *The location of defects in structures : a comparison of the use of natural frequency and mode shape data*. in *The 10th International Modal Analysis Conference*. 1992. San Diego, CA.
22. Adewuyi, A.P., Wu, Z.S., Serker, N.H.M.K., *Assessment of vibration-based damage identification methods using different measurement techniques.* Structural Health Monitoring, 2009. **8**(6): p. 443-461.
23. Seo, J., Hu, J.W., Lee, J., *Summary Review of Structural Health Monitoring Applications for Highway Bridges.* Journal of Performance of Constructed Facilities, 2015: p. 04015072-1-9.
24. Seo, J., Czaplewski, T.M., Kimn, J.H., Hatfield, G., *Integrated structural health monitoring system and multi-regression models for determining load ratings for complex steel bridges.* Measurement, 2015. **75**: p. 308-319.
25. Seo, J.P., B., Lu, P., Wipf, T., Dahlberg, J., *Bridge rating protocol using ambient trucks through structural health monitoring system.* Engineering Structures, 2013. **46**: p. 569-580.
26. Pharse, B., Lu, P., Wipf, T., Greimann, L., Seo, J., *Evolution of a Bridge Damage-Detection Algorithm.* Transportation Research Record: Journal of the Transportation Research Board, 2013. **2331**: p. 71-80.
27. Annamdas, V.G.M., Soh, C.K., *Application of electromechanical impedance technique for engineering structures: review and future issues.* journal of Intelligent Material Systems and Structures, 2010. **21**: p. 41-59.
28. Rose, J.L., *A baseline and vision of ultrasonic guided wave inspection potential.* Journal of pressure Vessel Technology, ASME, 2002. **124**: p. 273-282.
29. da Silva, S., Gonsalez, C.G., Lopes Jr., V. . *Adaptive filter feature identification for structural health monitoring in an aeronautical panel*. in *The Society for Experimental Mechanics Series*. 2011.
30. Antunes, P., Travanca, R., Varum, H., Andre, P., *Dynamic monitoring and numerical modelling of communication towers with FBG based accelerometers.* Journal of Constructional Steel Research, 2012. **74**: p. 58-62.
31. Shi, X., *Monitoring of Reinforced Concrete Corrosion*. 2018, Woodhead Publishing, Elsevier.

32. Lee, D.G., Mitrovic, M., Friedman, A., Carman, G.P.,Richards, L., *Characterization of fiber optic sensors for structural health monitoring.* Journal of Composite Materials, 2002. **36**: p. 1349-1366.
33. Ansari, F., *State-of-the-art in the applications of fiber-optic sensors to cementitious composites.* Cement and Concrete Composites, 1997. **19**: p. 3-19.
34. Antunes, P.F.C., Lima, H.F.T., Alberto, N.J., Rodrigues, H., Pinto, P.M., Nogueira, R.N., Varum, H., Costa, A.G., de Brito Andra, P.S., *Optical Fiber Accelerometer System for Structural Dynamic Monitoring.* Sensors, 2009. **9**: p. 1347-1354.
35. Flynn, E.B., Todd, M.D., *A Bayesian approach to optimal sensor placement for structural health monitoring with application to active sensing.* Mechanical Systems and Signal Processing, 2010. **24**: p. 891-903.
36. Schreier, H.M., Braasch, J.R., Sutton, M.A., *Systematic errors in digital image correlation caused by intensity interpolation, 39 (11) (2000) 2915–292.* Soc. Photo-Opt. Instrum. Eng., 2000. **39**(11): p. 2915-2921.
37. Crammond, G., Boyd, S.W., Dulieu-Barton, J.M., *Speckle pattern quality assessment for digital image correlation.* Optics and Lasers in Engineering, 2013. **51**: p. 1368-1378.
38. Yu, L.P., Pan, B., *The errors in digital image correlation due to overmatched shape functions.* Measurement Science and Technology. **26**(4): p. 045202.
39. Busca, G., Cigada, A., Mazzoleni, P., Zappa, E., *Vibration monitoring of multiple bridge points by means of a unique vision-based measuring system.* Experimental Mechanics, 2014. **54**: p. 255-271.
40. Ye, X.W., Ni, Y.Q., Wai, T.T., Wong, K.Y., Zhang, X.M., Xu, F., *A vision-based system for dynamic displacement measurement of long-span bridges: algorithm and verification.* Smart Structures and Systems, 2013. **12**: p. 363-379.
41. Ribeiro, D., Calcada, R., Ferreira, J., Martins, T., *Non-contact measurement of the dynamic displacement of railway bridges using an advanced video-based system.* Engineering Structures, 2014. **75**: p. 164-180.
42. Ye, X.W., Yi, T.H., Dong, C.Z., Liu, T., *Vision-based structural displacement measurement: System performance evaluation and influence factor analysis.* Measurement, 2016. **88**: p. 372-384.
43. Feng, D., Feng, M.Q., *Experimental validation of cost-effective vision-based structural health monitoring.* Mechanical Systems and Signal Processing, 2017. **88**: p. 199-211.
44. Gonzalez, R.C., Woods, R.E. (Eds.), *Digital Image Processing*, ed. 3rd. 2008, Upper Saddle River, NJ: Pearson Prentice Hall.
45. Ye, X.W., Yi, T.H., Dong, C.Z., Bai, H., *Multi-point displacement monitoring of bridges using a vision based approach.* Wind and Structures, 2015. **20**(2): p. 315-326.
46. Chen, J.G., Davis, A., Wadhwa, N., Durand, F., Freeman, W.T., Büyüköztürk, O., *Video Camera–Based Vibration Measurement for Civil Infrastructure Applications.* Journal of Infrastructure Systems, 2017. **B4016013**.
47. Chen, J.G., Wadhwa, N., Cha, Y. J., Durand, F., Freeman, W. T.,Buyukozturk, O., *Modal identification of simple structures with high-speed video using motion magnification.* Journal of Sound and Vibration, 2015. **345**: p. 58-71.
48. Giurgiutiu, V., Cuc, A., *Embedded non-destructive evaluation for structural health monitoring, damage detection, and failure prevention.* Shock Vibration Digest, 2005. **37**(2): p. 83-105.
49. Lynch, J.P., Loh, K.J., *A summary review of wireless sensors and sensor networks for structural health monitoring* Shock Vibration Digest, 2006. **38**(2): p. 91-128.
50. Kesavan, K., Ravisankar, K., Parivallal, S., Sreeshylam, P., Sridhar, S., *Experimental studies on fiber optic sensors embedded in concrete.* Measurement, 2010. **43**(2): p. 157-163.
51. Yehia, S., Landolsi, T., Hassan, M., Hallal, M., *Monitoring of strain induced by heat of hydration, cyclic and dynamic loads in concrete structures using fiber-optics sensors.* Measurement, 2014. **52**: p. 33-46.
52. Casas, J.R., Cruz, P.J., *Fiber optic sensors for bridge monitoring.* Journal of Bridge Engineering, 2003. **8**(6): p. 362-373.

53. Ge, Y., Elshafie, M.Z.E.B., Dirar, S., Middleton, C.R., *The response of embedded strain sensors in concrete beams subjected to thermal loading.* Construction and Building Materials, 2014. **70**: p. 279-290.
54. Hoult, N.A., Bennett, P.J., Middleton, C.R., Soga, K., *Distributed fibre optic strain measurements for pervasive monitoring of civil infrastructure*, in *International conference on structural health monitoring of intelligent infrastructure (SHMII-4)*, H.B. Meier Urs, Motavalli Masoud, Editor. 2009: Zurich, Switzerland.
55. Xia, Q., Quail, F., *Principles and validation of strain gauge shunt design for largedynamic strain measurement.* Sensors and Actuators A: Physical, 2016. **241**: p. 124-134.
56. Katafygiotis, L.S., Yuen, K. V., *Bayesian spectral density approach for modal updating using ambient data.* Earthquake Engineering and Structural Dynamics, 2001. **30**(8): p. 1103-1123.
57. Tegtmeier, F., Peters M., . *Determination of structural damage to buildings using microsensors based on strain gauge technology*. in *The XVI IMEKO World Congress*. 2000. Vienna.
58. Wada, T., Stein, S.J., Stein, M.A., Chitale, S.A. *The state-of-the-art of thick film technology for automotive sensors*. in *IEMT/IMC*. 1997.
59. Morten, B., Prudenziati, M., *Piezoresistive thick-film sensors*. Handbook of Sensors and Actuators. Vol. IV. 1994.
60. Zha, J.W., Zhang, B., Li, R.K.Y., Dang, Z.M., *High-performance strain sensors based on functionalized graphene nanoplates for damage monitoring.* Composites Science and Technology, 2016. **123**: p. 32-38.
61. Jabir, S.A.A., Gupta, N.K., *Condition monitoring of the strength and stability of civil structures using thick film ceramic sensors.* Measurement, 2013. **46**: p. 2223-2231.
62. Cho, J.W., Choi, J.S., Yoon, Y.S., *Electromechanical behaviour of hybrid/glass fiber composites with tension and bending*. Journal of Applied Polymers, 2002. **83**: p. 2447-2453.
63. Trung, T.Q., Tien, N.T., Kim, D., Jang, M., Yoon, O.J., Lee, N.E.A., *Flexible reduced graphene oxide field-effect transistor for ultrasensitive strain sensing.* Advanced Functional Materials, 2014. **24**: p. 117-124.
64. Sebastian, J., Schehl, N., Bouchard, M., Boehle, M., Li, L., Lagounov, A., Lafdi, K. , *Health monitoring of structural composites with embedded carbon nanotube coated glass fiber sensors.* Carbon, 2014. **66**: p. 191-200.
65. Toprakci, H.A.K., Kalanadhabhatla, S.K., Spontak, R.J., Ghosh, T.K., *Polymer nanocomposites containing carbon nanofibers as soft printable sensors exhibiting strain-reversible piezoresistivity.* Advanced Functional Materials, 2013. **23**: p. 5536-5542.
66. Li, W., Tang, X.Z., Zhang, H.B., Jiang, Z.G., Yu, Z.Z., Du, X.S., Mai, Y.W., *Simultaneous surface functionalization and reduction of graphene oxide with octadecylamine for electrically conductive polystyrene composites.* Carbon, 2011. **49**: p. 4724-4730.
67. Neild, S.A., Williams, M.S., McFadden, P.D., *Development of a vibrating wire strain gauge for measuring small strains in concrete beams.* Strain, 2005. **41**(1): p. 3-9.
68. Saw, H.S., Liew, J.Y.R., *Assessment of current methods for the design of composite columns in buildings.* Journal of Constructional Steel Research, 2005. **53**(2): p. 121-147.
69. Azhari, F., Banthia, N., *Cement-based sensors with carbon fibers and carbon nanotubes for piezoresistive sensing.* Cement & Concrete Composites, 2012. **34**: p. 866-873.
70. Sun, M.Q., Liew, R.J.Y., Zhang, M.H., Li, W., *Development of cement-based strain sensor for health monitoring of ultra high strength concrete.* Construction and Building Materials, 2014. **65**: p. 630-637.
71. Azhari, F., *Cement-based sensors for structural health monitoring*, in *Civil Engineering*. 2009, University of British Columbia.
72. Chen, P.W., Chung, D.D.L., *Carbon fiber reinforced concrete for smart structures capable of non-destructive flaw detection.* Smart Materials and Structures, 1993. **2**(1): p. 22-30.
73. Li, G.Y., Wang, P.M., Zhao, X., *Pressure-sensitive properties and microstructure of carbon nanotube reinforced cement composites.* Cement & Concrete Composites, 2007. **29**(5): p. 377-382.
74. Straser, E.G., Kiremidjian, A.S., *A Modular, Wireless Damage Monitoring System for Structures*, in *John A. Blume Earthquake Eng. Ctr.* 1998, Stanford University: Stanford, CA.

75. Graybeal, B., Phares, B.M., Rolander, D., Moore, M., Washer G., *Visual inspection of highway bridges.* Journal of Nondestructive Evaluation, 2002. **21**(3): p. 67-83.
76. Zhang, Y., Bai, L., *Rapid structural condition assessment using radio frequency identification (RFID) based wireless strain sensor.* Automation in Construction, 2015. **54**: p. 1-11.
77. Wong, A., Wong, F., Nadeem, A., *Government roles in implementing building information modeling systems: comparison between Hong Kong and the United States.* Construction Innovation Information Process Management, 2011. **11**(1): p. 61-76.
78. Isikdag, U., Aouad, G., Underwood, J., Wu S. *Building information models: a review on storage and exchange mechanisms* in *Bringing ITC Knowledge to Work, 24th W78 Conference, Maribor*. 2007.
79. Daliri, A., Galehdar, A., John, S., Wang, C., Towe, W., Ghorbani K., *Wireless strain measurement using circular microstrip patch antennas.* Sensors and Actuators A: Physical, 2012. **184**: p. 86-92.
80. Lynch, J.P., Wang, Y., Loh, K.J., Yi, J., Yun, C.B. *Wireless structural monitoring of the geumdang bridge using resolution enhancing signal conditioning*. in *24th International Modal Analysis Conference (IMACXXIV)*. 2006. St.Louis, MO.
81. Huynh, T.C., Park, J.H., Kim, J.T., *Structural identification of cable-stayed bridge under back-to-back typhoons by wireless vibration monitoring.* Measurement, 2016. **88**: p. 385-401.
82. Kim, J.T., Huynh, T.C., Lee, S.Y., *Wireless structural health monitoring of stay cables under two consecutive typhoons.* Structural Monitoring and Maintenance, 2014. **1**(1): p. 47-67.
83. Lee, S.Y., Huynh, T.C., Kim, J.T., *Structural identification of gravity-type caisson structure via vibration feature analysis.* Smart Structures and Systems, 2015. **15**(2): p. 259-281.
84. Yi, J.H., Yun, C.B., *Comparative study on modal identification methods using output-only information.* Structural Engineering and Mechanics, 2004. **17**(3-4): p. 445-446.
85. McCullagh, J.J., Galchev, T., Peterson, R.L., Gordenker, R., Zhang, Y., Lynch, J., Najafi, K., *Long-term testing of a vibration harvesting system for the structural health monitoring of bridges.* Sensors and Actuators A: Physical, 2014. **217**: p. 139-150.
86. Farinholt, K.M., Miller, N., Sifuentes, W., MacDonald, J., Farrar, C.R., *Energy harvesting and wireless energy transmission for embedded SHM sensor nodes.* Structural Health Monitoring, 2010. **9**: p. 269-280.
87. Galchev, T., McCullagh, J., Peterson, R.L., Najafi, K., Mortazawi, A. *Energy harvesting of radio frequency and vibration energy to enable wireless sensor monitoring of civil infrastructure*. in *SPIE 7983, Nondestructive Characterization for Composite Materials, Aerospace Engineering, Civil Infrastructure, and Homeland Security 2011,798314* 2011.
88. Sazonov, E., Haodong, L., Curry, D., Pilay, P., *Self-powered sensors for monitoringof highway bridges.* IEEE Sensors, 2009. **9**: p. 1422-1429.
89. Kwon, S.D., Park, J., Law, K., *Electromagnetic energy harvester with repulsivelystacked multilayer magnets for low frequency vibrations, Smart Mater. Struct.22 (2013) 055007.* Smart Materials and Structures, 2013. **22, 055007**.
90. Peigney, M., Siegert, D., *Piezoelectric energy harvesting from traffic-induced bridge vibrations.* Smart Materials and Structures, 2013. **22, 095019**.
91. Elvin, N., Elvin, A., Choi, D.H., *A self-powered damage detection sensor*. The Journal of Strain Analysis for Engineering Design, 2003. **38**(2): p. 115-124.
92. Lajnef, N., Chakrabartty, S., Elvin, N., *A piezo-powered floating-gate sensor array for long-term fatigue monitoring in biomechanical implants.* IEEE Transaction on Biomedical Circuits and Systems, 2008. **2**(3): p. 164-172.
93. Rahimi, M., Shah, H., Sukhatme, G.S., Heideman, J., Estrin D. *Studying the feasibility of energy harvesting in a mobile sensor network*. in *2003 IEEE International Conference on Robotics & Automation,*. 2003. Taipei. Taiwan.
94. Ono, K., *Application of acoustic emission for structure diagnosis.* Diagnost.-Diagnost. Struct. Health Monit, 2011. **2**(58): p. 3-18.
95. Nair, A., Cai, C., *Acoustic emission monitoring of bridges: review and casestudies.* Engineering Structures, 2010. **32**: p. 1704-1714.

96. Schumacher, T., Higgins, C., Lovejoy, S., *Acoustic emission monitoring ofconventionally reinforced concrete highway bridges under service conditions.* Nondestructive Testing of Materials and Structures, Springer, 2013. **6**: p. 847–853.
97. Saboonchi, H., Ozevin, D., Kabir, M., *MEMS sensor fusion: Acoustic emission and strain.* Sensors and Actuators A: Physical, 2016. **247**: p. 566-578.
98. Gallego, A., Martínez, E., *Emisión Acústica*. Niveles I y II AEND. 2016: FC Editorial.
99. Godínez-Azcuaga, V.F., Ley, O. *Structural health monitoring of aerospace structures using a low-power, wireless multichannel acoustic emission node*. in *5th International Symposium on NDT in Aerospace*. 2013. Singapore.
100. Sagasta, F., Zitto, M.E., Piotrkowski, R., Benavent-Climent, A., Suarez, E., Gallego, A., *Acoustic emission energy b-value for local damage evaluation in reinforced concrete structures subjected to seismic loadings.* Mechanical Systems and Signal Processing, 2017. **102**: p. 262-277.
101. Yapar, O., Basu, P.K., Volgyesi, P., Ledeczi, A., *Structural health monitoring of bridges with piezoelectric AE sensors.* Engineering Failure Analysis, 2015. **56**: p. 150-169.
102. Moore, P., Miller, R., Hill, R.K., *Acoustic emission testing*. Nondestructive testing handbook, ed. A.S.f.N. Testing. Vol. 6. 2005.
103. Harris, A.W., Oppenheim, I.J., Greve, D.W., *MEMS-based high-frequency vibration sensors.* Smart Materials and Structures, 2011. **20**(7).
104. Saboonchi, H., Ozevin, D., *MEMS acoustic emission transducers designed with high aspect ratio geometry.* Smart Materials and Structures, 2013. **22**.
105. Saboonchi, H., Ozevin, D., *Metal MUMPs-based piezoresistive strain sensors forintegrated on-chip sensor fusion.* Sensors, 2015. **15**: p. 568-578.
106. Aktan, A.E., Catbas, F.N., Grimmelsman, K.A., Pervizpour, M., *Develpoment of a Model Health Monitoring Guide for Major Bridges*, in *Federal Highway Administration Research and Development*. 2003, Drexel University.
107. Bao, Y., Beck, J.L., Li, H, *Compressive sampling for accelerometer signals in structural health monitoring.* Structural Health Monitoring, 2011. **10**(3): p. 235-246.
108. Bajwa, W.U., Haupt, J., Sayeed, A.M., Nowak, R. *Compressive wireless sensing*. in *Proceedings of the 5th International Conference on Information Processing in Sensor Networks (IPSN'06)*. 2006. Nashville, Tamil Nadu.
109. Takhar, D., Laska, J.N., Wakin, M.B., Duarte, M.F., Baron, D., Sarvotham, S., Kelly, F.K., Baraniuk, R.G. *A new compressive imaging camera architecture using optical-domain compression*. in *Proceedings of the Computational Imaging IV at SPIE Electronic Imaging*. 2006. San Jose, California.
110. Kirolos, S., Laska, J., Wakin, M., Duarte, M., Baron, D., Ragheb, T., Massoud, Y., Baraniuk, R. *Analog-to-information conversion via random demodulation*. in *Proceedings of the IEEE Dallas Circuits and Systems Workshop*. 2006. Dallas, Texas.
111. Chae, M.J., Yoo, H.S., Kim, J.Y., Cho, M.Y., *Development of a wireless sensor network system for suspension bridge health monitoring.* Automation in Construction, 2012. **21**: p. 237-252.
112. Kilic, G., Unluturk, M.S., *Testing of wind turbine towers using wireless sensor network and accelerometer.* Renewable Energy, 2015. **75**: p. 318-325.
113. Fushun, L., Huajun, L., Wei, L., Bin, W., *Experimental study of improved modal strain energy method for damage localisation in jacket-type offshore wind turbines.* . Renew Energy, 2014. **72**: p. 174-181.
114. Zhu, D., Wang, Y., Brownjohn, *Vibration testing of a steel girder bridge using cabled and wireless sensors.* Frontiers of Architecture and Civil Engineering in China, 2011. **5**(249).
115. Im, S.B., Hurlebaus, S., Kang, Y.J., *Summary Review of GPS Technology for Structural Health Monitoring.* Journal of Structural Engineering, 2013. **141**: p. 1653-1664.
116. Wong, K.Y., Man, K.L., Chan, W.Y., *Monitoring Hong Kong's bridges: Realtime kinematic spans the gap.* GPS World, 2001. **7**: p. 10-18.
117. Meng, X., Roberts, G.W., Dodson, A.H., Brown, C.J. *GNSS for bridge deformation: Limitations and solutions*. in *Third International Conference on Bridge Maintenance, Safety and Management*. 2006. Porto, Portugal.

118. Meng, X., Dodson, A.H., Roberts, G.W., *Detecting bridge dynamics with GPS and triaxial accelerometers*. Engineering Structures, 2007. **29**: p. 3178-3184.
119. Moschas, F., Stiros, S., *Noise characteristics of high-frequency, short-duration GPS records from analysis of identical, collocated instruments.* Measurement, 2013. **46**: p. 1488-1506.
120. Yi, T.H., Li, H.N., Gu, M., *Experimental assessment of high-rate GPS receivers for deformation monitoring of bridge.* Measurement, 2013. **46**: p. 420-432.
121. Yi, T.H., Li, H.N., Gu, M., *Full scale measurement of dynamic response of a suspension bridge subjected to environmental loads using GPS technology.* Science China Technological Sciences, 2010. **53**(2): p. 469-479.
122. Yi, T.H., Li, H.N., Gu, M., *Characterization and extraction of global positioning system multipath signals using an improved particle-filtering algorithm.* Measurement Science and Technology, 2011. **22**(075101): p. 11pp.
123. Kaloop, M.R., Hu, J.W., *Dynamic Performance Analysis of the Towers of a Long-Span Bridge Based on GPS Monitoring Technique.* Journal of Sensors, 2016. **2016**: p. 14 pages.
124. Moschas, F., Stiros, S. , *Dynamic deflections of a stiff footbridge using 100-Hz GNSS and accelerometer data.* Journal of Surveying Engineering, 2015. **141:04015003**.
125. Moschas, F., Avallone, A., Saltogianni, V., Stiros, S., *Strong motion displacement waveforms using 10-Hz precise point positioning GPS: An assessment based on free oscillation experiment.* International Association for Earhquake Engineering, 2015. **44**: p. 657-675.
126. Kaloop, M.R., Elbeltagi, E., Hu, J.W., Elrefai, A., *Recent Advances of Structures Monitoring and Evaluation Using GPS-Time Series Monitoring Systems: A Review.* International Journal o f Geo-Information, 2017. **6**(382).
127. Zumberge, J.F., Heflin, M.B., Jefferson, D.C., Watkins, M.M., Webb, F.H., *Precise point positioning for the efficient and robust analysis of GPS data from large networks.* Journal of Geophysical Research: Solid Earth, 1997. **102**: p. 5005-5017.
128. Yigit, C.O., Gurlek, E., *Experimental testing of high-rate GNSS precise point positioning (PPP) method for detecting dynamic vertical displacement response of engineering structures.* Geomatics Natural Hazards and Risk, 2017: p. 1-12.
129. Han, H., Wang, J., Meng, X., Liu, H., *Analysis of the dynamic response of a long span bridge using GPS/accelerometer/anemometer under typhoon loading.* Engineering Structures, 2016. **122**: p. 238-250.
130. Ingle, V.K., Proakis, J.G., *Digital signal processing using Matlab*. 1997, Boston (US): PWS Publishing Company.
131. Roberts, G.W., Cosser, E., Meng, X., Dodson, A., *High Frequency Deflection Monitoring of Bridges by GPS.* Journal of Global Positioning Systems, 2004. **3**(1-2): p. 226-231.
132. Lepadatu, A., Tiberius, C., *GPS for structural health monitoring – case study on the Basarab overpass cable-stayed bridge.* Journal of Applied Geodesy, 2014. **8**(1): p. 65-85.
133. Bogusz, J., Figurski, M., Nykiel, G., Szolucha, M., Wrona, M., *GNSS-based multi-sensor system for structural monitoring applications.* Journal of Applied Geodesy, 2012. **6**: p. 55-64.
134. Kavitha, S., Daniel, R.J., Sumangala, K., *A simple analytical design approach based on computer aided analysis of bulk micromachined piezoresistive MEMS accelerometer for concrete SHM applications.* Measurement, 2013. **46**: p. 3372-3388.
135. Lynch, J.P., Patridge, A., Law, K.H., Thomas, W., Kenny, W., Kiremidjian, A.S., Carryer, E., *Design of piezoresistive MEMS based accelerometer for integration with wireless sensing unit for structural monitoring.* Journal of Aerospace Engineering, 2003. **16**: p. 108-114.
136. Kavitha, S., Daniel, R.J., Sumangala, K., *High performance MEMS accelerometers for concrete SHM applications and comparison with COTS accelerometers.* Mechanical Systems and Signal Processing, 2015. **66-67**: p. 410-424.
137. Kavitha, S., Daniel, R.J., Sumangala, K., *Design and Analysis of MEMS Comb Drive Capacitive Accelerometer for SHM and Seismic Applications.* Measurement, 2016. **93**: p. 327-339.
138. Walmsley, R.G., Kiyarna, L.K.,, Milligan, D.M., Alley, R.L., Erickson, D.L., Hartwell, P.G., *Micro-G silicon accelerometer using surface electrodes*, in *IEEE - SENSORS* 2009. p. 971-974.

139. Bao, M.H., Middelhoek, S., *Handbook of Sensors and Actuators, Micromechanical Transducers*. Vol. 8. 2000: Elsevier.
140. Vogl, A., Wanga, D.T., Storasa, P., Bakkea, T., Taklo, M.M.V., Thomson, A., Balgard, L., *Design, process and characterisation of a high-performance vibration sensor for wireless condition monitoring.* Sensors and Actuators A: Physical, 2009. **153**(2): p. 155-161.
141. Acar, C., Shkel, A.M., *Experimental evaluation and comparative analysis of commercial variable - capacitance MEMS accelerometers.* Journal of Micromechanics and Microengineering, 2003. **13**: p. 634-645.
142. Acar, C., Shkel, A.M., *Comparative Characterization of Low-g Capacitive MEMS Accelerometers*. Structural Health Monitoring from Diagnostics and Prognostics to Structural Health Management. 2003, USA: D Estech Publications.
143. *ADXL 150/250 Specification Data Sheets.* Analog Devices Inc, 1998.
144. Gonenil, E.I., Butler, Z.C., Donald, P., *Surface micromachined MEMS accelerometer on flexible polymide substrate.* IEEE Sensors, 2011. **11**: p. 2318-2326.
145. Kavitha, S., Daniel, R.J., Sumangala, K., *Design and analysis of bulk micromachined piezoresistive MEMS accelerometer for concrete SHM applications.* Digital Sensors and Sensor Systems: Practical Design, 2012. **144**(9): p. 62-75.
146. Li, G., Tseng, A.A., *Transient and impact dynamics of a Micro-accelerometer.* Journal of Materials Processing and Manufacturing Science, 2000. **9**: p. 143-156.
147. Abosrra, L., Ashour, A.F., Youseffi, M., *Corrosion of steel reinforcement in concrete of different compressive strengths.* Construction and Building Materials, 2011. **25**: p. 3915-3925.
148. Cheng, Y., Hanif, A., Chen, E., Ma, G.,Li, Z., *Simulation of a novel capacitive sensor for rebar corrosion detection.* Construction and Building Materials, 2018. **174**: p. 613-624.
149. Ann, K.Y., Song, H.W., *Chloride threshold level for corrosion of steel in concrete.* Corrosion Science, 2007. **49**(11): p. 4113-4133.
150. Shi, X., Xie, N., Fortune, K., Gong, J., *Durability of steel reinforced concrete in chloride environments: an overview.* Construction and Building Materials, 2012. **30**: p. 125-138.
151. González, J.A., Molina, A., Escudero, M.L., Andrade, C., *Errors in the electrochemical evaluation of very small corrosion rates-I. Polarization resistance method applied to corrosion of steel in concrete,.* Corrosion Science, 1985. **25**: p. 917-930.
152. Liu, C., Bi, Q., Leyland, A., Natthews, A., *An electrochemical impedance spectroscopy study of the corrosion behaviour of PVD coated steels in 0.5 N NaCl aqueous solution: Part II.: EIS interpretation of corrosion behaviour.* Corrosion Science, 2003. **45**: p. 1257-1273.
153. Sathiyanarayanan, S., Natarajan, P., Saravanan, K., Srinivasan, S., *Corrosion monitoring of steel in concrete by galvanostatic pulse technique.* Cement & Concrete Composites, 2006. **28**: p. 630-637.
154. Li, W., Kong, Q., Ho, S.C.M., Mo, Y.L., Song, G., *Feasibility study of using smart aggregates as embedded acoustic emission sensors for health monitoring of concrete structures.* Smart Materials and Structures, 2016. **25**(11): p. 115031.
155. Qin, L., Ren, H., Dong, B., Xing, F., *Development of technique capable of identifying different corrosion stages in reinforced concrete.* Applied Acoustics, 2015. **94**: p. 53-56.
156. Talakokula, V., Bhalla, S., Gupta, A., *Corrosion assessment of reinforced concrete structures based on equivalent structural parameters using electro-mechanical impedance technique.* Journal of Intelligent Material Systems and Structures, 2014. **25**(4): p. 484-500.
157. Yoo, J.H., Park, Z.T., Kim, J.G., Chung, L., *Development of a galvanic sensor system for detecting the corrosion damage of the steel embedded in concrete structures: Part 1. Laboratory tests to correlate galvanic current with actual damage.* Cement & Concrete Composites, 2003. **33**(12): p. 2057-2062.
158. Pereira, E.V., Figueira, R.B., Salta, M.M.L., Da Fonseca, I.T.E., *A galvanic sensor for monitoring the corrosion condition of the concrete reinforcing steel: relationship between the galvanic and the corrosion currents.* Sensors, 2009. **9**(11): p. 8391-8398.
159. Park, Z.T., Choi, Y.S., Kim, J.G., Chung, L., *Development of a galvanic sensor system for detecting the corrosion damage of the steel embedded in concrete structure: Part 2. Laboratory electrochemical testing of sensors in concrete.* Cement and Concrete Research, 2005. **35**(9): p. 1814-1819.

160. Perveen, K., Bridges, G.E., Bhadra, S., Thomson, D.J. *An embedded inductively coupled printed circuit board based corrosion potential sensor.* in *Instrumentation and Measurement Technology Conference (I2MTC), 2013 IEEE International. IEEE*. 2013. Piscataway, NJ.
161. Bhadra, S., Thomson, D.J., Bridges, G.E., *A wireless embedded passive sensor for monitoring the corrosion potential of reinforcing steel.* Smart Materials and Structures, 2013. **22**(7): p. 075019.
162. Myers, J.J., Hernandez, E., *Implementation of radio frequency identification (RFID) sensors for monitoring of bridge deck corrosion in Missouri.*, in *Final Report for the Center for Transportation Infrastructure and Safety/NUTC Program*. 2014, Missouri University of Science and Technology: Rolla, MO.
163. Murthy, S.G.N. *Batteryless Wireless RFID based embedded sensors for long term monitoring of reinforced concrete structures*. in *International Symposium Non-Destructive Testing in Civil Engineering*. 2015.
164. Uva, G., Porco, F., Fiore, A., Porco, G., *Structural monitoring using fiber optic sensors of apre-stressed concrete viaduct during construction phases.* Case Studies in Nondestructive Testing and Evaluation, 2014. **2**: p. 27-37.
165. Al-Fakih, E., *The use of fiber Bragg grating sensors in biomechanics and rehabilitation applications: the state-of-the-art and ongoing research topics.* Sensors, 2012. **12**.
166. Torres, B., Zaforteza, I.P., Calderón, P.A., Adam, J.M., *Analysis of the strain transfer in a new FBG sensor for Structural Health Monitoring.* Engineering Structures, 2011. **33**: p. 539-548.
167. Cheng, L.K., Toet, P.M., *Innovative fiber bragg grating sensors for highly demanding applications: Considerations, concepts, and designs*. Opto-Mechanical Fiber Optic Sensors. 2018: Elsevier.
168. Li, H.N., Li, D.S., Song, G.B., *Recent applications of fiber optic sensors to health monitoring in civil engineering.* Engineering Structures, 2004. **26**(11): p. 1647-1657.
169. Delepine-Lesoille, S., Merliot, E., Boulay, C., Quétel, L., Delaveau, M., Courteville, A., *Quasi-distributed optical fibre extensometers for continuous embedding into concrete: design and realization.* Smart Materials and Structures, 2006. **15**(4): p. 931.
170. Bourne-Webb, P., Amatya, B., Soga, K., Amis, T., Davidson, C., Payne, P., *Energy pile test at Lambeth College, London: geotechnical and thermodynamic aspects of pile response to heat cycles.* Geotechnique, 2009. **59**: p. 237-248.
171. Majumder, M., Gangopadhyay, T.M., Chakraborty, A.K. , *Fibre Bragg gratings in structural health monitoring—present status and applications.* Sensors and Actuators A: Physical, 2008. **147**(1): p. 150-164.
172. Rodrigues C., C., F., Félix C., Figueiras J., *FBG based strain monitoring in the rehabilitation of a centenary metallic bridge.* Engineering Structures, 2012. **44**: p. 281-290.
173. Ansari, F., *Practical implementation of optical fiber sensors in civil structural health monitoring.* Journal of Intelligent Material Systems and Structures, 2007. **18**(8): p. 879-889.
174. Costa, B.J.A., Figueiras, J.A., *Fiber optic based monitoring system applied to a centenary metallic arch bridge: Design and installation.* Engineering Structures, 2012. **44**: p. 271-280.
175. Moyo, P., Brownjohn, J.M.W., Suresh, R., Tjin, S.C., *Development of fiber Bragg grating sensors for monitoring civil infrastructure.* Engineering Structures, 2005. **27**(12): p. 1828-1834.
176. Adeli, H., Jiang, X., *Dynamic fuzzy wavelet neural network model for structural system identification.* Journal of Structural Engineering, 2006. **132**(1): p. 102-111.
177. Ngoi, B.K.A., Paul, J., Zhao, L.P., Fang, Z.P., *Enhanced lateral pressure tuning of fiber Bragg gratings by polymer packaging.* Optics Communication, 2004. **242**: p. 425-430.
178. Dawood, T.A., Shenoi, R.A., Sahin, M., *A procedure to embed fibre Bragg grating strain sensors into GFRP sandwich structures.* Composites A, 2007. **38**: p. 217-226.
179. Chung, W., Kang, D., *Full-scale test of a concrete box girder using FBG sensing system.* Engineering Structures, 2008. **30**: p. 643-652.
180. Dally, J.E., Riley, W.F., *Experimental stress analysis*. 2nd Edition. 1978: McGraw-Hill.
181. Kister, G., Winter, D., Badcock, R.A., Gebremichael, Y.M., Boyle, W.J.O., Meggitt, B.T., Grattan, K.T.V., Fernando, G.F., *Structural health monitoring of a composite bridge using*

Bragg grating sensors. Part 1: Evaluation of adhesives and protection systems for the optical sensors. Engineering Structures, 2007. **29**: p. 440-448.
182. Kang, H.K., Bang, J.H., Hong, C.S., Kim, C.G., *Simultaneous measurement of strain, temperature and vibration frequency using a fiber optic sensor.* Journal of Measurement Science and Technology, 2002. **13**: p. 1191-1196.
183. Fernández-Valdivielso, C., Matías, I.R., Arregui, F.J., *Simultaneous measurement of strain and temperature using a fiber Bragg grating and a thermochromic material.* Sensors and Actuators A: Physical, 2002. **101**: p. 107-116.
184. Poloso, T., *Fibre Bragg optical sensing technology*, in *Smart Materials*. 2001. p. 7-10.
185. Li, D., Zhou, Z., Ou, J., *Dynamic behavior monitoring and damage evaluation for arch bridge suspender using GFRP optical fiber Bragg grating sensors.* Optics & Laser Technology, 2012. **44**: p. 1031-1038.
186. Li, D.S., Zhou, Z., Ou. J.P., *Development and sensing properties study of FRP–FBG smart stay cable for bridge health monitoring applications.* Measurement, 2011. **44**: p. 722-729.
187. Pharse, B., Lu, P., Wipf, T., Greimann, L., Seo, J., *Field Validation of a Statistical-Based Bridge Damage-Detection Algorithm.* Journal of Bridge Engineering, 2013. **18**: p. 1227-1238.
188. Xia, Q., Cheng, Y.Y., Zhang, J., Zhu, F.Q., *In-Service Condition Assessment of a Long-Span Suspension Bridge Using Temperature-Induced Strain Data.* Journal of Bridge Engineering, 2016. **04016124**.
189. Ni, Y.Q., Xia, Y.X., *Strain-Based Condition Assessment of a Suspension Bridge Instrumented with Structural Health Monitoring System.* International Journal of Structural Stability and Dynamics, 2016. **16 (2016)**(1640027): p. 23pp.
190. Lau, C.K., Wong, K.Y., Ho, K.S., *The wind and structural health monitoring system (WASHMS) for the three longspan cable-supported bridges in Hong-Kong.* IABSE congress report = Rapport du congrès AIPC = IVBH Kongressbericht, 1996. **15**: p. 104-112.
191. Chan, T.H.T., Yu, L., Tam, H.Y., Ni, Y.Q., Liu, S.Y., Chung, W.H., Cheng, L.K., *Fiber Bragg grating sensors for structural health monitoring of Tsing Ma bridge: Background and experimental observation.* Engineering Structures, 2006. **28**: p. 648-659.
192. Rodrigues C., F.C., Lage A., Figueiras J., *Development of a long-term monitoring system based on FBG sensors applied to concrete bridges.* Engineering Structures, 2010. **32**(8): p. 1993-2002.
193. Zhou, G.D., Yi, T.H., Chen, B., *Innovative Design of a Health Monitoring System and Its Implementation in a Complicated Long-Span Arch Bridge.* Journal of Aerospace Engineering, 2016. **B4016006**: p. 17pp.
194. Wu, B., Wu, G., Lu, H., Feng, D., *Stiffness monitoring and damage assessment of bridges under moving vehicular loads using spatially-distributed optical fiber sensors.* Smart Materials and Structures, 2017. **26(2017)**(035058): p. 21pp.
195. Ojio, T., Yamada, K. *Bridge weigh-in-motion systems using stringers of plate girder bridges*. in *3rd Int. Conf. on Weigh-In- Motion (ICWIM3)*. 2002.
196. Connolly, C., *Fiber-optic-based sensors bring new capabilities to structural monitoring.* Sensor Review, 2006. **26**(3): p. 236-243.
197. Shehata, E., Rizkalla, S., *Intelligent sensing for innovative bridges.* Journal of Intelligent Material Systems and Structures, 1999. **10**(4): p. 304-313.
198. Elamari, A., Inaudi, D., Pflug, L., Gisin, N., Breguet, J., Vurpillot, S., *Low-coherence deformation sensors for the monitoring of civil engineering structures. Sens Actuators 1994;44:125–30.* Sensors and Actuators A: Physical, 1994. **44**: p. 125-130.
199. Inaudi, D., Casanova, N., Vurpillot, S., Kronenberg, P., Martinola, G., Steinmann, G., Mathier, J.F. *SOFO: Structural Monitoring with Fiber Optic Sensor*. in *Monitoring and Safety Evaluation of Existing Concrete Structures*. 1999. Vienna, Austria.
200. Stupar, D.Z., Bajic´ , J.S., Dakic´ , B.M., Slankamenac, M.P., Zˇivanov, M.B., *The possibility of using a plastic optical fibre as a sensing element in civil structural health monitoring.* Physica Scripta, 2013. **2013**: p. 014031.
201. Hong, C.Y., Zhang, Y.F., Liu, L.Q., *Application of distributed optical fiber sensor for monitoring the mechanical performance of a driven pile.* Measurement, 2016. **88**: p. 186-193.

202. Measures, R.M., *Structural monitoring with fibre optic technology*, Elsevier, Editor. 2001, Academic Press. p. 716.
203. Misra, A., Chen, C.H., *Analytical solution for micropile design under tension and compression.* Geotechnical and Geological Engineering, 2004. **22**: p. 199-225.
204. Leung, C.K.Y., Wan, K.T., Chen, L., *A novel optical fiber sensor for steel corrosion in concrete structures.* Sensors, 2008. **8**: p. 1960-1976.
205. Nguyen, T.H., Venugopala, T., Chen, S., Sun, T., Grattan, K.T., Taylor, S.E., Basheer, P.A.M., Long, A.E., *Fluorescence based fibre optic pH sensor for the pH 10-13 range suitable for corrosion monitoring in concrete structures.* Sensors and Actuators B: Chemical 2014. **191**: p. 498-507.
206. Torres-Luque, M., Bastidas-Arteaga, E., Schoefs, F., Sa´nchez-Silva, M., Osma, J.F., *Non-destructive methods for measuring chloride ingress into concrete: state-of-the-art and future challenges.* Construction and Building Materials, 2014. **68**: p. 68-81.
207. Tan, C.H., Shee, Y.G., Yap, B.K., Adikan, F.R.M., *Fiber Bragg Grating Based Sensing System: Early Corrosion Detection for Structural Health Monitoring.* Sensors and Actuators A: Physical, 2016. **246**: p. 123-128.
208. Kersey, A.D., Davis, M.A., Patrick, H.J., LeBlanc, M., Koo,K.P., Askins, C.G., Putnam,M.A., Friebele, E.J., *Fibre grating sensors.* Journal of Lightwave Technology, 1997. **15**: p. 1442-1463.
209. Johnson, I.D., McCluskey, D.K., Tan, C.K.L., Tracey, M.C., *Mechanical Characterization of Bulk Sylgard 184 for Microfluidics and Microengineering.* Journal of Micromechanics and Microengineering, 2014. **24**: p. 1-7.
210. Tan, C.H., Adikan, F.R.M., Shee, Y.G., Yap, B.K., *Non-destructive fiber Bragg grating based sensing system: Early corrosion detection for structural health monitoring.* Sensors and Actuators A: Physical, 2017. **268**: p. 61-67.
211. Sharma, T., Madras, G., *Effect of crosslinker on the swelling and adsorption properties of cationic superabsorbent.* Indian Academy of Sciences, 2016. **39**: p. 613-626.
212. Rytter, T., *Vibration Based Inspection of Civil Engineering Structure*, in *Department of Building Technology and Structure Engineering*. 1993, Aalborg University: Denmark.
213. Kleckers, T., Günther,B. , *Optical Versus Electrical Strain Gages: A Comparison.* HBM Measurements, 2008.
214. Roths, J., Wilfert, A., Kratzer, P., Jülich, F., Kuttler, R., *Strain calibration of opticalFBG-based strain sensors.* (EWOFS'10) Fourth European workshop on optical fibre sensors, International Society for Optics and Photonics, 2010. **76530F-F-4**.
215. Sreeshyiarn, P., Ravisankar, K., Parivallal, S., Kesavan, K., Sridhar, S., *Condition monitoring of prestressed concrete structures using vibrating wire sensors.* International Journal of COMADEM, 2008. **11**(3): p. 46-54.
216. Neville, A.M., *Properties of concrete*, ed. P. Hall. 1997.
217. Chowdhury, S.N., Bellegou, H., Castro, M., Longrais, P., Feller, J.F., *Crossed investigation of damage in composites with embedded quantum resistive strain sensors (sQRS), acoustic emission (AE) and digital image correlation (DIC).* Composites Science and Technology, 2018. **160**: p. 79-85.
218. Chowdhury, S.N., Bellegou, H., Pillin, I., Castro, M., Longrais, P., Feller, J.F., *Non-intrusive health monitoring of infused composites with embedded carbon quantum piezo-resistive sensors.* Composites Science and Technology, 2016. **123**: p. 286-294.
219. Gao, L., Thostenson, E.T., Zhang, Z., Chou, T.W., *Coupled carbon nanotube network and acoustic emission monitoring for sensing of damage development in composites.* Carbon, 2009. **47**: p. 1381-1388.
220. Park, H.S., Sohn, H.G., Kim, I.S., Park, J.H., *Application of GPS to monitoring of wind-induced responses of high-rise buildings.* The Structural Design of Tall and Special Buildings, 2008. **17**(1): p. 117-132.
221. Li, Z.N., Tang, J., Li, Q.S., *Optimal sensor locations for structural vibration measurements.* Applied Acoustics, 2004. **65**: p. 807-818.

222. Rao, A.R.M., Lakshmi, K., Krishnakumar, S., *A Generalized Optimal Sensor Placement Technique for Structural Health Monitoring and System Identification.* Procedia Engineering, 2014. **86**: p. 529-538.
223. Yi, T.H., Li,H.N., Zhang, X.D., *Sensor placement on Canton Tower for health monitoring using asynchronous-climb monkey algorithm.* Smart Materials and Structures, 2012. **125023**: p. 12pp.
224. Yi, T.H., Li, H.N., Zhang, X.D., *A modified monkey algorithm for optimal sensor placement in structural health monitoring.* Smart Materials and Structures, 2012. **105033**: p. 9pp.
225. Yi, T.H., Li, H.N., Wang, C.W., *Multiaxial sensor placement optimization in structural health monitoring using distributed wolf algorithm.* Structural Control and Health Monitoring, 2016. **23**: p. 719-734.
226. Loutas, T.H., Bourikas, A., *Strain sensors optimal placement for vibration-based structural health monitoring. The effect of damage on the initially optimal configuration.* Journal of Sound and Vibration, 2017. **410**: p. 217-230.
227. Cong, D.D., Trung, H.D., Thoi, T.N., *An efficient approach for optimal sensor placement and damage identification in laminated composite structures.* Advances in Engineering Software, 2018. **119**: p. 48-59.

Table 1. Characteristics of piezoelectric material strain gauge [59]

Material	Gauge Factor	Temperature Coefficient of Resistance – ppm/^{0}C	Temperature Coefficient of Gauge Factor- ppm/^{0}C	Stability
Metal sheets and films	1-2	20	100	Excellent
Silicon single crystals	50-80	1000	-1500	Good
Thick Film resistor	2-35	50-200	-300	Very Good

Table 2. Basic properties of the CBSS [70]

	Compressive Strength (MPa)	Elastic Modulus (GPa)	Poisson's Ratio	Resistivity (Ω m)	Gauge Factor
Air-drying	122 ± 4	41.8 ± 2.0	0.17 ± 0.01	$(1.41 \pm 0.10) * 10^3$	42 ± 10
Oven-drying	134 ± 3	40.7 ± 2.2	0.17 ± 0.01	$(3.34 \pm 0.32) * 10^3$	202 ± 13

Table 3. Comparison of Capacitive and Piezoresistive accelerometers with COTS accelerometers [141, 142]

Device/ Manufacturer	Range	Measured sensitivity	Flat frequency response range (Hz)	DC – 100 Hz, 0-2g resolution (μg)	Amplifying electronics
Silicon Design (SD2012-10)	0-10	399.3 mV/g	1-200	124	Yes
M1220D (Motorola)	0-8	241.4 mV/g	1-90	1237	Yes
Jerome [97]	0-10	1.250 mV/g	0-680	20	No
ADXL210A (Analog Device)	0-10	108.0 mV/g	1-16	258	Yes
7290A-10 (Endevco)	0-2	199.9 mV/g	1-200	84	Yes
Capacitive accelerometer	0-2	301 mV/g/V	0-30	9.6	No
Piezoresistive accelerometer	0-2	4.0 mV/g/V	0-45	12.72	No

Table 4. Comparison of two ADXL series accelerometers with other MEMS accelerometers [137]

Device/ Manufacturer	Range (g)	Specified sensitivity	Resonance frequency (Hz)	Noise floor (μg/$\sqrt{Hz}$)	Micro machining process	MEMS type
Colibrys (MS9002)	0-2	1000 (mV/g)	100	18	BM	Silicon
Endevco (7290A)		1000 (mV/g)	1300		BM	Silicon
Silicon Designs, INC. (1221)	0-2	2 (V/g)	400	5	BM	Non-Silicon Nickel
Kavitha et al. [138]	0-2	4 (mV/g/V)	100	4.53	BM	Silicon
Li and Tseng [139]	0-2	0.40 (V/g)	500	1.6	BM and SM	Silicon
Device A	0-0.1	1915 (mV/g/V)	100	1.3	SM	Polysilicon
Device B	0-2	106.8 (mV/g/V)	500	4.64	SM	Polysilicon

Table 5. Comparative study for the different sensors used for health monitoring of structure.

Sensors	Type	Material	Damage Type Detected	Working Principle	Advanta
Machine Based Vision Technology	Digital and Video Photography	High Resolution Digital Camera	Crack Patterns, Crack Growth	Superimposition of damage templates	Non Co No com required detectio
Metallic thin film strain gauge	Electrical, Wired	Thin Metallic Film	Strain	Change in Strain	Econom Compac
Thick film ceramic strain sensors	Electrical, Wired	Thick Piezoresistive material-Ceramic	Strain	Piezoresistive Effect-Voltage Change	Durable Resistan
Carbon based graphene sensor	Electrical, Wired	Carbon Nanomaterials-Graphene	Strain	Change in Electronic Energy Band	Lightwe Sensitiv
Cement based strain sensor	Electrical, Wired	Cement	Strain	Change in Volume Electric Resistivity	Suitable in Concr
Wireless strain sensor	Electrical, Wireless	Electronic Equipment	Strain	Radio frequency identification	Automa Monitor
Acoustic Emission Sensor	Electrical, Wired,	Piezoelectric material, MEMS	Strain	Change in Elastic Waves	Low am damage threshol
Wireless Accelerometers	Electrical, Wireless	Electronic Equipment	Acceleration	Measure three way acceleration of a structure	Econom monitor
GPS Based Accelerometer	Electrical, Wireless	GPS	Acceleration	Change in vibrational frequency using a proper digital filter	Sensitiv frequenc sensing
Micro Electro-Mechanical System (MEMS) Technology Sensors	Electrical, Wireless	Piezoelectric material	Strain Acceleration	Piezoresistivity and capacitive	Low ba reductio consump sensitivi
Corrosion Sensors	Electrical,Wired, Wireless	Piezoceramic material, galvanic couple	Corrosion (Rusting and pH change)	AE waves, Cathode Anode arrangement, RF signals	Can be u embedde sensor fo

					detectio
FBG Sensor	Optical	Optic Fiber	Multiple	Light refractivity	Effectiv damage points in from Ele Influenc
Fiber Optics Sensor	Optical	Optic Fiber	Multiple	Light Refractivity	Effectiv detectio of fiber, Electron Influenc
FBG based Accelerometer	Optical	Optic Fiber	Acceleration	Light Refractivity	Immune electrom
FBG based Corrosion Sensor	Optical	Optic Fiber	Corrosion	Light Refractivity	Immune electric tempera

Table 6. Comparative study on some of the recent OSP algorithm

Sl No	**OSP Algorithm**	**Method**	**Advantage**	**Disadvantage**
1	Fitness Function Approach [221]	The missing mode shape value is calculated with the help of normal interpolation of the neighbouring points.	Simple and efficient with less calculations and lower risk of missing sensor data	The number of interpolation required for complex structure is more.
2	Bayesian Approach [35]	The algorithms works on the platform of global detection evaluating with the use of Bayes risk-based performance metric.	Useful for obtaining the maximum performance of sensor by cost reduction	Large number of calculations are to be solved when the technique is applied on complex structure
3	Frequency Effective Independence Approach (FEfi) [222]	The algorithm uses data from Frequency Response Functions (FRF) to obtain dynamic information that can be used for placement of sensors	The method is applicable for frequencies from low range to high range	There is an increase in calculations for optimal sensor placement (OSP) in case of complex structure.
4	Monkey Algorithm (MA) [224]	The algorithm uses coding method which involves the steps of monkey; climb process, watch-jump process and somersault process and Modal Assurance Criterion (MAC) for sensor placement detection.	This method can be used to solve problems such as non linearity, high dimensionality and non-differentiability at a faster convergence rate, thus less calculations are required.	The algorithm is not suitable for modern multi axial sensors which can detect acceleration in all the three directions.
5	Asynchronous-Climb Monkey Algorithm (AMA) [223]	Uses Darwinian Principle of natural selection which is better in selecting the modes and exchanging the measured structural information than the original MA.	Uses iterative loop to pin-point the required sensor location	
6	Distributed Wolf Algorithm [225]	This algorithm involves the working of wolf pack i.e., searching, attacking and food distribution and using swarm intelligent algorithm to improve for efficient for solving.	The shuffling strategy embedded in DWA includes higher searching capacity and better convergence of results	The algorithm includes complex mathematical calculations which requires sufficient amount of time.
7	Fisher Information Matrix (FIM) norm [226]	The algorithm makes use of convergence criterion to decide the threshold redundancy by using strain mode shapes from two directions simultaneously.	Developed mainly for OSP of FBG Sensors. Does not use the acceleration or displacement data directly, hence less chance of missing out any location where sensor is not	For less damage case, the algorithm shows the need for more number of sensors. However it may be so that the current placement of sensor could be the

			present.	optimal position.
8	Iterated Improved Reduced System (IIRS) Method [227]	A reduced order model for OSP is developed which performs optimized damage detection for validating if the sensor layout is optimum for damage detection.	Shows its capacity to diagnose damage for the lower incomplete modes with the use of Jaya Algorithm	The method is a new technique has so far proved to be robust

Fig. 1. Schematic of strain gauge shunt on the target surface [55]

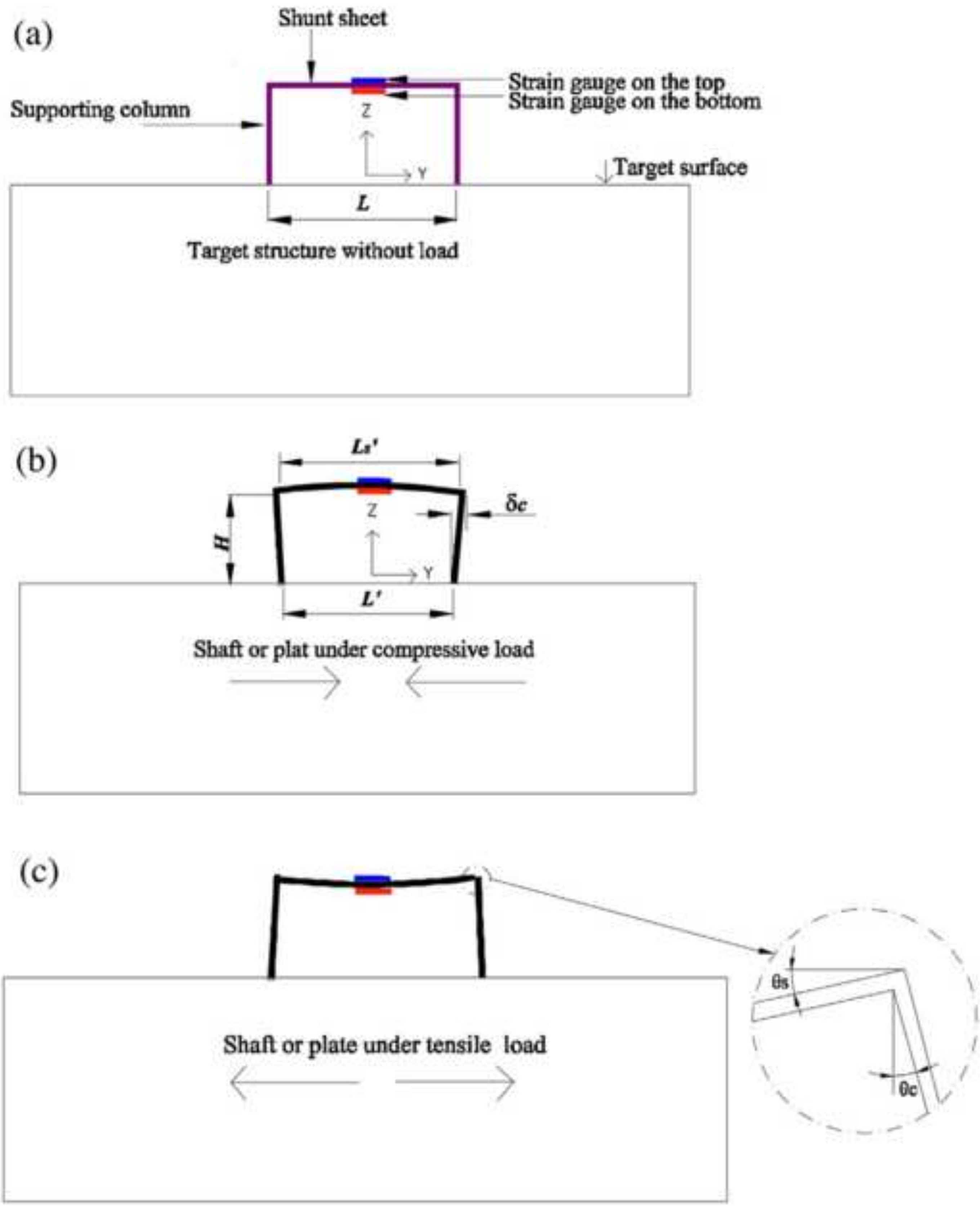

Figure(s)

Fig. 2. Comparison of Thick-film ceramic sensor to FSG for tension and compression [61]

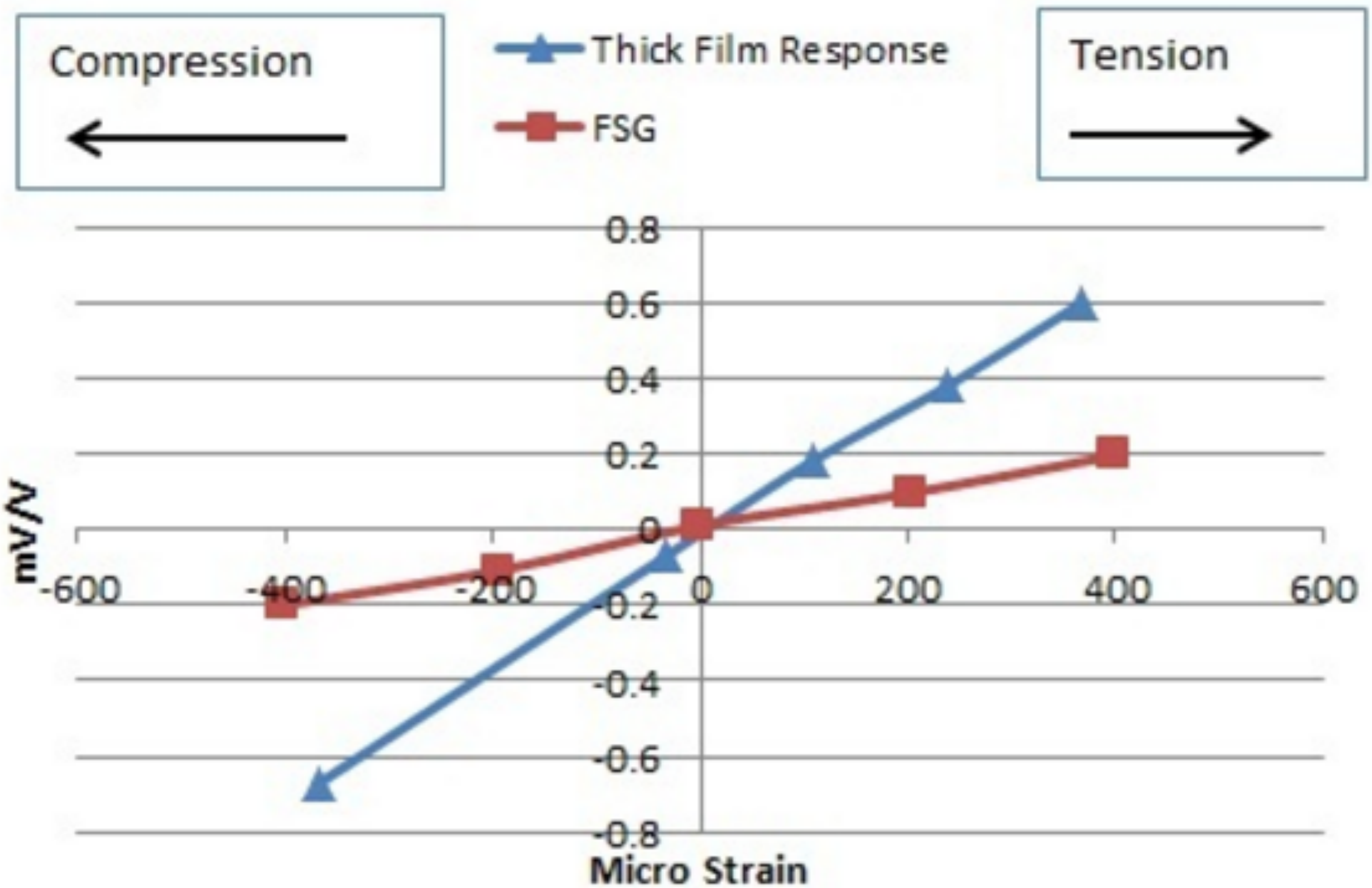

Fig. 3. Piezoresistive behaviour of graphene based sensor under; a) successive tensile load, b) under incremental cyclic load [60]

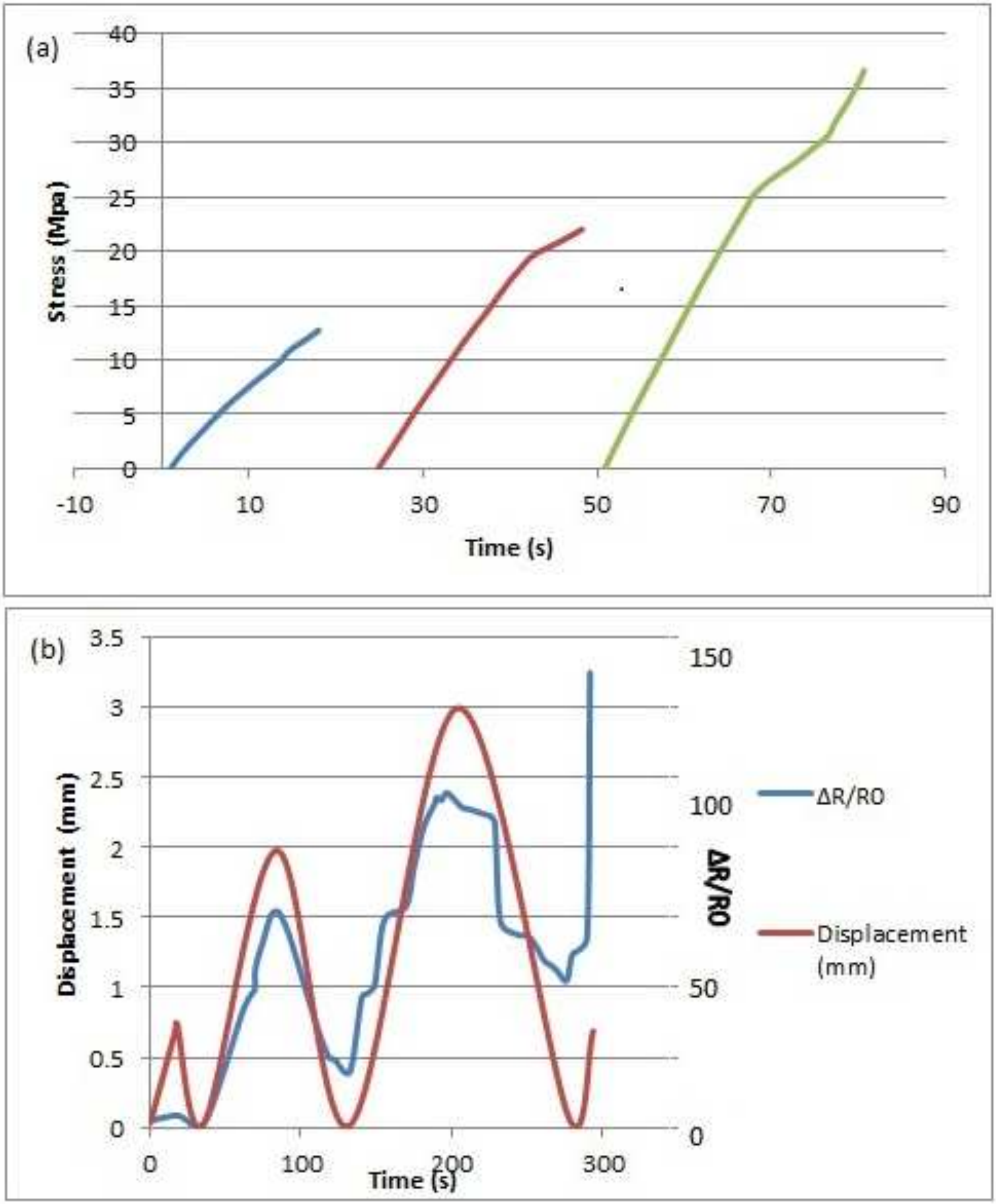

Fig. 4. Results from cyclic compression test for stress 60 MPa: a) Strain vs Time, b) stress and $\Delta R/R_0$ vs time [70]

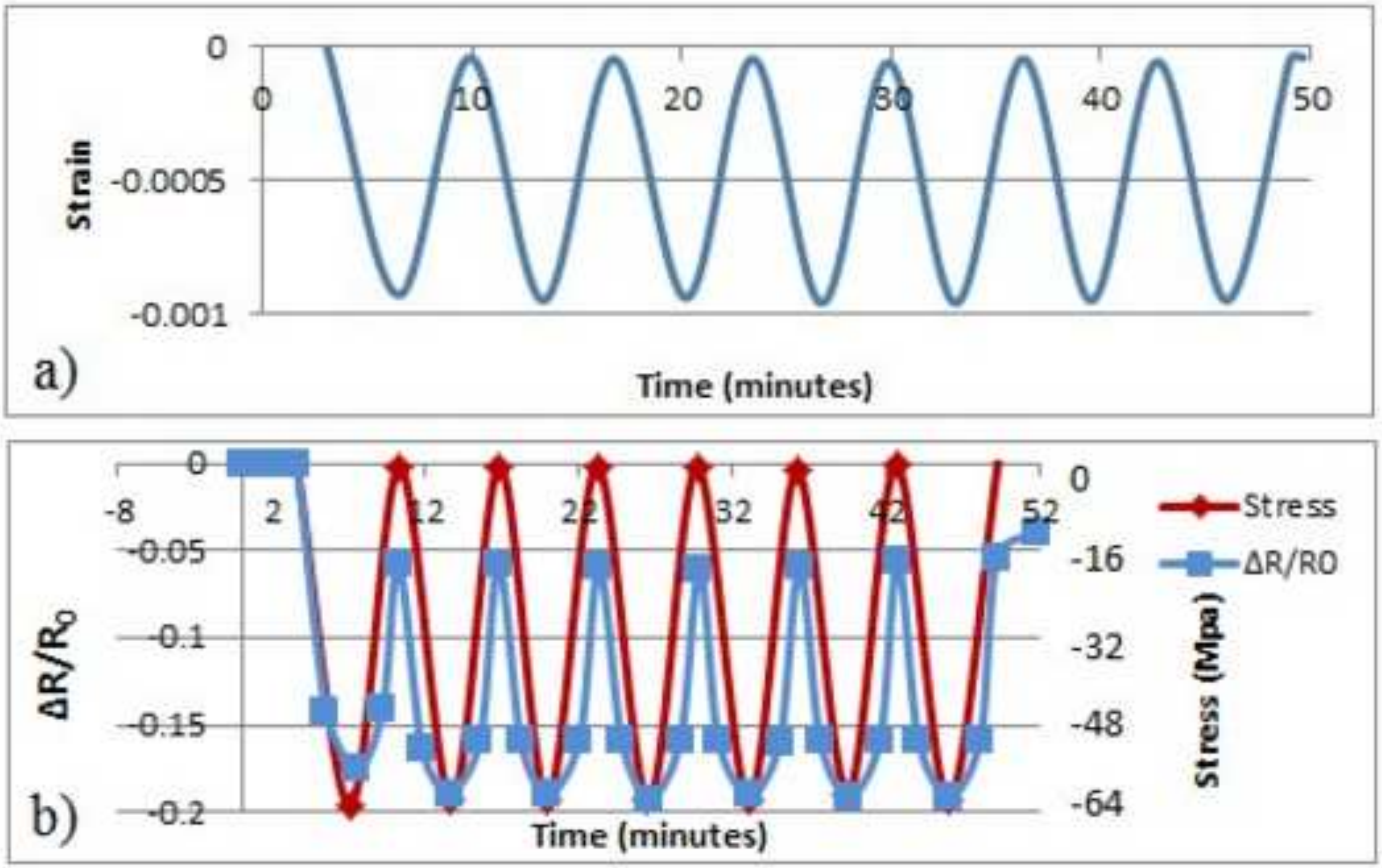

Figure(s)

Fig. 5. Results from cyclic compression test for stress 120 MPa: a) Strain vs Time, b) stress and $\Delta R/R_0$ vs time [70]

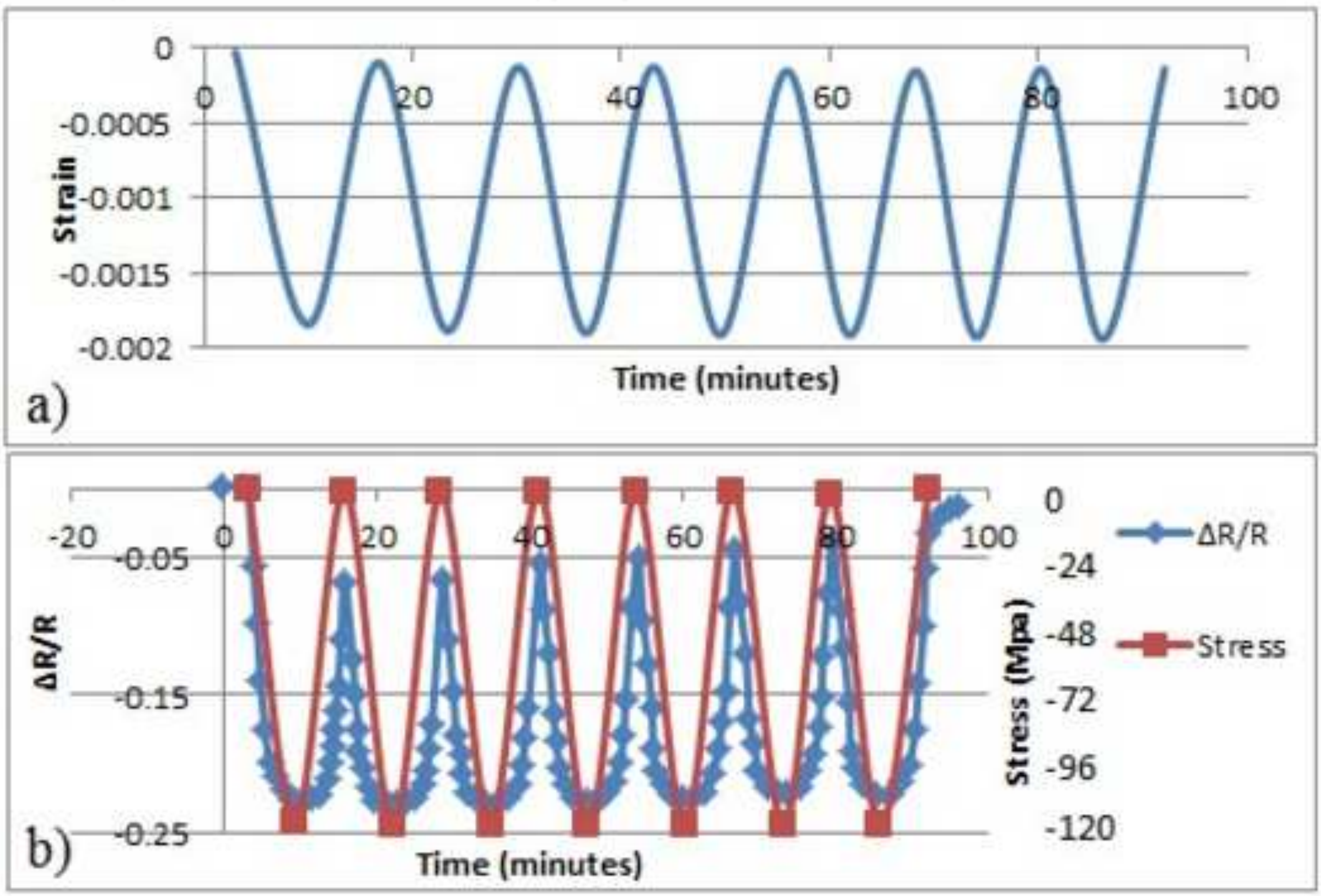

Fig. 6. Cumulative energy for Wired and Wireless AE sensor [99]

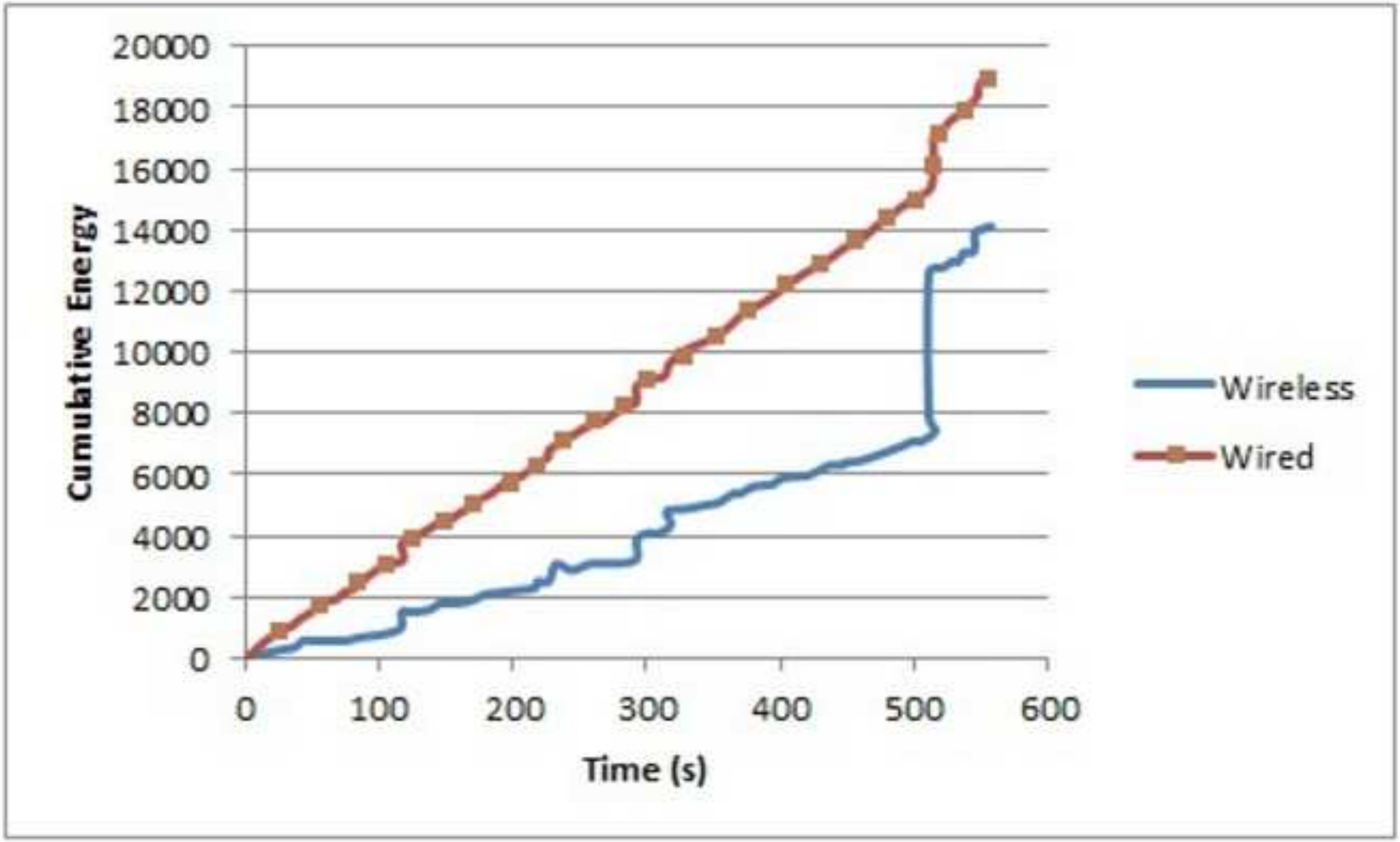

Fig. 7. Behaviour of energy b-value with increase in Peak Acceleration [100]

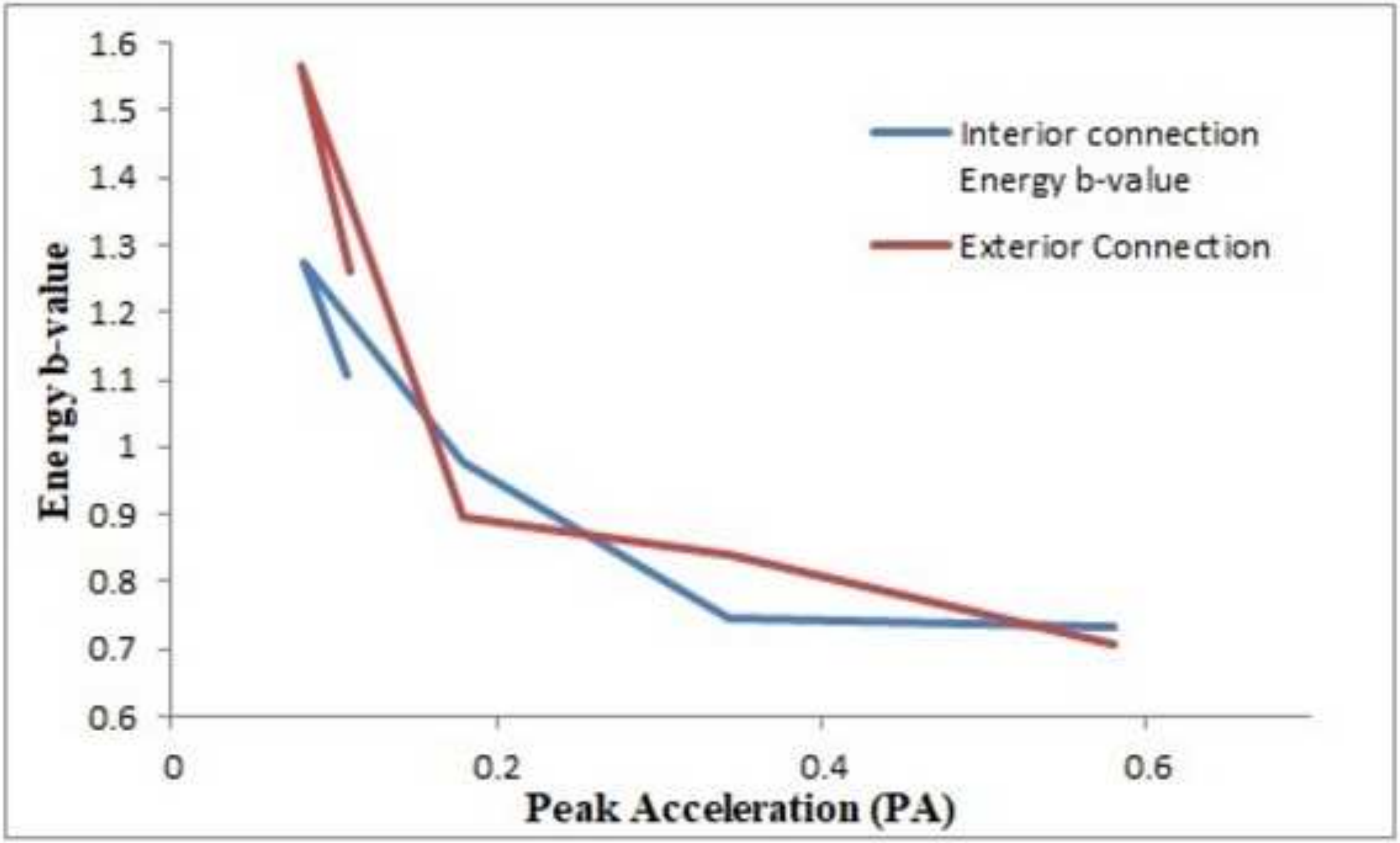

Fig. 8 5s acceleration data obtained for cabled and wireless accelerometer for; a) location 6 and b) location 10 [114]

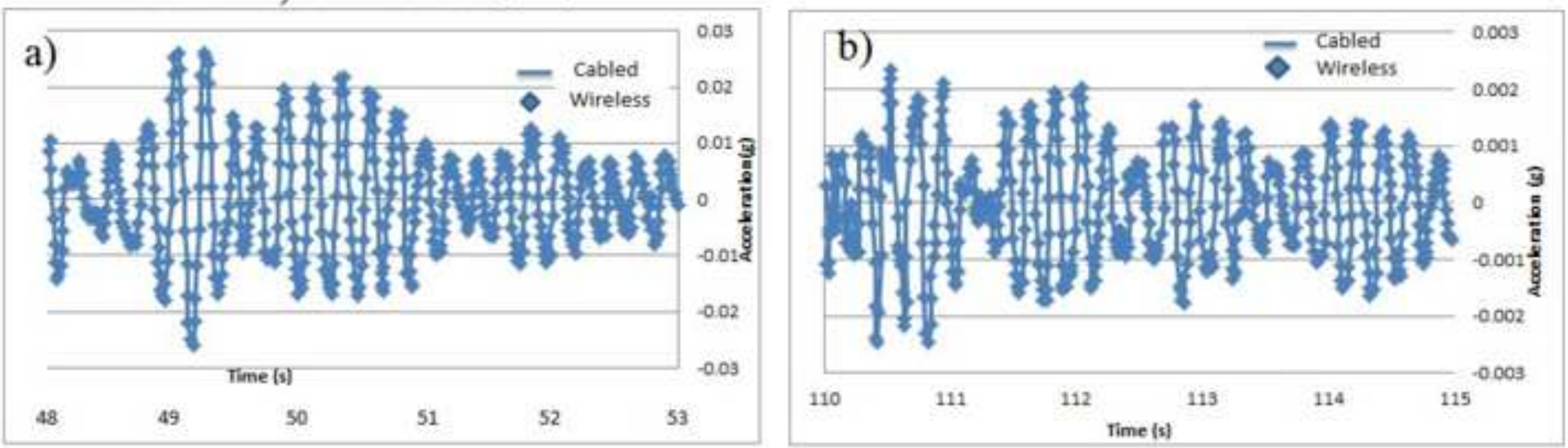

Figure(s)

Fig. 9 . Vertical Acceleration data in Event 1 for; a) Re-sampled acceleration (10 Hz), and b) GPS accelerometer [118]

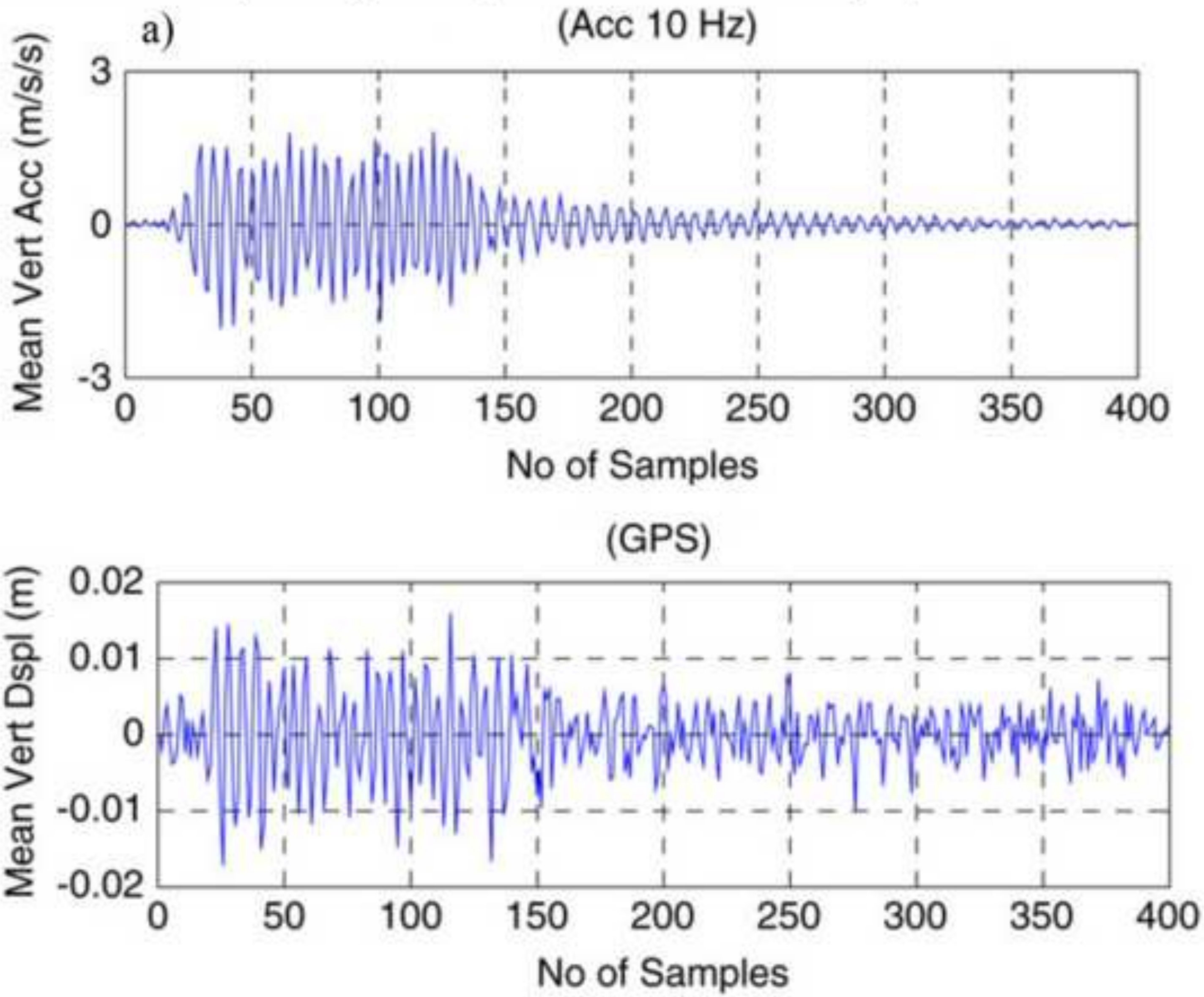

Fig. 10. Performance of : a) Piezoresistive MEMS accelerometer and b) capacitive MEMS accelerometer [137]

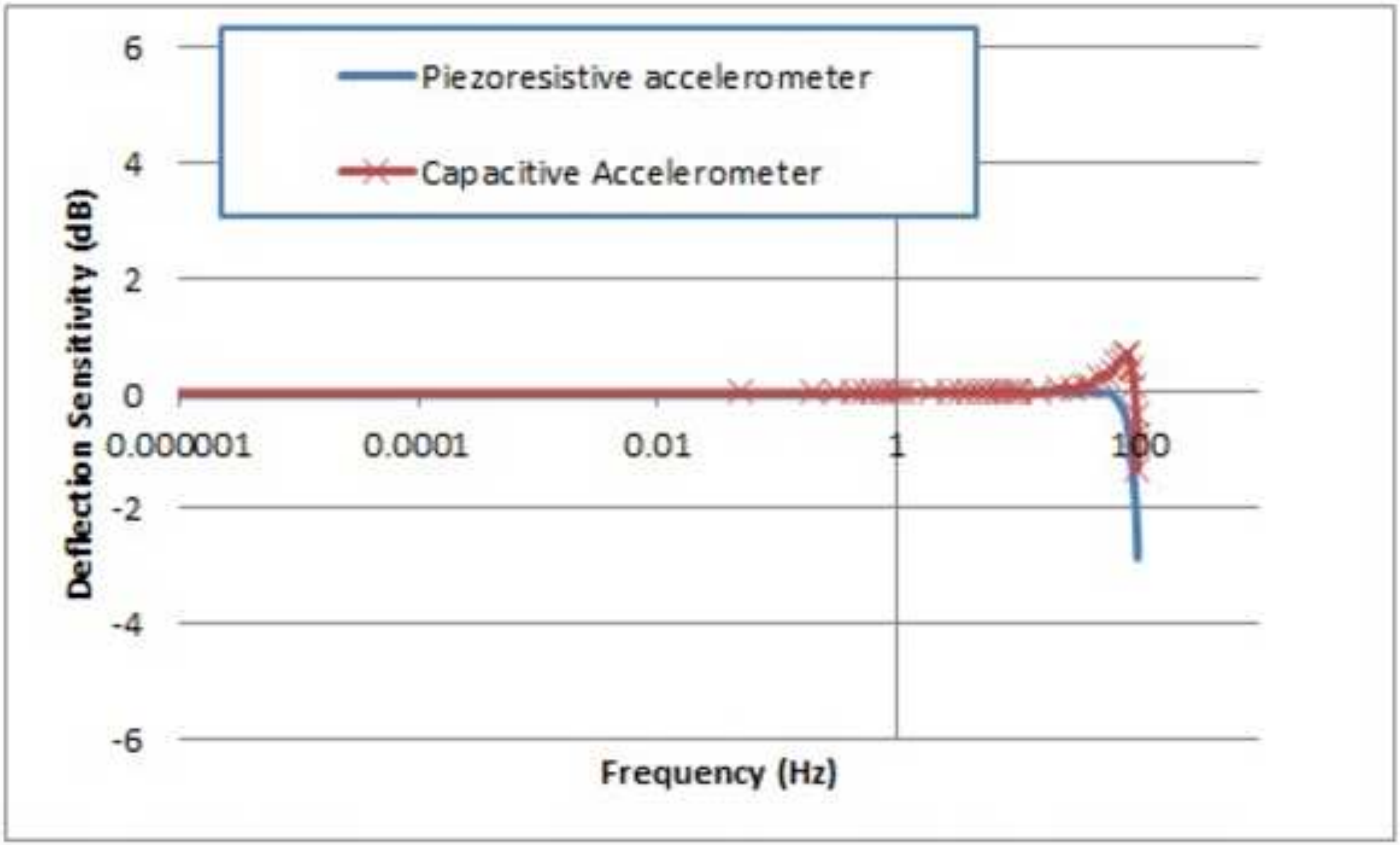

Fig. 11. Single mode optical fiber

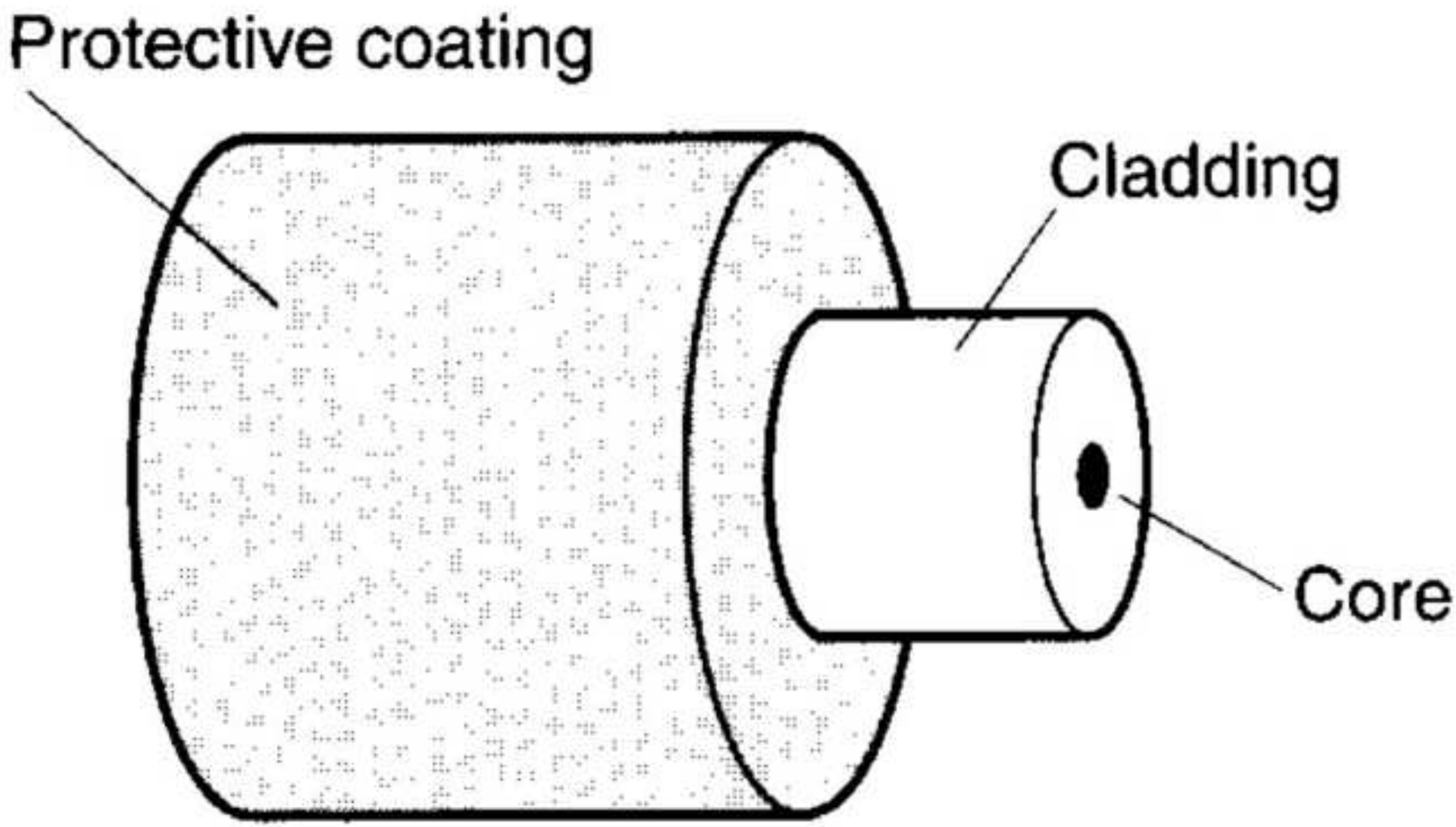

Fig. 12. Transmission and Reflection Spectra from a FBG sensor [166]

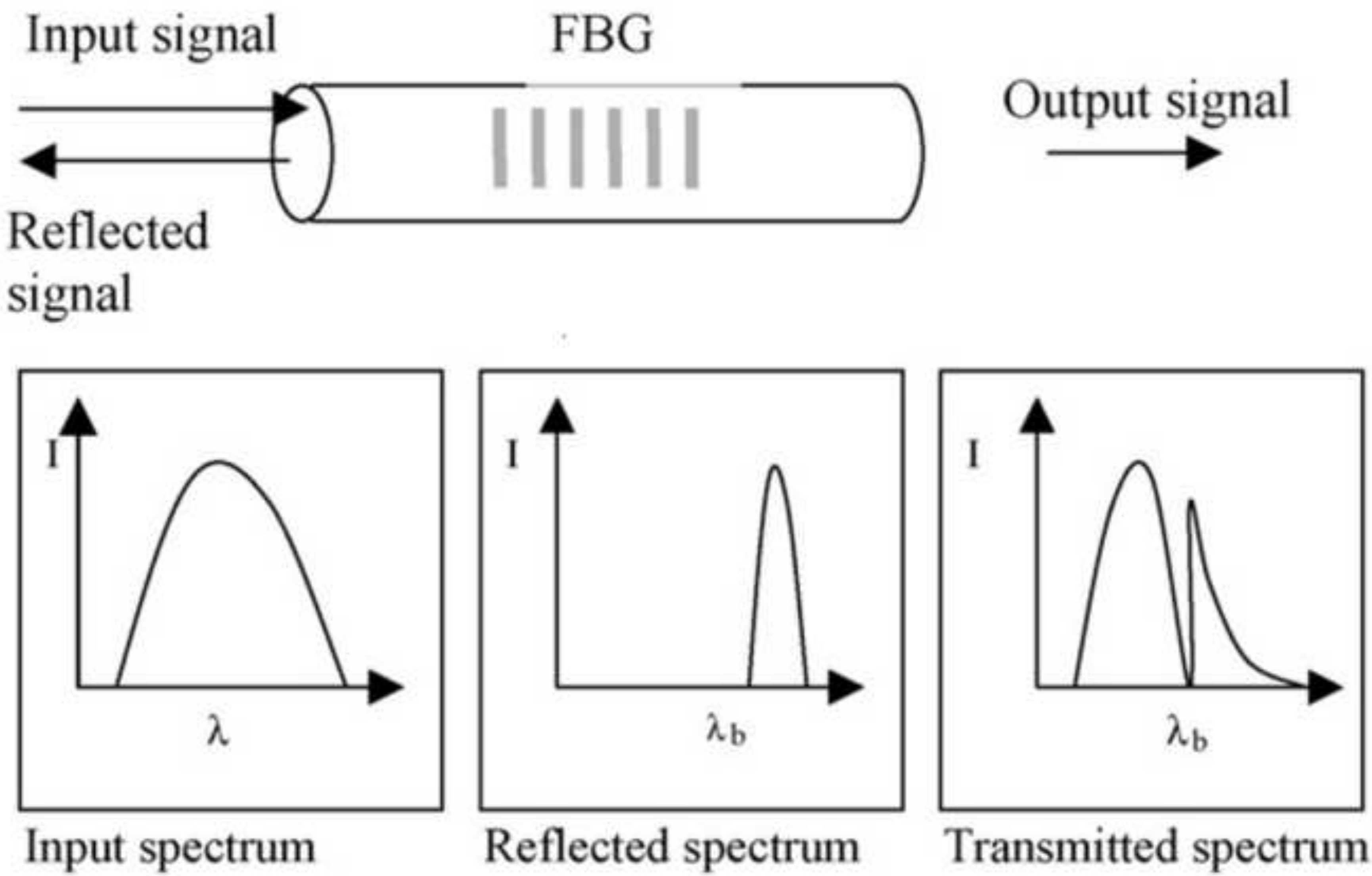

Fig. 13 . Graphical interpretention of the theoritical and experimental results [164]

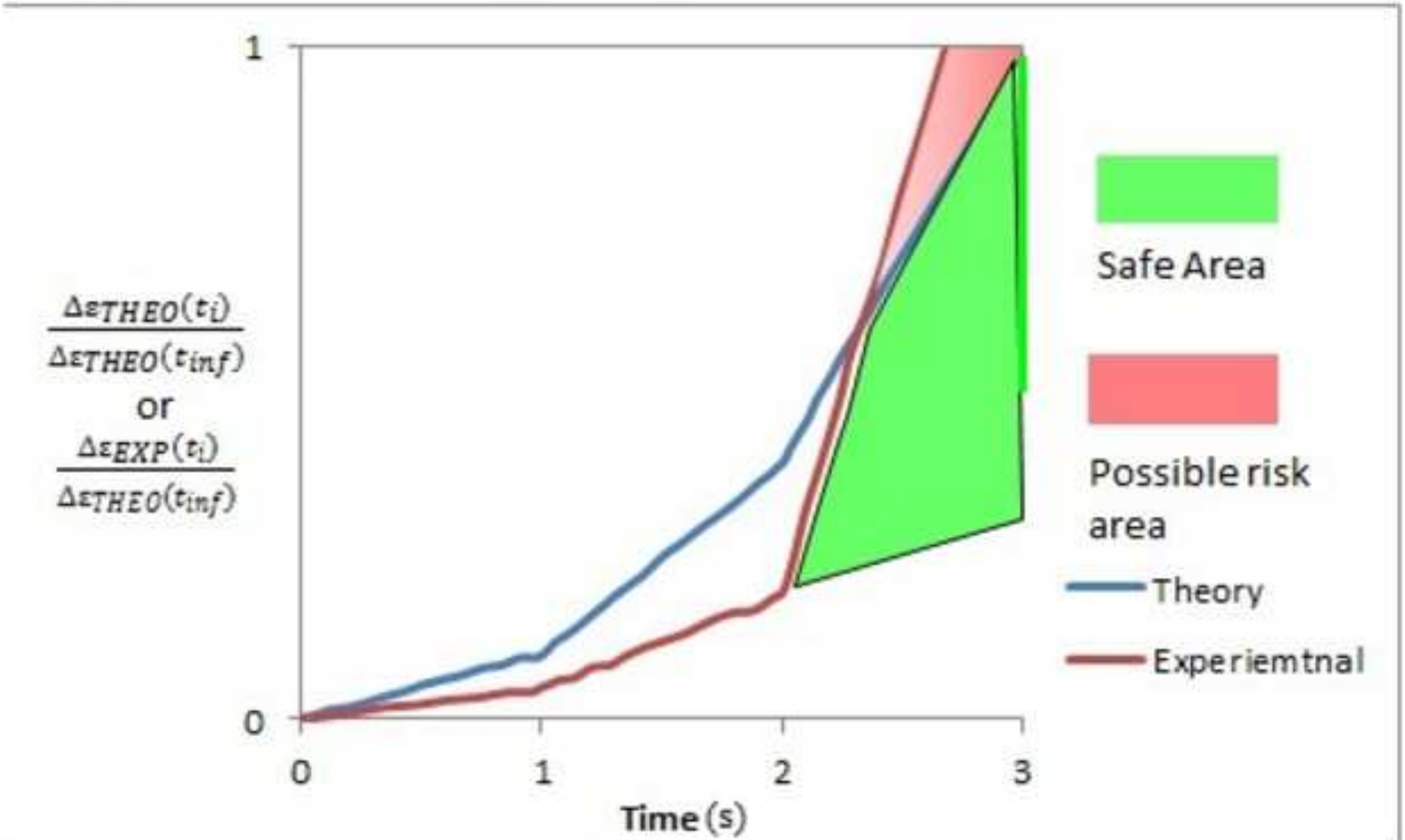

Fig. 14. Temperature compensated strain data [53]

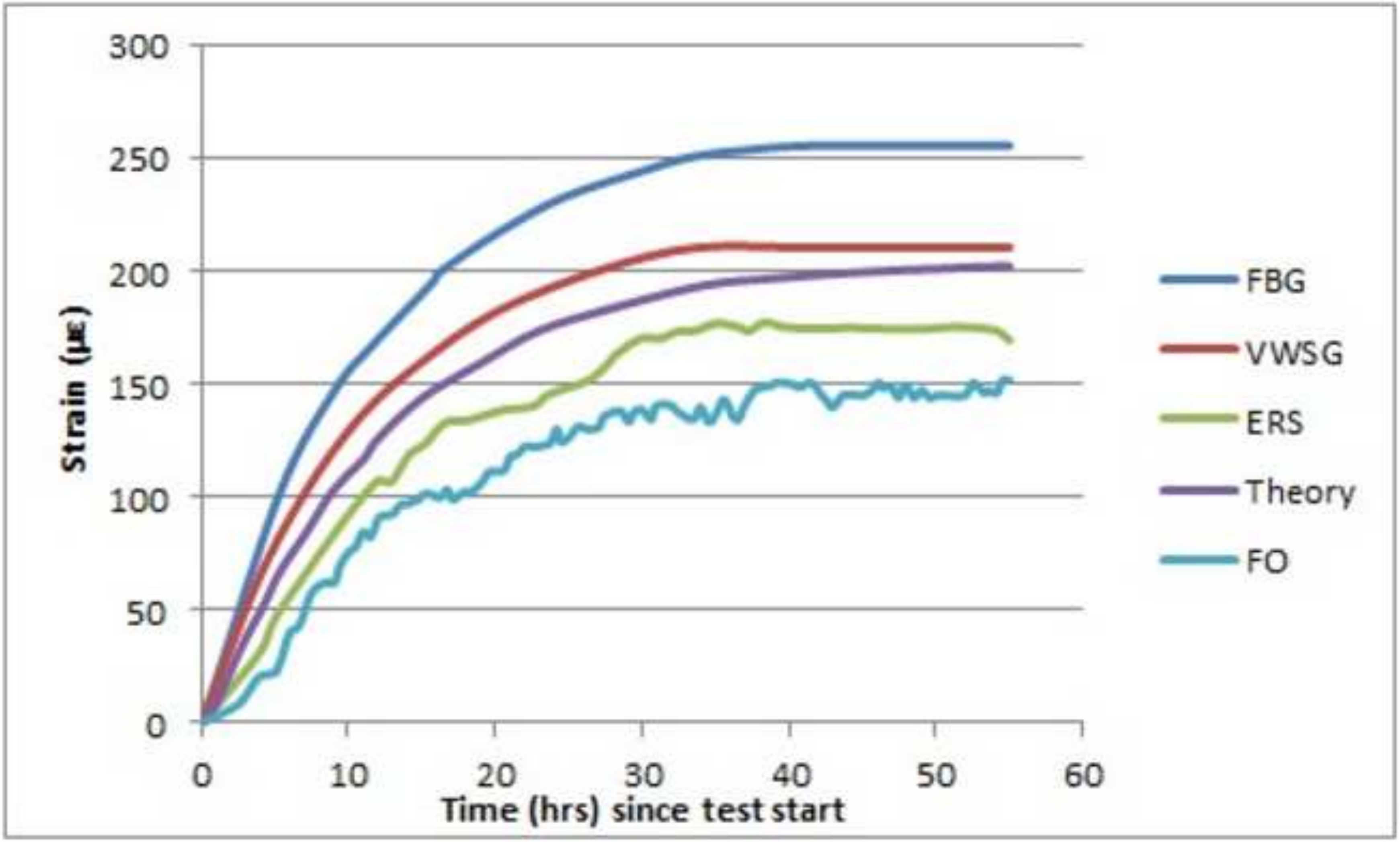

Fig. 15. Strain measurements for tempearture gradient case [53]

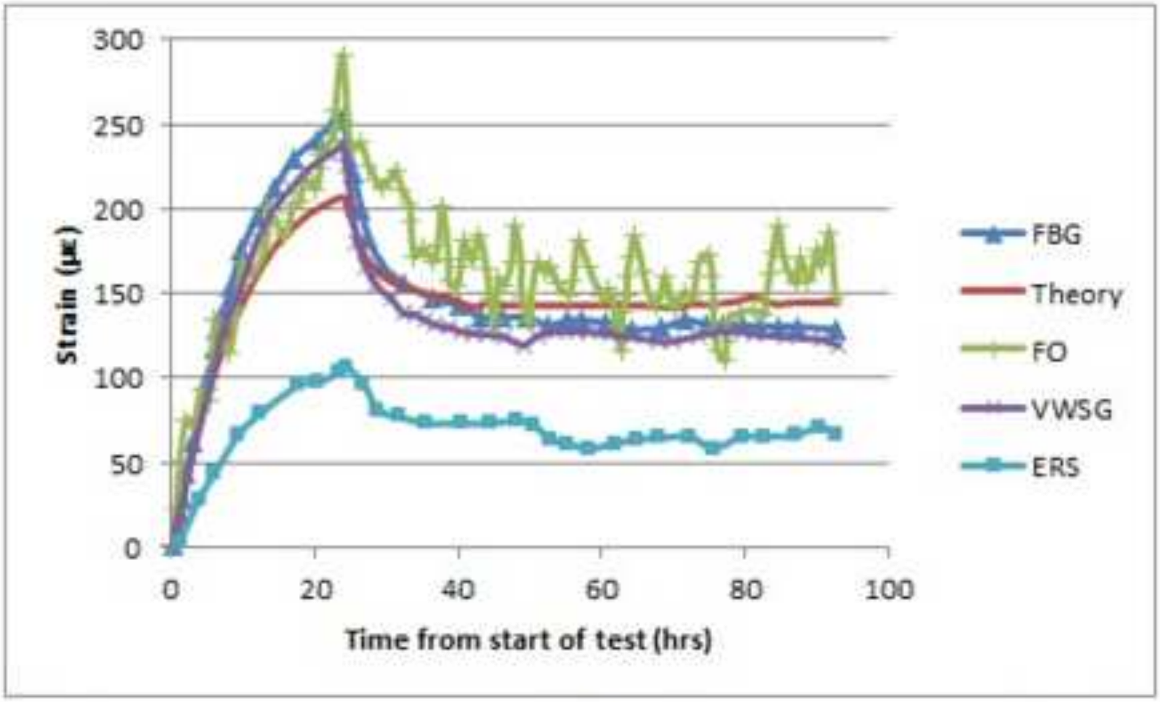

a) Tempearture compensated strain measurements (top)

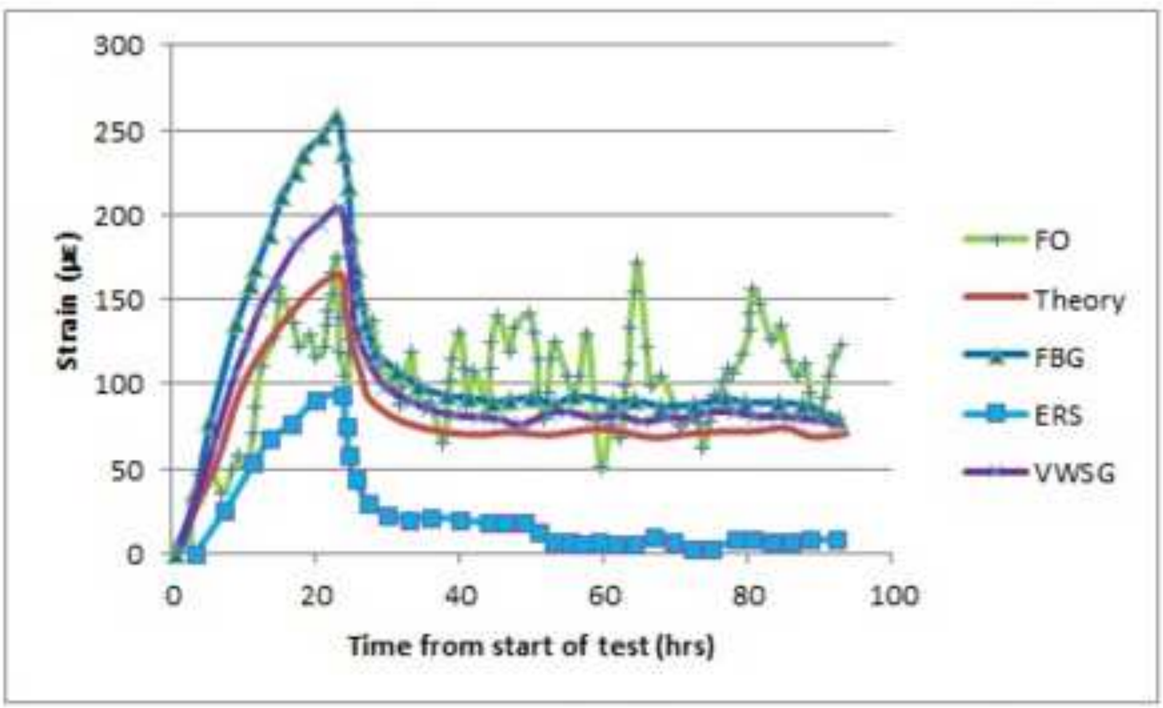

b) Tempearture compensated strain measurements (bottom)

Fig. 16. Static response evaluation of FOS and ERS [174]

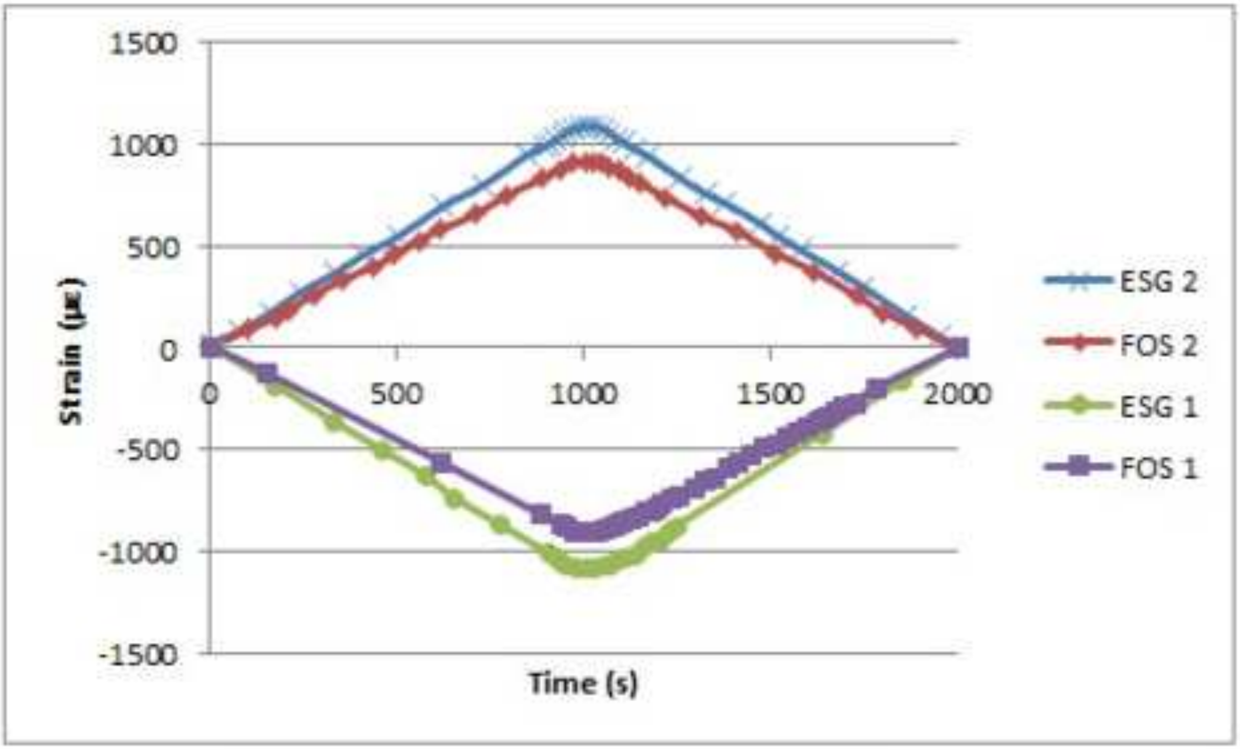

a) ERS vs FOS of length 4cm.

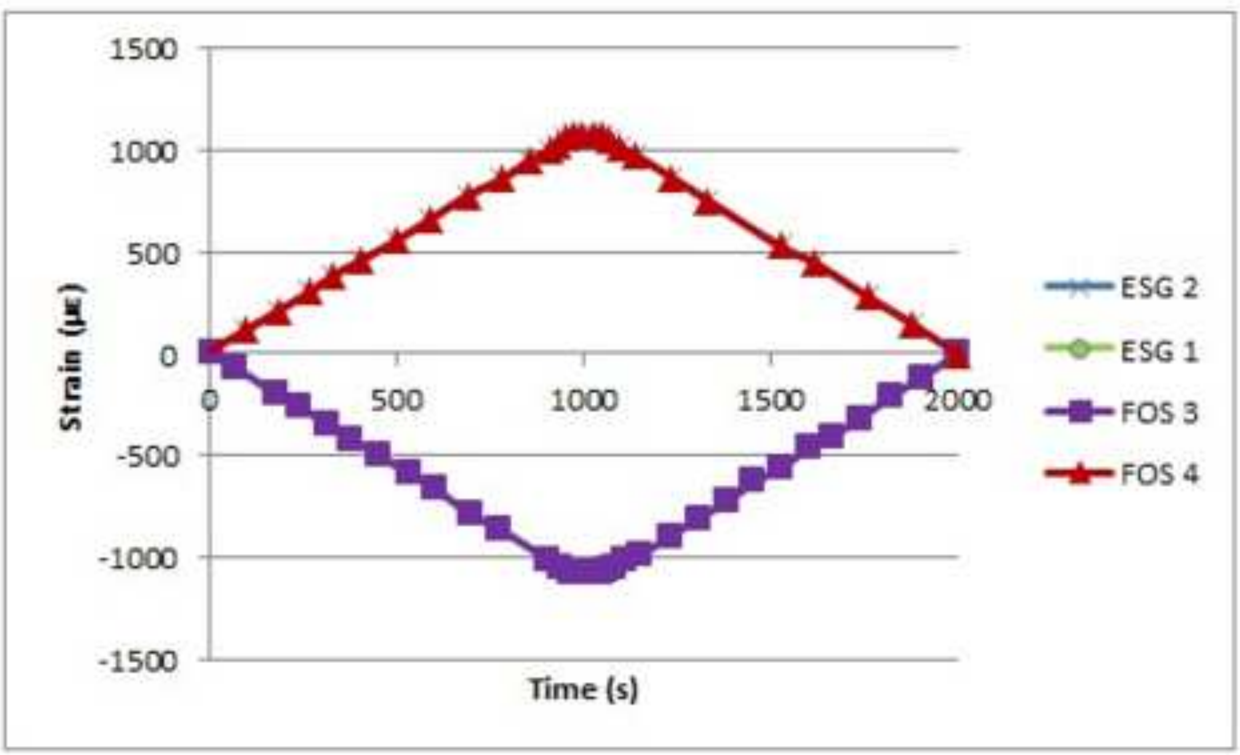

b) ERS vs FOS of length 10 cm.

Fig. 17 . Practical and theoritical strain vs steel temperature for one cycle temperature test [174]

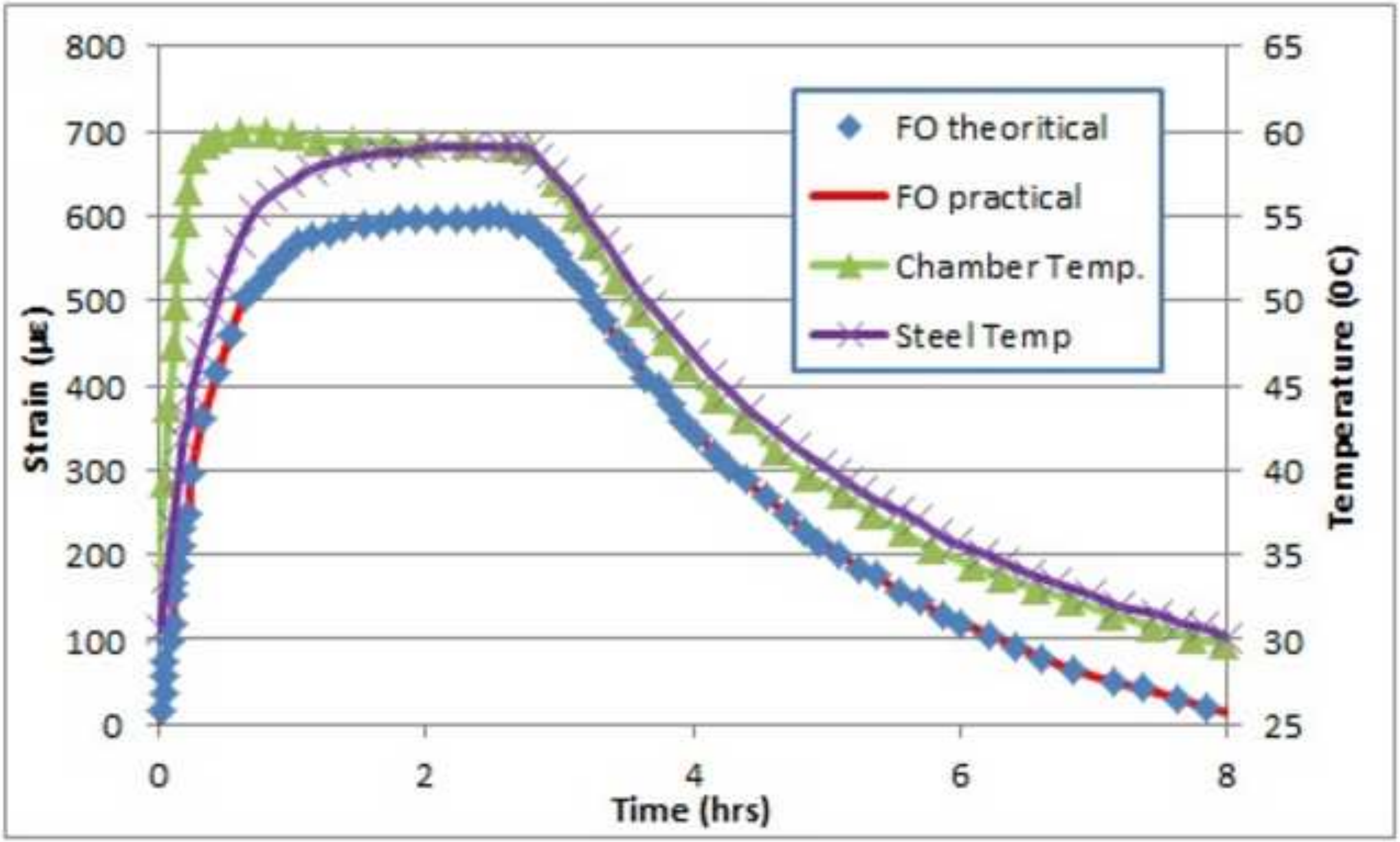

Fig. 18. Strain measurement for sQRS (S_h), DIC and AE sensors for cyclic load [217]

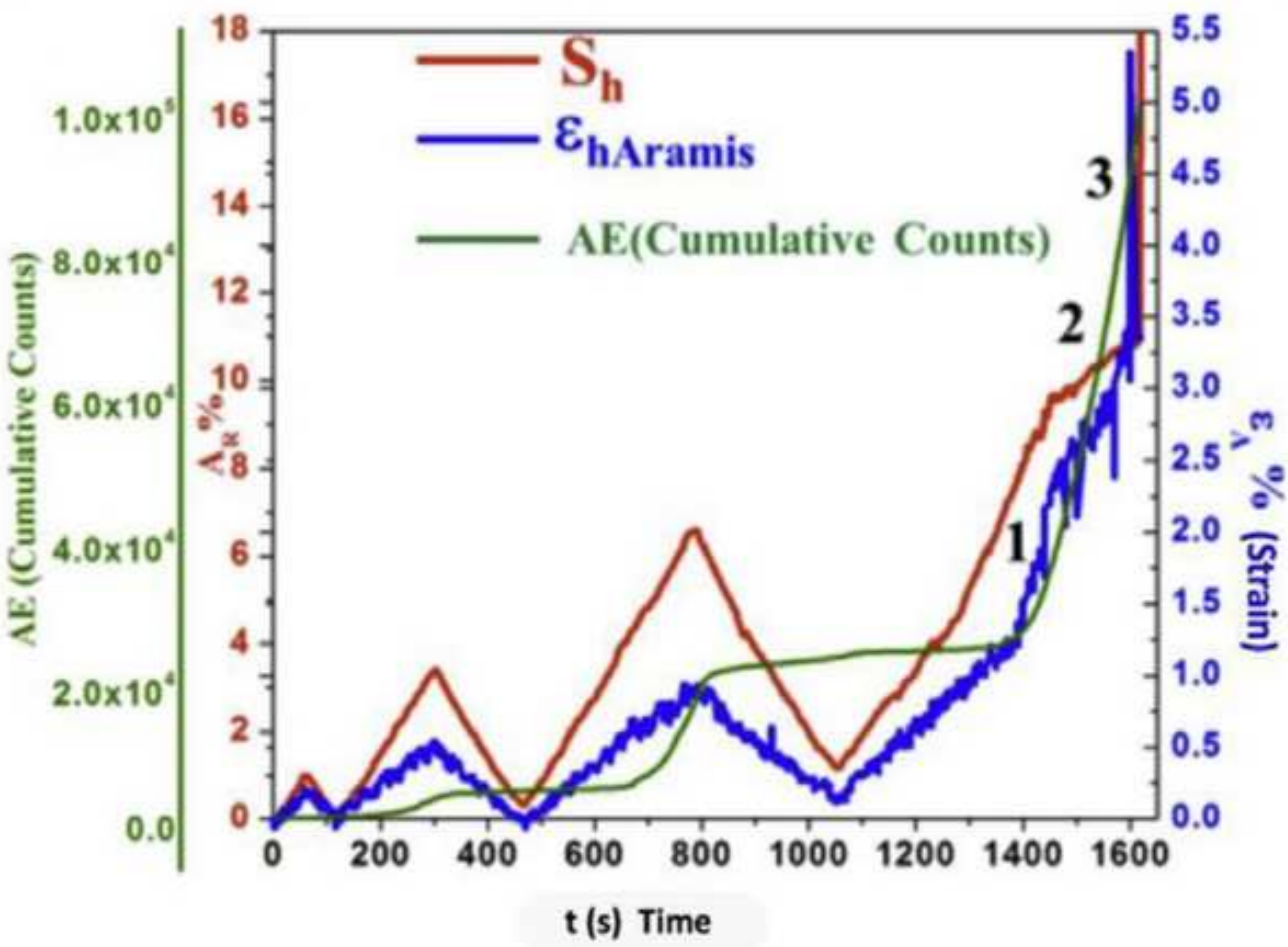

Fig. 19. Acceleration measurement by GPS, laser displacement meter and accelerometer [220]

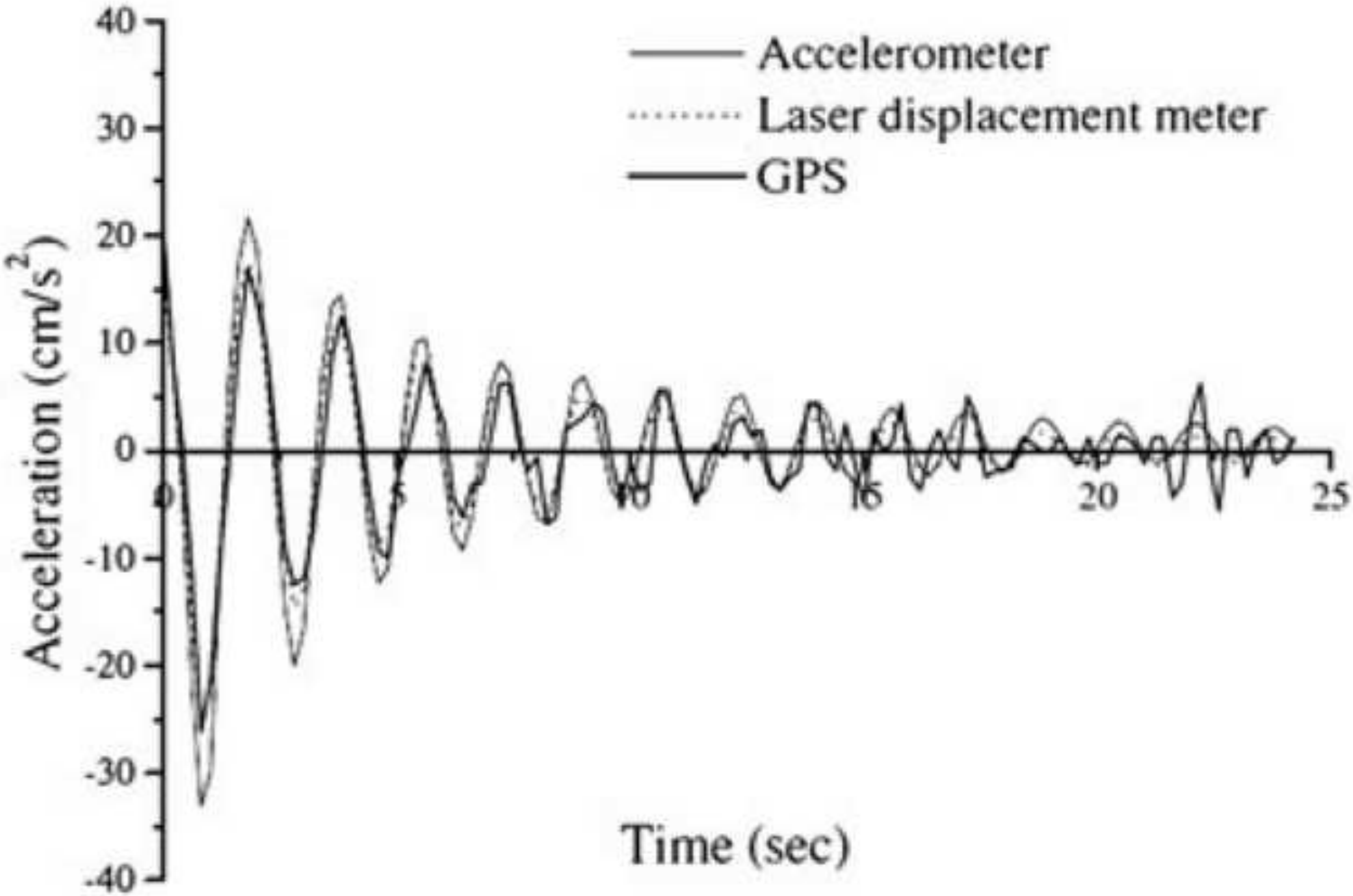

Figure(s)

Fig. 20. Horizontal displacement time series from DGPS and PPP processing with FFT [128]